Chem Soc Rev

Strapped calix[4]pyrroles: From syntheses to applications

Journal:	*Chemical Society Reviews*
Manuscript ID	CS-SYN-07-2019-000528.R2
Article Type:	Review Article
Date Submitted by the Author:	05-Dec-2019
Complete List of Authors:	Peng, Sangshan; Hunan University State Key Laboratory of Chemo/Biosensing and Chemometrics, College of Chemistry and Chemical Engineering; He, Qing; Hunan University State Key Laboratory of Chemo/Biosensing and Chemometrics, College of Chemistry and Chemical Engineering Vargas-Zuniga, Gabriela; University of Texas, Chemistry and Biochemistry Qin, Lei; University of Texas at Austin, Chemistry Hwang, Inhong; University of Texas at Austin, Department of Chemistry Kim, Sung Kuk; Gyeongsang National University, Department of Chemistry and Research Institute of Natural Sciences Heo, Nam Jung; Gyeongsang National University, Chemistry Lee, Chang-Hee; Kangwon National University, chemistry Dutta, Ranjan; Kangwon National University, chemistry Sessler, Jonathan; Univ Texas Austin, Chemistry; Shanghai University,

ARTICLE

Strapped calix[4]pyrroles: From syntheses to applications

Sangshan Peng,[a] Qing He,*[a] Gabriela I. Vargas-Zúñiga,[b] Lei Qin,[b] Inhong Hwang,[b] Sung Kuk Kim,*[c] Nam Jung Heo,[c] Chang-Hee Lee,*[d] Ranjan Dutta,[d] and Jonathan L. Sessler*[b,e]

Received 00th January 20xx,
Accepted 00th January 20xx

DOI: 10.1039/x0xx00000x

Supramolecular chemistry is a central topic in modern chemistry. It touches on many traditional disciplines, such as organic chemistry, inorganic chemistry, physical chemistry, materials chemistry, environmental chemistry, and biological chemistry. Supramolecular hosts, *inter alia* macrocyclic hosts, play critical roles in supramolecular chemistry. Calix[4]pyrroles, non-aromatic tetrapyrrolic macrocycles defined by sp^3 hybridized *meso* bridges, have proved to be versatile receptors for neutral species, anions, and cations, as well as ion pairs. Compared to the parent system, octamethylcalix[4]pyrrole and its derivatives bearing simple appended functionalities, strapped calix[4]pyrroles typically display enhanced binding affinities and selectivities. In this review, we summarize advances in the designs and syntheses of strapped calix[4]pyrroles, as well as their broad utility in molecular recognition, supramolecular extraction, separation technology, ion transport, and as agents capable of inhibiting cancer cell proliferation. Future challenges within this sub-field are also discussed.

1 Introduction

Over the past 50 years, supramolecular chemistry has witnessed tremendous growth and has emerged as one of the central disciplines in modern chemistry.[1] The importance of the field is underscored by two Nobel Prizes in Chemistry awarded to Charles Pedersen, Donald J. Cram, and Jean-Marie Lehn "for their development and use of molecules with structure-specific interactions of high selectivity" in 1987 and to Jean-Pierre Sauvage, Sir J. Fraser Stoddart, and Bernard L. Feringa "for their development of molecular machines" in 2016, respectively. Currently, supramolecular chemistry impinges on numerous fields of science as diverse as biology, materials science, medicine, analytical chemistry, environmental remediation, separation science, and nanotechnology.[2, 3]

Receptor-based molecular recognition is one of the core tenants of supramolecular chemistry.[4, 5] Not surprisingly, therefore, the design and synthesis of supramolecular hosts possessing high affinity and adequate selectivity for various targeted substrates represents an ongoing challenge that continues to attract considerable attention.[6] Considerable effort has been devoted to creating functional receptors for specific guest species (*i.e.*, neutral molecules, cations, anions, or ion pairs).[1, 2, 7-9] For instance, crown ethers and their derivatives proved early on to be elegant receptors for cationic metal ions;[10, 11] calix[n]arenes were found capable of capturing neutral species or cationic guests, as well as anions;[12-16] cyclodextrins are recognized for their ability to bind relatively hydrophobic guests, particularly, in water.[17-20] Moreover, within the past 10 years, pillararenes have attracted tremendous interest due to their appealing structures, unusual binding properties, and ability to support self-assembly.[21-25] The so-called cucurbiturils, have been shown to be capable of serving as molecular containers for a variety of guests, including peptides, dyes, saccharides, and proteins, such as human insulin.[26, 27] They have thus shown promise for applications that range from supramolecular and biochemistry to those that lie squarely in the medicinal,[28-32] chemosensing,[33-36] and catalysis domains.[37-39]

Over the past two decades, calixpyrroles, *inter alia* calix[4]pyrroles, have emerged as important members of the supramolecular chemistry pantheon due to their ability to act as receptors for anions, cations, and ion pairs.[9, 40] The first calixpyrrole, octamethylcalix[4]pyrrole (**1**), was prepared by Baeyer in 1886.[41] In 1996, Sessler and co-workers reported that calix[4]pyrroles could serve as simple-to-prepare anion receptors.[42] Subsequently, a large number of calix[4]pyrrole-

[a] State Key Laboratory of Chemo/Biosensing and Chemometrics, College of Chemistry and Chemical Engineering, Hunan University, Changsha 410082, P. R. China. E-mail: heqing85@hnu.edu.cn
[b] Department of Chemistry, The University of Texas at Austin, 105 East 24th Street, Stop A5300, Austin, Texas 78712, USA. E-mail: sessler@cm.utexas.edu
[c] Department of Chemistry and Research Institute of Natural Science, Gyeongsang National University, Jinju 660-701, Korea. E-mail: sungkukkim@gnu.ac.kr
[d] Department of Chemistry, Kangwon National University and IMSFT, Chun-Cheon 24341, Korea. E-mail: chhlee@kangwon.ac.kr
[e] Center for Supramolecular Chemistry and Catalysis, Shanghai University, Shanghai 200444, P. R. China.

based anion- and ion pair receptors were developed by functionalizing the backbone of parent calix[4]pyrrole at its *meso* positions or at one of more *β*-pyrrolic sites. To date, several reviews have been published on the topic of calix[4]pyrrole chemistry.[40, 43-50] Most of these reviews have focused on monocyclic calix[4]pyrrole systems. Only one review, entitled, "Strapped and other topographically nonplanar calixpyrrole analogues. Improved anion receptors", published about ten year ago by two of our groups, provides coverage of so-called strapped calix[4]pyrroles. Such systems feature one or more bridging "straps" that span the calix[4]pyrrole backbone to create a bi- or polycyclic system (Fig. 1).[46] However, over the past ten years strapped calix[4]pyrrole have garnered considerable attention and have led to advances that have yet to be recapitulated in the case of simple calix[4]pyrroles. For instance, as compared to calix[4]pyrroles, strapped calix[4]pyrroles often display enhanced affinities and greater selectivity towards anionic or ion pair guests.[51-56]

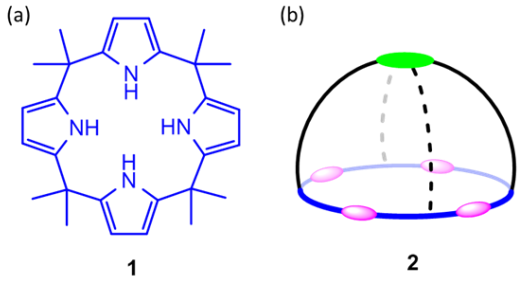

Fig. 1 (a) Chemical structures of parent calix[4]pyrrole **1** and (b) generalized representation of a strapped calix[4]pyrrole **2** bearing at least one "closed" strap.

The increased binding affinities and enhanced selectivity typically seen for strapped calix[4]pyrroles are ascribed to what may be termed a "strap effect". This effect has its origins in a number of determinants, including: 1) the presence of additional cooperative binding sites on the straps; 2) enhanced preorganization and substrate complementarity provided by the strapped calix[4]pyrrole *per se*; 3) deeper encapsulation of targeted guests within the cavity of the multi-macrocyclic receptors. A related contributing factor is that the presence of straps reduces the freedom of the host, which makes guest binding more entropically favourable.

This review summarizes progress made in the area of strapped calix[4]pyrrole chemistry, with a particular emphasis on work appearing in the last decade or so. According to the nature of the functional groups introduced onto the straps, the strapped calix[4]pyrroles considered in this review will be organized into six classes, namely simple strapped calix[4]pyrroles; crown-ether-strapped calix[4]pyrroles; calixarene-strapped calix[4]pyrroles; hemispherand-strapped calix[4]pyrroles; calix[4]pyrrole-strapped calix[4]pyrroles; and other uncommon strapped calix[4]pyrroles. This review will highlight the design and synthesis of strapped calix[4]pyrroles, their unique structures and coordination chemistry, as well as their potential utility in applications involving ion sensing, extraction, assembly, and through-membrane transport, among other potential applications.

2 Simple strapped calix[4]pyrroles

This section provides an overview of strapped calix[4]pyrroles where the straps contain only simple binding motifs and limited recognition sites, such as benzene-strapped calix[4]pyrroles, pyrrole-strapped calix[4]pyrroles, pyridine-strapped calix[4]pyrroles, naphthalene-strapped calix[4]pyrroles, *etc*. The design strategy and synthesis of the calix[4]pyrroles in question, as well as their applications in anion or ion pair binding, will be discussed in detail.

In 2002, Lee and co-workers designed and synthesized the first strapped calix[4]pyrrole **4** (Fig. 2). This team showed that adding even a simple strap provided a means to tune the anion binding properties of the constituent calix[4]pyrrole.[57] The strapped receptor **4** was obtained in 16% yield via the acid-catalysed condensation of strap-bridged bis-dipyrromethane **3** with acetone (present in excess; Fig. 2). Using this approach both macrocycles making up the bicyclic product **4** are formed simultaneously in the final step. This makes the synthesis relatively straightforward. As true for most non-strapped calix[4]pyrroles,[48, 50, 58, 59] the conformation of **4** was found to undergo a change from the *1,3-alternate* form to the corresponding cone form upon the binding of a fluoride or chloride anion. ^{1}H NMR spectroscopic analyses in DMSO–d_6 revealed that there exists one additional hydrogen bond between the encapsulated fluoride/chloride anion and the inner aromatic proton located between the two carbonyl groups in **4**. This interaction is in addition to the classic pyrrolic NH-to-bound anion hydrogen bond effects seen in the case of non-strapped calix[4]pyrroles.

Quantitative determinations of the anion binding affinities of receptor **4** were carried out in DMSO-d_6 solution using standard ^{1}H NMR spectroscopic titrations and isothermal titration calorimetry (ITC) analyses. As expected, the benzene-strapped calix[4]pyrrole **4** displayed a higher affinity for both the fluoride and chloride anions relative to the parent calix[4]pyrrole **1**. For instance, the affinity constant, K_a, for the chloride anion was estimated be (1.01 ± 0.10) × 10^5 M^{-1} on the basis of ITC measurements carried out in DMSO, while the corresponding value involving the unstrapped host **1** was only 1.27 × 10^3 M^{-1} under otherwise identical conditions. A fluoride-for-chloride ^{1}H NMR spectroscopic competition experiment in DMSO-d_6 allowed the binding constant for fluoride anion recognition (K_a = 3.9 x 10^6 M^{-1}) to be estimated. Based on Job plots, the binding stoichiometry for the recognition of both the fluoride and chloride anions was assigned as 1:1. Careful analysis of the X-ray crystal structures revealed that the cone angle is smaller in chloride complex than in the corresponding fluoride complex. This was taken as evidence that the fluoride anion forms a tighter hydrogen bonding complex with the pyrrole N–H protons, which in turn serves to make the overall complex more planar.

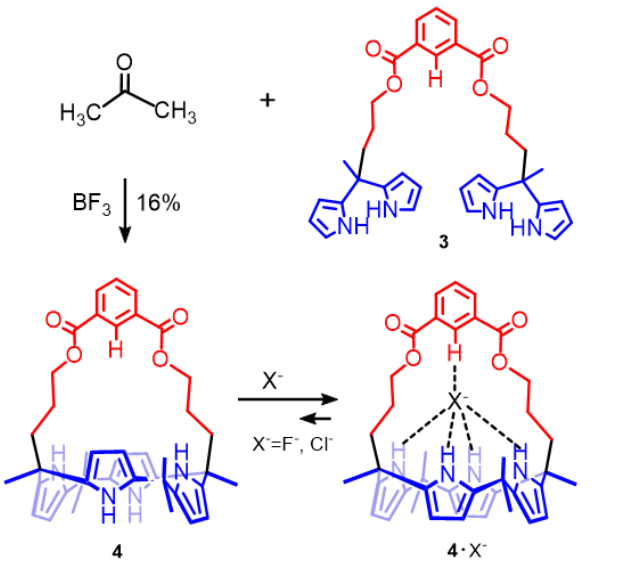

Fig. 2 Synthesis of benzene-strapped calix[4]pyrrole **4** and the structure of **4**·X⁻.

To enhance further the anion recognition properties of calix[4]pyrroles, Lee and Sessler, *et al.* reported three new calix[4]pyrroles (**5**–**7**) strapped with *m*-orcinol-derived diethers of different lengths (Fig. 3).[60] Qualitative support for bromide and chloride binding came from ^{1}H NMR spectroscopic studies carried out in CD_3CN. The central aromatic CH proton of the aryl portion on the strap was seen to undergo a downfield shift upon the addition of anions. This was taken as evidence that it acts as a CH hydrogen bond donor and interacts with the bound anion. As expected, the binding affinities of **5**–**7** towards the bromide (3.0×10^4 M^{-1} for **5**, 3.1×10^4 M^{-1} for **6**, and 1.2×10^5 M^{-1} for **7**, respectively) and chloride (3.6×10^6 M^{-1} for **5**, 1.4×10^6 M^{-1} for **6**, and 1.4×10^6 M^{-1} for **7**, respectively) anions were substantially enhanced relative to those of **1** (4.5×10^3 M^{-1} for Br^- and 5.0×10^4 M^{-1} for Cl^-, respectively) (Table 1). Specifically, as determined by quantitative ITC analyses in acetonitrile, the association constant K_a corresponding to the interaction between receptor **5** and the chloride anion was over one order of magnitude larger than that seen for the parent system **1**. An enhancement factor of nearly 7-fold was also seen relative to the unstrapped fluorinated calix[4]pyrrole **8** that served as a high affinity benchmark at the time of the study. It was found that the binding affinity could be further tuned by changing the strap length. Among the three diether strapped systems **5**–**7**, the shortest strap yielded the highest chloride anion affinity, while the longest one showed the greatest affinity for the bromide anion. Taken together, these findings led to the suggestion that the anion binding affinity and selectivity of calix[4]pyrrole-based hosts could be modulated readily via the introduction of appropriately chosen straps.

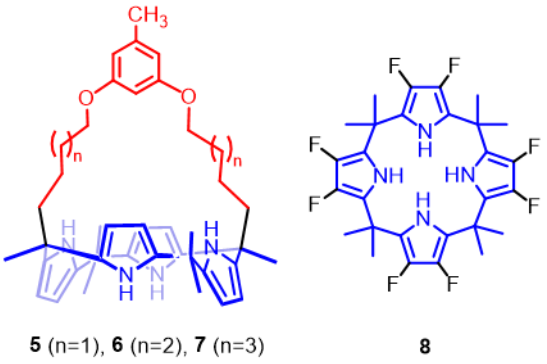

Fig. 3 Chemical structures of **5**–**8**.

Table 1 Association Constants (K_a) Corresponding to the Interaction of **1**, **5-8** with the Bromide and Chloride Anions in CH_3CN[a 60]

	K_a (M^{-1})	
Receptors	Cl^-	Br^-
1[b]	5.0×10^4	4.5×10^3
5	3.6×10^6	3.0×10^4
6	1.4×10^6	3.1×10^4
7	1.4×10^6	1.2×10^5

[a] Determined by ITC at 303 K. [b] From ref. 61 at 298 K. Tetra-n-butylammonium was used as the counterion in all cases.

As an initial test of this proposition, several new benzene-strapped calix[4]pyrroles **9**–**13** (Fig. 4) containing amide units, rather than ether or ester, within the strap were prepared by the same groups.[62] The presence of amide moieties within the straps was expected to provide additional hydrogen-bonding donor sites and to improve the anion binding affinities. In the case of receptor **10** and the chloride ion, a receptor:anion ratio of 2:1 (**10**$_2$·Cl^-) at a relatively high receptor concentrations and an equilibrium between 1:1 and 2:1 (receptor:anion) complexes (Fig. 5) was inferred from ^{1}H NMR spectroscopic analyses and ITC measurements carried out in acetonitrile–d_3 and dry acetonitrile, respectively. On the basis of these studies, it was proposed that the cavity defined by the strap is unable to accommodate the chloride ion well because of a size mismatch. Consequently, anion binding occurs preferentially outside the central pocket (**10**·Cl^-) (Fig. 5). Nevertheless, the binding affinity obtained was larger than that seen for various unstrapped calix[4]pyrroles; presumably, this reflects the fact that the amide groups provide additional hydrogen-bonding donors that enhance the anion-receptor interactions. In the case of the fluoride or bromide anions, receptor:anion ratios of 1:1 (**10**·F^-) and 2:1 (**10**$_2$·Br^-) dominate, respectively (Fig. 5). These findings support the notion that both the size of the anion and the nature of the strap play important roles in modulating the binding affinities. Not surprisingly, and consistent with the proposed outside binding modes, varying the strap length had little influence on the anion selectivities. Although the corresponding trans receptors (**12** and **13**) were also isolated,

the pyrrolic NH protons in these systems were found not to participate effectively in anion binding. The inherent rigidity of these systems presumably precludes adopting the cone conformation that favours anion binding.

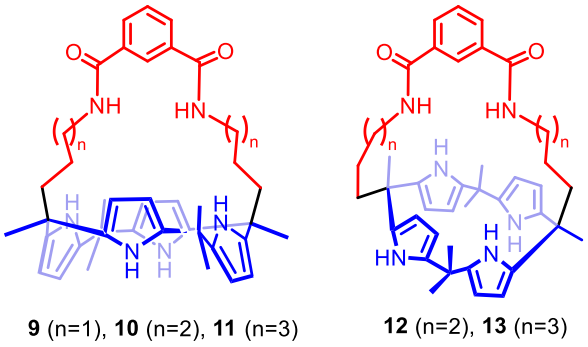

Fig. 4 Chemical structures of **9**, **10**, **11**, **12**, and **13**.

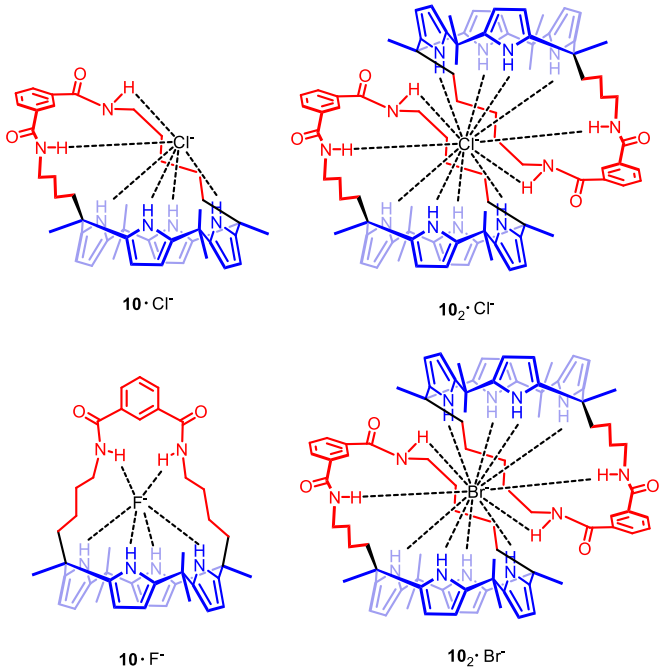

Fig. 5 Binding modes proposed for the interaction of **10** with F^-, Cl^-, and Br^-.

As noted above, in the case of the complex **4**·Cl^-, a hydrogen bonding interaction between the aryl hydrogen and the chloride ion was inferred and served to rationalize the relatively enhanced binding affinity. In order to investigate the extent to which the C–H···Cl^- interaction contributes to the chloride ion binding process, Lee and co-workers synthesized the pyrrole- and furan-strapped congeners **14** and **15** (Fig. 6), and compared their chloride anion binding affinities with that of receptor **4**.[51] As deduced from an X-ray diffraction analysis, the N–H···Cl^- contact distance was 0.63 Å shorter than the benzene–H···Cl^- bond distance, leading to the suggestion that the hydrogen bonding interaction in **14**·Cl^- is stronger than that in **4**·Cl^-. The same conclusion was reached on the basis of a theoretical study involving density functional theory (DFT).[63] The furan-strapped system, lacking a proton donor, was characterized by the weakest chloride anion affinity among these three receptors. Based on the results of an ITC study conducted in acetonitrile, the chloride association constants K_a were found to be 2.2×10^6 M^{-1}, 1.8×10^7 M^{-1}, and 1.9×10^5 M^{-1} for hosts **4**, **14**, and **15**, respectively. It was suggested by the authors that not-so-weak hydrogen bonding interactions, such as C–H···Cl^- bonds, could be exploited in the design of anion receptors. This idea was seminal in its time.

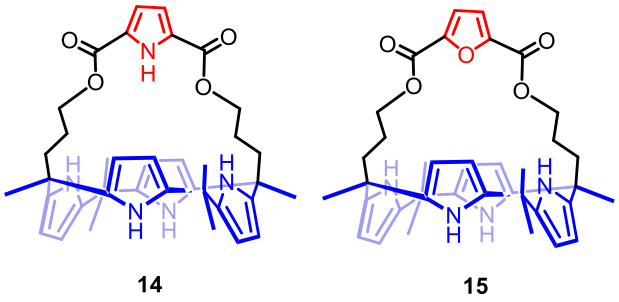

Fig. 6 Chemical structures of **14** and **15**.

In addition to their utility in the above-mentioned studies, Sessler and co-workers found that the pyrrole-strapped calix[4]pyrrole **14** was capable of binding the fluoride and chloride anions effectively even in a highly polar environment consisting of 4:1 (v/v) DMSO–H_2O.[64]

Detailed study of the anion binding properties of receptors **1**, **4**, **14**, and **15** was extended to include other anions, *i.e.*, fluoride, bromide, and benzoate.[65] As determined via ITC analyses carried out in CH_3CN solution, the binding affinities towards the bromide and benzoate anions were enhanced in the case of the benzene- and pyrrole-strapped systems relative to the corresponding furan-strapped congener. However, the values were similar to those seen for the parent *meso*-octamethylcalix[4]pyrrole.

Based on ITC studies (in acetonitrile) and ^1H NMR spectroscopic measurements (in DMSO-d_6) it was inferred that the interactions between **14** and the fluoride anion proceeded via two sequential steps, involving anion binding in the first step followed by deprotonation of the pyrrolic NH proton on the strap upon adding further anion equivalents. In contrast to **14**·Cl^-, where the bound chloride ions interact directly with the pyrrolic NH proton of the strap, a methanol molecule is involved in the stabilization of complex **14**·F^-; it does so by bridging between the encapsulated fluoride ion and the pyrrolic NH as inferred from a single crystal X-ray diffraction analysis (Fig. 7).

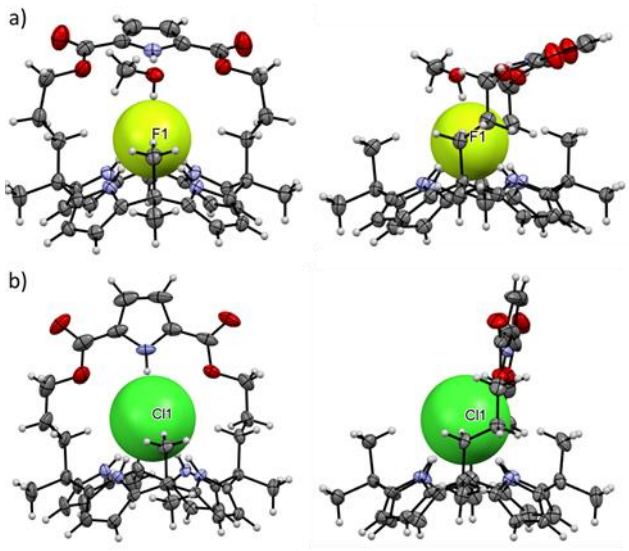

Fig. 7 Single crystal X-ray structures of the anion complexes (a) **14**·F^-·CH_3OH and (b) **14**·Cl^- (left: front view; right: side view). These figures were generated using data downloaded from the Cambridge Crystallographic Data Centre (CSD Nos. 737942 and 682548)

Generally, the binding of ion pairs is considered advantageous compared to the complexation of either individual cations or anions. These improvements, typically true in terms of both affinity and selectivity, are ascribed to favourable electrostatic interactions between the co-bound ions and a reduction in competitive solvation effects.[9, 66, 67] It is well known that calix[4]pyrroles are capable of binding certain ion pairs, especially CsX (X = F, Cl, Br).[48] In order to determine the effect, if any, of a strap on the ion pair binding of calix[4]pyrroles, Sessler, *et al.* conducted a detailed study wherein the pyrrole-strapped calix[4]pyrrole **14** and the parent calix[4]pyrrole **1** were used as comparable hosts.[68] An X-ray diffraction analysis revealed that receptor **14** is able to complex CsF in the form of a 1:1 complex (Fig. 8a). In this case, the fluoride anion is bound to the NH protons of the calix[4]pyrrole framework, as well as to the NH proton of the pyrrole unit within the strap. A bridging methanol molecule is seen as noted above.[65] The Cs^+ cation was found bound to the bowl-shaped calix[4]pyrrole cavity ("cup") via multiple presumed cation–π interactions. The cation also interacts with the carbonyl oxygen atom on another receptor, as well as a methanol molecule. The net result is that a two-dimensional coordination polymer is present in the solid state (Fig. 8b).

In contrast to what was seen in the case of CsF, in the solid state both CsCl and CsBr were found to bind to **14** without a co-coordinated solvent (methanol). In the case of these latter salts, the cation interacts with the anion of an adjacent complex, thus forming a linear coordination polymer (Fig. 9). Receptor **14** was not found to bind CsI appreciably, if at all. On the basis of solution phase studies ($CH_3OH/CDCl_3$, 1:4, v/v), it was concluded that in **14**·CsF the fluoride anion interacts with the NH proton of the strap (Fig. 10). The binding affinity was also found to be much larger than that for **1**·CsF. This latter inference was based on the fact that saturation is achieved when **14** is treated with 1.0 equiv. of CsF, whereas 15.0 equiv. of CsF proved necessary to achieve a comparable level of saturation in the case of **1**. Presumably as the result of the enhanced anion affinity seen in the case of **14**, this particular receptor proved capable of extracting CsF successfully from the solid state into a chloroform receiving phase.

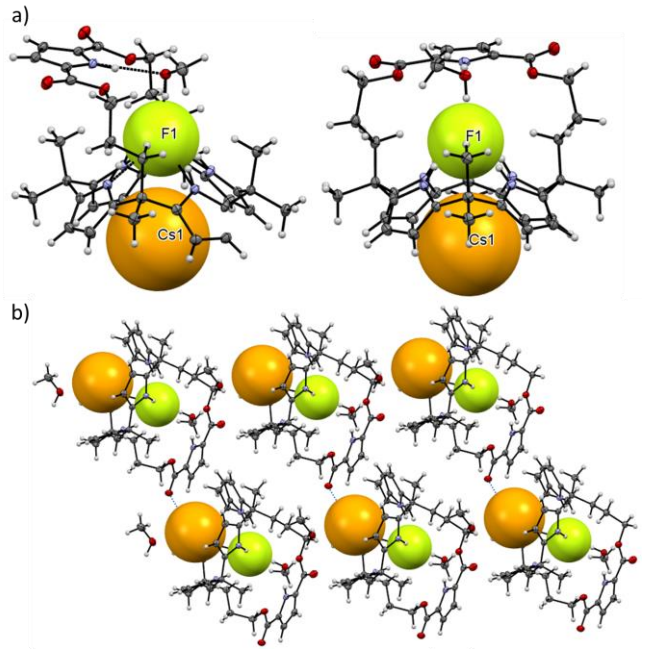

Fig. 8 (a) Two different views of the single crystal X-ray diffraction structure of **14**·CsF·CH_3OH and (b) Two-dimensional coordination polymer network seen in the crystal lattice of **14**·CsF·CH_3OH. This figure was generated using data downloaded from the Cambridge Crystallographic Data Centre (CSD Nos. 1851192).

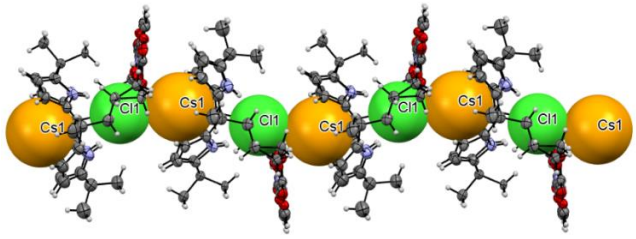

Fig. 9 Partial view of the extended structure seen in the crystal lattice of **14**·CsCl. This figure was generated using data downloaded from the Cambridge Crystallographic Data Centre (CSD Nos. 1851190).

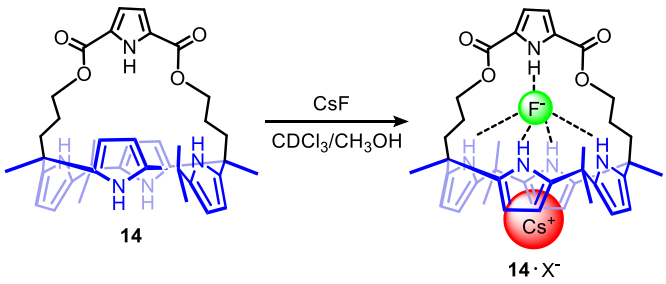

Fig. 10 Binding mode for complex **14**·CsF thought to pertain in $CH_3OH/CDCl_3$ (1:4, v/v) solution.

Lee and co-workers reported a benzene-strapped

calix[4]pyrrole **16** and showed that it functioned as a cyanide-selective chemosensor. This system was prepared by introducing a 1,3-indanedione group onto a *β*-pyrrolic position of the calix[4]pyrrole backbone (Fig. 11).[55] The starting strapped system **4** was first subjected to Vilsmeier-Haack formylation, followed by Knoevenagel condensation with 1,3-indanedione, thus affording targeted compound **16** as a major product. In $CD_3CN/DMSO$-d_6 (10:3, v/v) solution, receptor **16** was found to interact with the cyanide anion both via binding within the cavity and through nucleophilic addition to the indanedione vinyl group (Fig. 11). The latter reaction produces a bleaching of the initial yellow colour of $CH_3CN/DMSO$(100:3, v/v) solutions of **16**. This bleaching was only observed for the cyanide anion, even in the presence of other anions, a finding ascribed to the fact that the indandione-derived vinyl group reacts with the cyanide anion with near 100% selectivity.

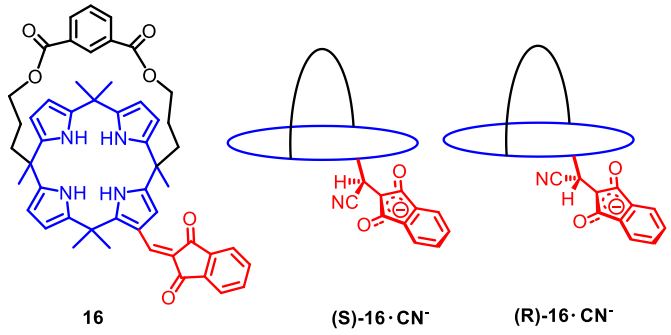

Fig. 11 Molecular structure of **16** and its cyanide adducts.

The cryptand-like calix[4]pyrrole **17** (Fig. 12), featuring two pyrroles and one phenyl group on the strap, was also prepared and studied as an anion receptor by Lee and co-workers.[69] This system was found to bind the fluoride and chloride ions with exceptionally high affinities relative to the unstrapped parent calixpyrrole **1** and the benzene-strapped congeners discussed above, as evidenced by ITC analyses carried out in DMSO. An unusual upfield shift in the pyrrolic NH proton signals for the strap was observed in the ^{1}H NMR spectrum upon titration with a fluoride anion source (i.e., the corresponding tetrabutylammonium salt, TBAF) in DMSO-d_6. It was suggested that the main interaction between the bound anion and the ancillary pyrrolic subunit involved an anion–π interaction, rather than hydrogen bonding per se.

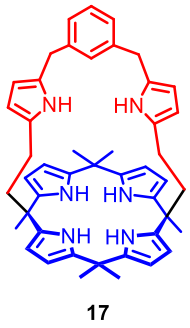

Fig. 12 Molecular structure of the cryptand-like calix[4]pyrrole **17**.

In 2015, Panda and co-workers reported a calix[4]pyrrole-based anion receptor **18** containing a catechol-derived diether strap (Fig. 13).[70] The cavity defined by this specific strap is relatively constrained such that only the *cis*-like configuration of the receptor was obtained during the condensation reaction leading to **18**. Receptor **18** displayed a strong preference for the F^- anion. It also exhibited a higher affinity towards the Cl^- anion than towards Br^- in acetonitrile, thus showing high selectivity relative to the resorcinol strapped calix[4]pyrrole **6**. Encapsulation of two methanol molecules was also observed in the solid state structure of receptor **18**.

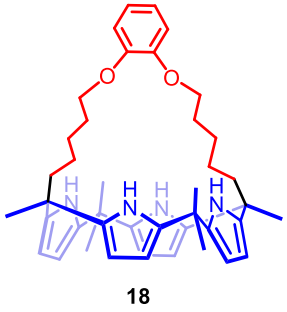

Fig. 13 Molecular structure of the catechol derived strapped calix[4]pyrrole **18**.

The same group also synthesized two strapped calix[4]pyrroles containing diether straps and a naphthalene moiety introduced as a fluorescent reporter unit (Fig. 14).[71] In the case of the first of these, **19**, the binding constant corresponding to the formation of a chloride anion complex proved to be one order of magnitude higher than the corresponding value for the fluoride anion in acetonitrile. This unusual selectivity was attributed to the better size match between the chloride anion and the cavity defined by the strap, as deduced from DFT calculations. In addition, the binding affinities for these two anions obtained via ITC analyses and fluorescence spectroscopic studies in acetonitrile, proved similar to one another. However, in the case of the second system, **20**, the differences between the K_a values obtained by these two methods were substantial, especially for relatively large anions, *e.g.*, $H_2PO_4^-$, CN^-. It was proposed that a tilting away of the fluorophore forced by the large ions negated the anion–fluorophore interaction and led to a lack of emission quenching.

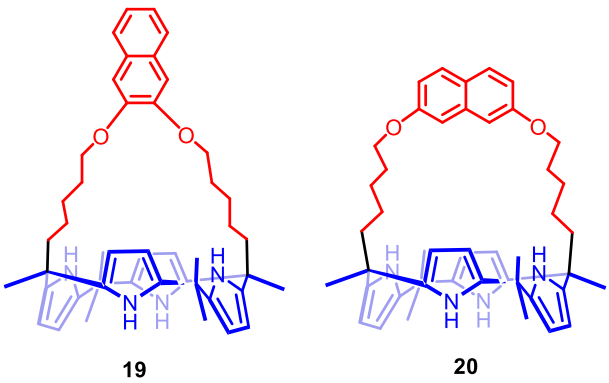

Fig. 14 Structure of the naphthalene-strapped fluorescent calix[4]pyrrole isomers **19** and **20**.

Following the above study, the same group synthesized four calix[4]pyrroles bearing very short catechol-derived diether straps (**21**–**24**, Fig. 15).[72] As revealed by single crystal X-ray diffraction analyses of **21**, **22**, and **23**, in the solid state all three calix[4]pyrrole units exist in the 1,3-*alternate* conformation. Moreover, the straps were found to be almost orthogonal to the mean plane of the macrocycles. This set of receptors exhibited high selectivity toward the fluoride ion, as deduced from ^{1}H NMR and fluorescence emission spectroscopic studies, as well as ITC analyses. The F^- binding affinity of **21** and **22** could be further enhanced by introducing electron withdrawing groups onto the benzene moiety as seen in the case of **23** and **24**. The binding mode for the host/F^- complex as inferred from DFT calculations was considered unique. Specifically, it was suggested that the calix[4]pyrrole macrocycles adopt a 1,3–*alternate* conformation forcing the fluoride ion to bind to the distal to the strap (Fig. 16). Support for this conclusion came from the minimal shift seen for the NH proton in the ^{1}H NMR spectrum in CD_3CN upon exposure to a F^- source and the correspondingly weak binding affinities determined via ITC analyses in acetonitrile.

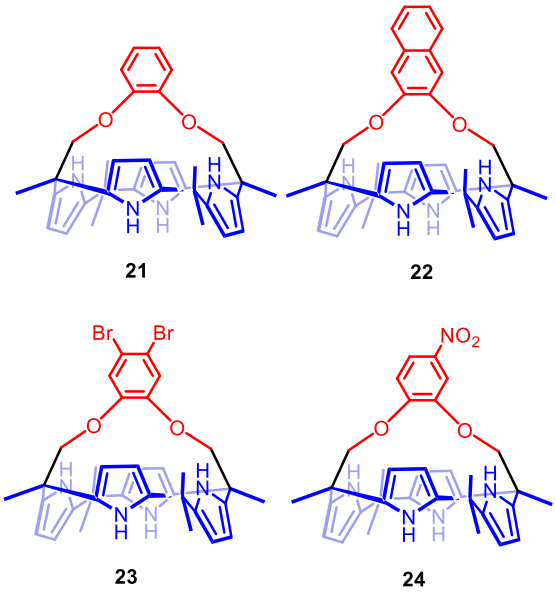

Fig. 15 Catechol-derived diether-strapped calix[4]pyrroles containing exceptionally short straps.

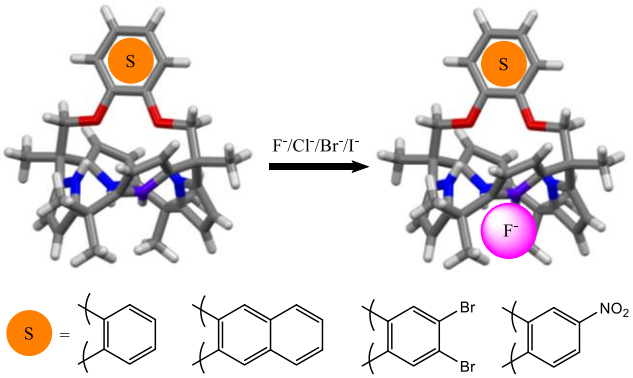

Fig. 16 Proposed binding modes for the F^- complexes of calix[4]pyrroles **21**–**24**.

It is regarded as a particular challenge to recognize and extract the sulfate (SO_4^{2-}) anion selectively from aqueous source phases because of its high hydration energy (–1080 kJ mol^{-1}).[73] In an effort to address this challenge, Sessler and co-workers prepared two cage-like calix[4]pyrroles, **25** and **26** (Fig. 17).[74] These systems, first reported in 2014, displayed improved affinities for the sulfate anion (as its TBA^+ salt) in CD_2Cl_2 compared to the parent calix[4]pyrrole. A 1:1 complex of **25**·$(TMA)_2SO_4$ was formed in the solid state as confirmed by a single crystal structural analysis (Fig. 18). The bound sulfate anion was found to interact with all six of the pyrrolic NH protons via hydrogen bonds. One oxygen atom from the SO_4^{2-} anion was bound to the calixpyrrole, whereas another one was seen to interact with the bipyrrole unit on the strap. Both of the TMA^+ counter cations were bound to the host via presumed CH–π interactions (Fig. 18). Presumably as the result of the strong binding produced by these receptor-anion interactions, calix[4]pyrroles **25** and **26** were found to solubilize $(TMA)_2SO_4$ into chloroform under conditions of solid-liquid extraction. Furthermore, the strapped systems **25** and **26** allowed the sulfate anion to be extracted effectively from an aqueous source phase into chloroform when used in conjunction with A336Cl (A336$^+$ = methyltrialkyl(C8-10)-ammonium cation) (Fig. 19). The extraction efficiency was enhanced by >10-fold compared to what was achieved with the parent calix[4]pyrrole **1**.

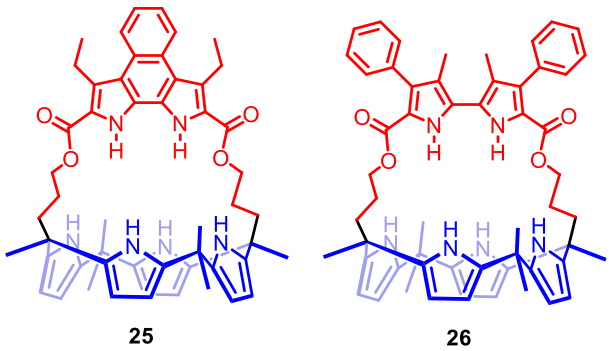

Fig. 17 Molecular structures of the bipyrrole-strapped calix[4]pyrroles **25** and **26**.

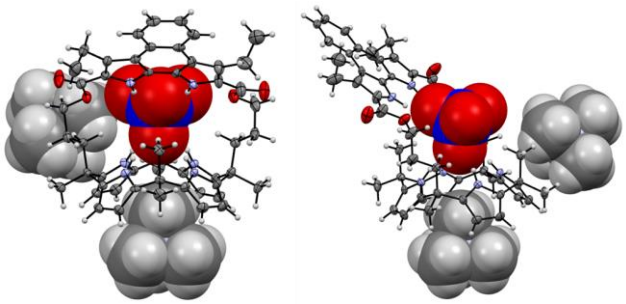

Fig. 18 Two views of the single crystal structure of **25**·$(TMA)_2SO_4$. Solvent molecules are omitted for clarity. These figures were generated using data downloaded from the Cambridge Crystallographic Data Centre (CSD Nos. 1017884).

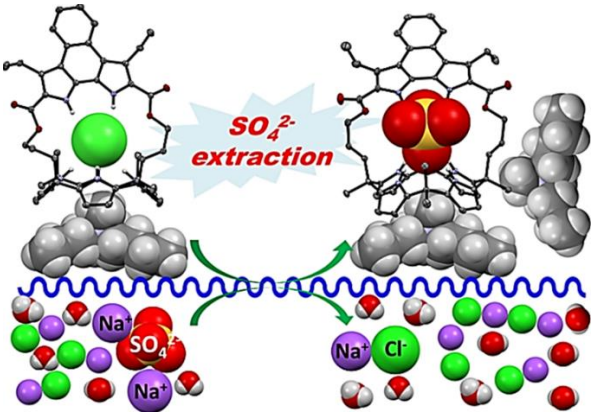

Fig. 19 Illustration of the liquid-liquid extraction of SO_4^{2-} with **25** as the extractant and A336Cl as the co-extractant. Reproduced from ref. 74 with permission. Copyright American Chemical Society, 2014.

The potential hazard and ubiquity of the azide anion provides an incentive to develop receptors that allow for its recognition with high affinity and selectivity.[75-77] However, the linear configuration and symmetrically distributed negative charge of the N_3^- anion imposes considerable geometric constraints in terms of receptor design.[78] In 2018, the Kim and Sessler groups reported that pyrrole- and naphthobipyrrole-strapped calix[4]pyrroles **14** and **25** could be utilized as neutral, nonionizable receptors for the linear azide anion.[79] Roughly two orders of magnitude higher affinities for the azide anion were observed in the case of **14** and **25** relative to the unfunctionalized macrocycle **1** in acetonitrile. Presumably, this reflects the presence of pyrrole and naphthobipyrrole subunits within the straps that serve as auxiliary hydrogen bonding donors. As revealed by both single crystal X-ray diffraction structural studies and DFT calculations, receptor **14** could capture CsN_3 via two different binding modes, namely, vertical and horizontal. These different geometries result in disparate N–N bond lengths within the bound azide anion (Fig. 20). In contrast, only a vertical azide anion binding mode was observed in the case of **25**·CsN_3 (Fig. 21). In both complexes (**14**·CsN_3 and **25**·CsN_3) the Cs^+ cation was found bound to the calix[4]pyrrole bowl via presumed cation–π interactions in the solid state.

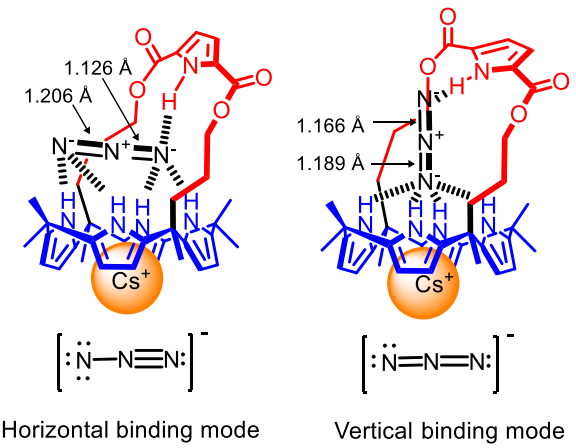

Fig. 20 Two binding modes for complex **14**·CsN_3 and the azide anion resonance forms invoked to explain the observed metric parameters.

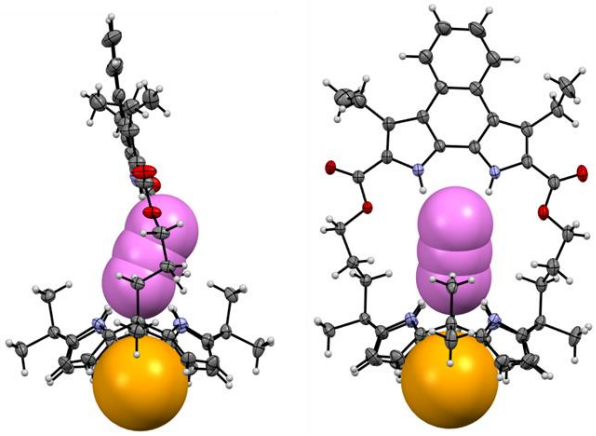

Fig. 21 Two different views of the single crystal X-ray diffraction structure of **25**·CsN_3. These images were generated using data downloaded from the Cambridge Crystallographic Data Centre (CSD Nos. 1586344).

Introducing chromogenic reporter groups generally endows receptors with the ability to act as chemosensors. Ideally, these sensors permit the convenient detection of analytes via direct naked-eye or spectroscopic means.[80-84] With such considerations in mind, Sessler and co-workers reported a simple strapped calix[4]pyrrole **27** (Fig. 22a) featuring a coumarin unit that served as a potential fluorophore.[85] The fluorescence intensity of the receptor was found to be controlled by the dual "input parameters" of cations and anions. When cations (e.g., Na^+, Li^+, or Mg^{2+}) were added to acetonitrile solutions of **27**, the fluorescence intensity was enhanced. The emission could then be quenched via the subsequent addition of tetrabutylammonium chloride (TBACl) (Fig. 22b). These findings were interpreted in terms of a quenching and reactivation of a photoinduced electron transfer (PET) process as illustrated in Fig. 23. The association constants corresponding to the interaction of **27** with three representative anions (Cl^-, Br^- and AcO^-; TBA^+ salts) were determined via fluorescence titrations and ITC analyses; a good concordance was seen (Table 2).

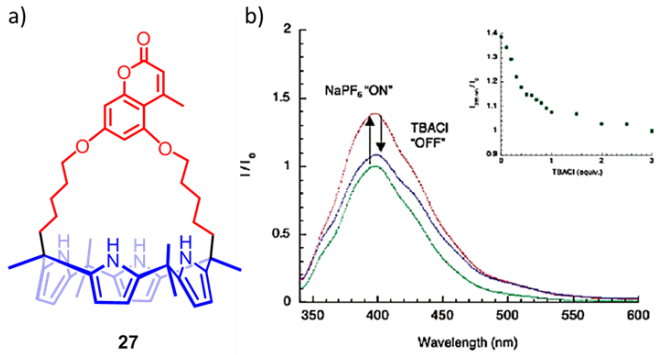

Fig. 22 (a) Structure of **27** and (b) the change in its fluorescence intensity before and after addition of excess $NaPF_6$, as well as the further addition of 1 equiv. of TBACl. Reproduced from ref. 85 with permission. Copyright American Chemical Society, 2005.

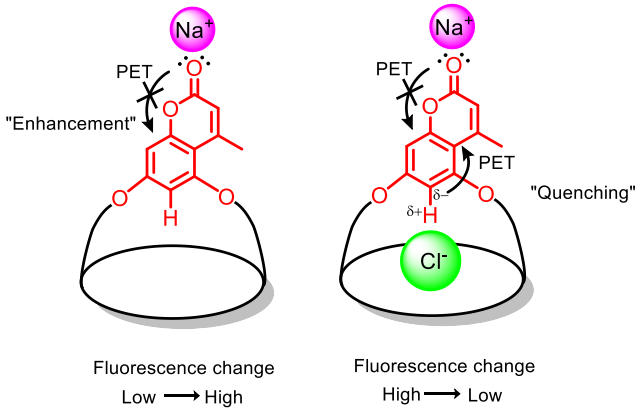

Fig. 23 Schematic representation of the interactions of **27** with NaCl. The cation (Na^+) is thought to bind weakly to the oxygen lone pairs and lead to an enhancement in the fluorescence intensity. The binding of the anion (Cl^-) activates a different PET mode and quenches the fluorescence signal.

Table 2 Association Constants (K_a) Corresponding to the Interaction of **27** with Anions in 3% H_2O/CH_3CN, $NaPF_6/CH_3CN$, and CH_3CN at 298 K

	K_a (M^{-1})		
Anion source	3% H_2O/CH_3CN[a]	$NaPF_6/CH_3CN$[a]	CH_3CN[b]
TBACl	1.9×10^6	2.3×10^6	3.6×10^6
TBABr	3.7×10^4	1.0×10^5	1.1×10^5
$TBACH_3CO_2$	8.9×10^5	1.3×10^6	1.9×10^6

[a] Determined by fluorescence emission spectroscopy. [b] Determined by ITC; average of three determinations at two concentrations.

An acridine moiety, designed to serve as a fluorogenic reporter, was also used to produce a strapped calix[4]pyrrole (Fig. 24).[86] Although the resulting host (**28**) displayed a high affinity for chloride anions in dry acetonitrile, little change in the spectral intensity was produced. This was rationalized by the authors in terms of either 1) an overly weak interaction between the attached acridine moiety and portions of the receptor involved in binding or 2) energy quenching caused by π–π interactions among multiple molecules.

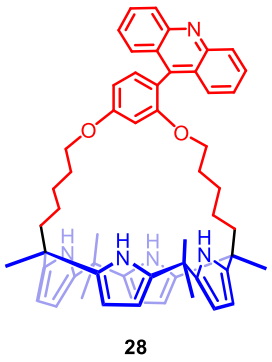

Fig. 24 Molecular structure of the strapped-calix[4]pyrrole **28** bearing an acridine moiety.

A calix[4]pyrrole-based compound (**29**) containing a dipyrrolylquinoxaline as a part of the strap was synthesized by Lee and co-workers (Fig. 25).[87] In this case, the dipyrrolylquinoxaline subunit was designed to act as a chromophore and enable the receptor to provide a colorimetric response upon anion binding. Compound **29** exhibited a high selectivity for the fluoride ion over other halide anions in organic media. Of note is that the two pyrrole rings on the strap adopt a conformation that is almost perpendicularly to the quinoxaline ring upon fluoride anion binding (Fig. 25). Evidence for this binding mode came from an ^1H NMR spectral analysis of the host-guest complex in $CD_3CN/DMSO–d_6$ (9:1 v/v) solution.

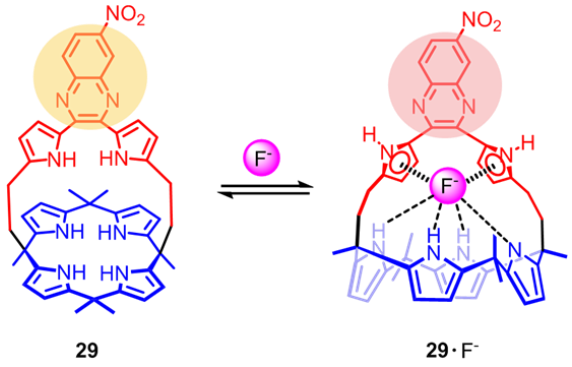

Fig. 25 Molecular structure of dipyrrolylquinoxaline-strapped calix[4]pyrrole **29** and the proposed binding mode present in complex **29**·F^-.

In 2013, the Lee group also reported two systems wherein a pyrene moiety, designed to serve as a fluorescence probe, was linked to the pyrrole-strapped calix[4]pyrrole. These two systems differ in that the calix[4]pyrrole anion recognition site and the pyrene probe site were connected directly or via a triple bond to give **30** and **31**, respectively (Fig. 26).[88] Anion-dependent fluorescence quenching was seen for both receptors upon titration with a fluoride ion source in 5% acetonitrile/toluene. Although different linkages between the strap pyrrole group and the pyrene unit are present in **30** and **31**, similar anion-dependent fluorescence quenching was seen for both receptors.

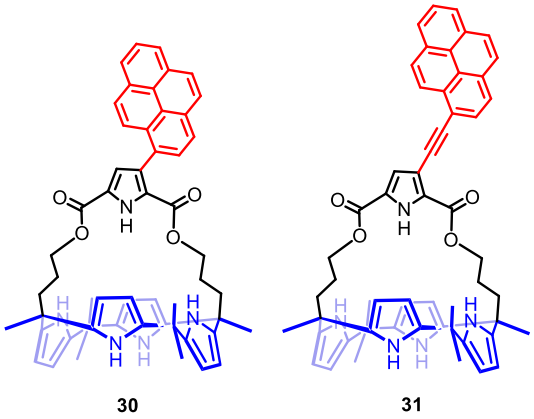

Fig. 26 Molecular structure of the pyrene-bearing strapped calix[4]pyrroles **30** and **31**.

Recently, a similar strategy employing pyrene as the fluorophore was used to prepare the strapped fluorogenic calix[4]pyrrole **32** (Fig. 27a).[89] In this system, the basic tertiary amine is expected to act not only as a fluorescence quencher of the pyrene via PET but also an additional hydrogen bond acceptor for anions, such as hydrogen sulfate, that contain an OH group that can act as an hydrogen bond donor. As confirmed by ^{1}H NMR spectroscopic and ITC analyses, receptor **32** proved capable of binding F^-, Cl^-, $HP_2O_7^{3-}$ and HSO_4^- (as their TBA^+ salts) in chloroform and acetonitrile. Selectivity for F^- was seen, a finding ascribed to the relative rigidity and small size of the strap. The changes in the fluorescence intensity of receptor **32** proved distinctly different when titrated with different anions (Fig. 27b). The addition of F^- and $HP_2O_7^{3-}$ quenched the fluorescence while treatment with HSO_4^- served to enhance the emission intensity. These disparate observations were rationalized in terms of F^- binding leading to facilitated PET from the nitrogen atom lone pair to the pyrene. In contrast, protonation of the strap nitrogen atom served to inhibit this PET process (Fig. 28). Thus, receptor **32** was able to act as a "turn off" or "turn on" sensor for anions depending on the nature of the guest ions.

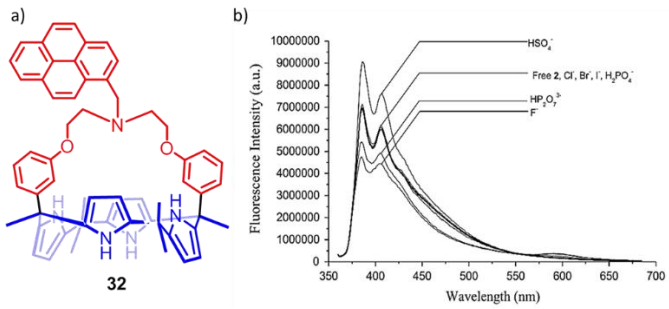

Fig. 27 (a) Structure of strapped calix[4]pyrrole **32** and (b) fluorescence spectra of **30** upon addition of different anions (TBA^+ salts) in 10% DMSO in acetonitrile. Reproduced from ref. 89 with permission. Copyright Taylor and Francis Ltd., 2017.

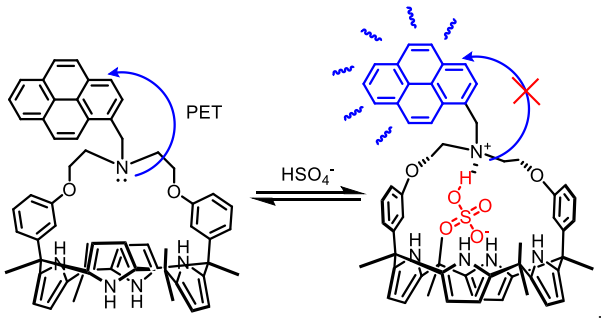

Fig. 28 Proposed interactions between receptor **32** and the hydrogen sulfate anion and the effect of anion binding on a key internal PET process regulating the fluorescence emission intensity.

Receptor mediated cross-membrane transport of anions has attracted considerable attention of late. This interest reflects an appreciation that studies of synthetic anion transporters may help elucidate the mechanisms underlying anion transport disorders and could provide a potential means for treatment.[90-92] With the above considerations in mind, Gale and co-workers synthesized the 1,2,3-triazole-strapped calix[4]pyrrole **33** (Fig. 29a) via click chemistry.[54] The triazole motif was designed to provide an extra C–H···Cl^- hydrogen bond upon the addition of chloride ion (as its TBA^+ salt). Support for this postulate came from ^{1}H NMR spectral studies carried out in acetonitrile–d_3. On the basis of supporting ITC analyses in acetonitrile involving the analogous TEA^+ (tetraethylammonium) salt, it was concluded that the binding affinity corresponding to the interaction between **33** and the chloride ion was improved by approximately one order of magnitude relative to the comparative value for the simple macrocycle **1**. When incorporated into unilamellar 1-palmitoyl-2-oleoylphophatidylcholine (POPC) based vesicles, receptor **33** was found to promote the transport of Cl^- across the POPC bilayer membrane. This chloride anion transport was seen in the presence of Cs^+, as well as in the presence of Na^+, K^+, and Rb^+ (Fig. 29b).

A key predicate underlying these studies was the supposition that the sulfate anion is highly hydrophilic and thus not likely to be transported efficiently across the lipid layer. In fact, when the salt in the buffer solution was changed from $NaNO_3$ to Na_2SO_4, the chloride release rate remained largely unchanged in the case of the CsCl-containing vesicles. In contrast, the corresponding release rates were considerably lower in the case of the vesicles containing NaCl, KCl, and RbCl. Based on these results, it was proposed by the authors that two mechanisms were involved in the observed chloride release, namely ion pair co-transport (in the case of CsCl) and chloride–nitrate antiport (in the case of NaCl, KCl, and RbCl).

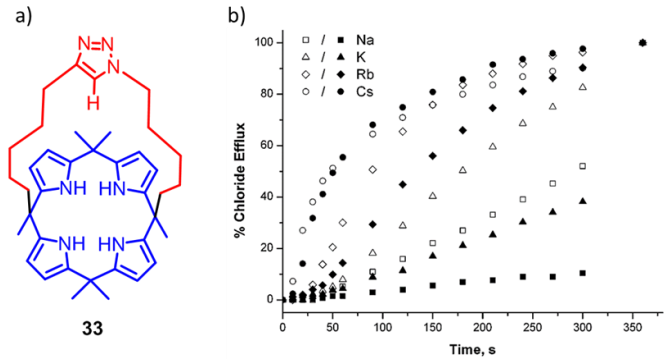

Fig. 29 (a) Structure of the triazole-strapped calix[4]pyrrole **33** and (b)chloride flux across POPC vesicles incorporating **33** and containing different chloride ion salts. Open and closed symbols denote buffer solution contains $NaNO_3$ and Na_2SO_4, respectively. Reproduced from ref. 54 with permission. Copyright The Royal Society of Chemistry , 2009.

In order to investigate in greater detail the role of the strap in terms of regulating the anion transport efficiency and mechanism of calix[4]pyrroles as transporters, the Gale group synthesized three bis-1,2,3-triazole strapped calix[4]pyrroles, namely **34**–**36** (Fig. 30).[56] Single crystal X-ray diffraction analyses of the chloride complexes in the solid state revealed differences among the binding modes in the case of these receptors. In the case of **35**·Cl^- (Fig. 31a), only one of the triazoles interacts with the bound Cl^- (as do the four pyrrolic NHs). However, the chloride ion was bound by all six hydrogen bond donors in the case of receptor **36** (Fig. 31b). ^1H NMR spectra obtained in CD_2Cl_2 provided support for the notion that the bis-triazole-strapped calix[4]pyrroles provide relatively enhanced anion affinities compared to simpler systems. The length of the alkyl chain linking the bis-triazole group was found to have a large effect on the chloride anion transport efficiency as inferred from transmembrane transport studies involving CsCl. As the length increased, the transport efficiency improved. At the same time, the transport mechanism changed from one involving predominant co-transport in the case of compound **34** to chloride/nitrate antiport in the case of compound **36**.

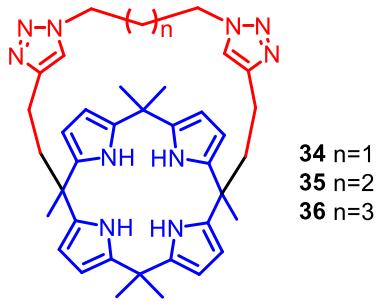

Fig. 30 Molecular structures of bis-1,2,3-triazole strapped calix[4]pyrroles **34–36**.

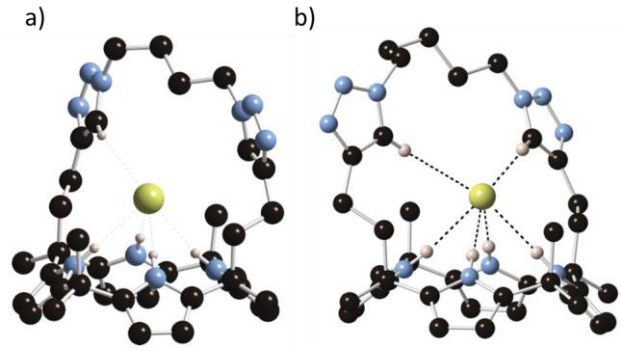

Fig. 31 Binding modes seen for (a) **35**·Cl^- and (b) **36**·Cl^-. Reproduced from ref. 56 with permission. Copyright The Royal Society of Chemistry, 2010.

Employing **33** and **36** as the anion receptors, Gale and co-workers developed what was expected to be a dual host approach to salt transport.[93] Systems **33** and **36** were utilized as the anionophores, while valinomycin was used as the cationophore. Upon the concurrent addition of the anionophore and cationophore, chloride transport through a vesicle-type lipid bilayer membrane was enhanced compared to what was seen using only the anionophore or only the cationophore, as well as the sum of these two individual processes (Fig. 32a). These observations were interpreted in terms of a synergistic co-transport effect as illustrated in Fig. 32b.

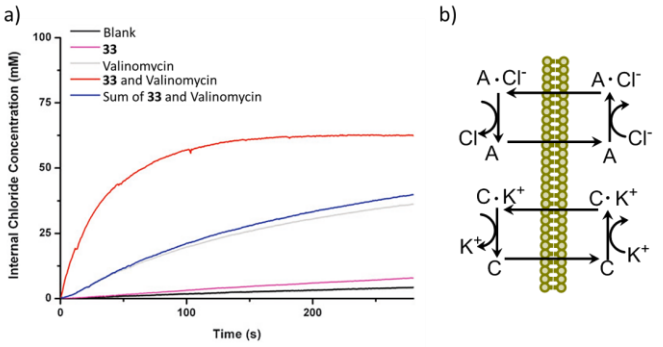

Fig. 32 (a) Change in internal chloride concentration of unilamellar POPC vesicles seen upon addition of **33**, valinomycin and both **33** and valinomycin and (b) a dual host approach to the co–transport of KCl by a cationophore and anionophore (designated as C and A, respectively). Reproduced from ref. 93 with permission. Copyright The Royal Society of Chemistry, 2011.

Thereafter, the same research group proposed a dual host approach to achieve effective Cl^-/HCO_3^- antiport across POPC lipid bilayers. In this instance, the triazole-strapped calix[4]pyrroles **33** and **36** were employed as the chloride transporters, while the thiourea derivative **37** (Fig. 33a) was used as the bicarbonate transporter.[94] The combination of these two kinds of receptors was found to enhance the Cl^-/HCO_3^- antiport rate relative to the sum of the transport rates achieved using the individual receptors.

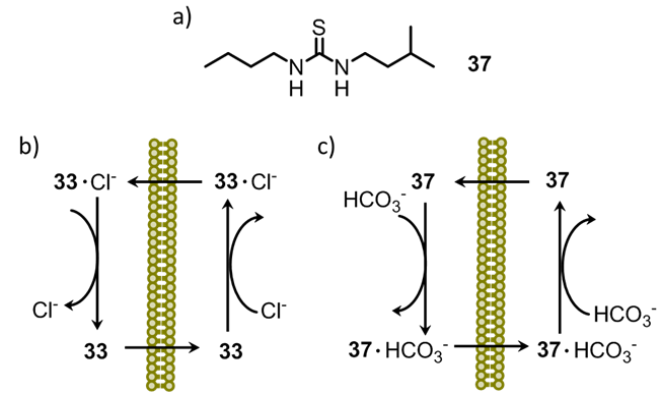

Fig. 33 (a) Molecular structure of the optimized bicarbonate transporter **37**, (b) chloride uniport by compound **33** and c) bicarbonate uniport by compound **37**.

In recent years, naturally occurring F^- anion channels have been found in bacterial cells. These channels display high selectivity for F^- over Cl^- and are thought to help reduce bacterial fluoride toxicity.[95, 96] Inspired by this discovery, Gale and co-workers studied fluoride anion transport across lipid bilayers mediated by the strapped calix[4]pyrroles **34**–**36**.[91] Valinomycin (Vln), capable of facilitating K^+ uniport, and monensin (Mon), capable of facilitating K^+/H^+ antiport, were employed as electrogenic and electroneutral cationophores, respectively. The results obtained were interpreted in terms of compounds **34**–**36** serving to facilitate F^- and Cl^- transport through coupling to K^+ co-transport as illustrated in Fig. 34. Receptors **34** and **35**, bearing shorter straps, exhibited a preference for fluoride ion transport as compared to receptor **36** with a relatively large cavity. The Cl^- vs H^+/OH^- transport selectivity was studied by means of an HPTS (a pH-sensitive dye) transport assay. On this basis it was concluded that **34**–**36** operate predominantly via a Cl^- transport mechanism, as opposed to an alternative H^+/OH^- mechanism. No loss in Cl^- > H^+/OH^- selectivity was observed when the transport ability of **34** was studied in the presence of natural fatty acids. In contrast, a large selectivity loss was observed in the case of **36**. This latter finding was ascribed to **36** being bound to the fatty acid headgroup and to a subsequent flip-flop of the anionic form of the fatty acid, which serves to enhance proton shuttling (Fig. 35).

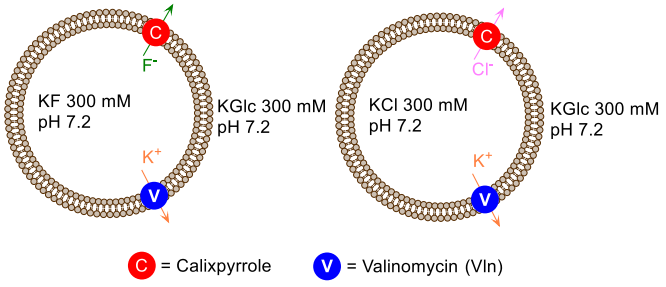

Fig. 34 Illustration of Vln-coupled fluoride and chloride efflux mediated via an electrogenic process.

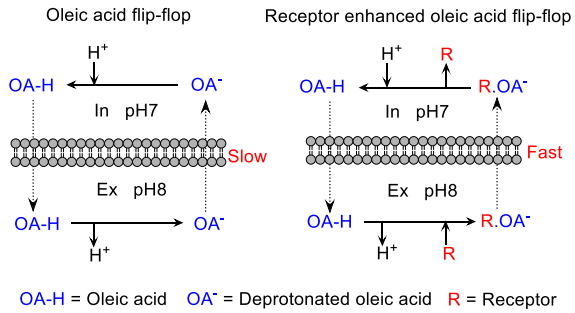

Fig. 35 Schematic designed to show the flip-flop of oleic acid and a related receptor enhanced oleic acid flip-flop process.

In 2014, two pyridine diamide-strapped calix[4]pyrroles (compounds **38** and **39**, Fig. 36) were prepared by Gale, Sessler, Shin, *et al.*[97] These systems were tested for their anion recognition capabilities and as through-membrane transporters. It was found that the NH peaks of both the pyrrole and amide protons in the ^1H NMR spectrum underwent significant downfield shifts upon the addition of NaCl, KCl, and CsCl to **38** in 10% D_2O/DMSO–d_6. This was taken as an indication that both sets of protons interact with the chloride ion via hydrogen bonding interactions. On the basis of a single crystal X-ray diffraction analysis it was concluded that the sodium counter-cation is bound to exterior of these receptors involving the carbonyl oxygen atoms of the amide groups (Fig. 37).

Ion transport tests involving liposomal phospholipid model bilayers revealed that both **38** and **39** are capable of transporting chloride anion with a moderate efficiency via a chloride/nitrate antiport mechanism in the presence of hydrophobic extravesicular nitrate ions. Greatly enhanced chloride flux rates were seen when monensin was added as a sodium ionophore. Presumably, this enhancement reflects a coupled process involving Na^+/Cl^- co-transport.

These two synthetic receptors were incubated with several cancer and normal cell lines in an effort to explore their chloride anion transport properties under *in vitro* conditions. On the basis of a number of control studies, involving the use of different cellular conditions and channel inhibitors, it was concluded that receptors **38** and **39** function predominantly as chloride anion transporters. The resulting chloride anion influx was thought to account for the caspase-dependent cell apoptosis induced by these two agents.[58, 98] In contrast, compound **40**, a control system that lacks the diamide groups present in **38** and **39**, proved ineffective as a transporter and had little effect on cell proliferation. On the basis of these studies, it was concluded that under conditions of cellular incubation, sodium counter cations enter the cells mainly through cellular sodium channels, while chloride anion transport is mediated by **38** and **39**.

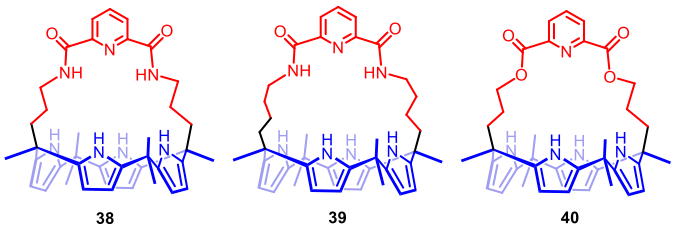

Fig. 36 Molecular structures of diamide-strapped calix[4]pyrroles **38** and **39**, as well as the diester control system **40**.

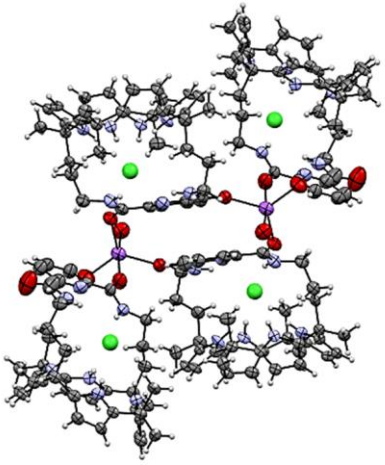

Fig. 37 Partial view of **38**·NaCl; solvent molecules and two non-attributable tetramethylammonium (TMA^+) cations are omitted for clarity. This figure was generated using data downloaded from the Cambridge Crystallographic Data Centre (CSD Nos. 990430).

It is widely appreciated that autophagy levels are generally higher in cancer cells than in normal cells[99] and that tumour cells are typically resistant to apoptosis.[100] Autophagy-disrupting agents and effective apoptosis inducers are thus attractive as a potential approach to treating cancer.[101, 102] In 2017, Gale, Sessler, Shin, *et al.* reported that synthetic ion transporters can both disrupt autophagy and induce apoptosis. They arrived at this conclusion by exploring a series of squaramide-based receptors as potential ion transporters.[103] In 2019, the same research team reported a detailed mechanistic study of how synthetic ion transporters affect apoptosis and autophagy in cancer cells. In this case compounds **38**, **8**, and **41** (Fig. 38) were used as the synthetic transporters, while the parent macrocycle **1**, which displayed no transport activity in cells, was studied as a control.[104] Ion transport tests involving lipid bilayer models led to the conclusion that component **38** transported Cl^- in an electrogenic fashion (chloride uniporter), while **41** acted in an electroneutral fashion (HCl co-transporter). It was also concluded that **8** functions in a nonspecific manner (i.e., mediating transport via both electrogenic and electroneutral processes).

A series of *in vitro* studies led to the suggestion that these transporters induced cancer cell death via the mechanisms depicted in Fig. 39. Briefly, all the synthetic ion transporters (except **1**) were found to increase the intracellular concentrations of both the sodium and chloride ions. This increase produces osmotic stress within the cells and induces a series of processes leading to generation of reactive oxygen species (ROS) and caspase-dependent apoptosis. Moreover, receptors **8** and **41,** but not **38**, were also found to induce cancer cell death via inhibition of autophagy. These two electroneutral transporters were found capable of exporting chloride ions from the lysosome and increasing the lysosomal pH. This has the effect of perturbing lysosome functions deemed vital for the autophagy process.

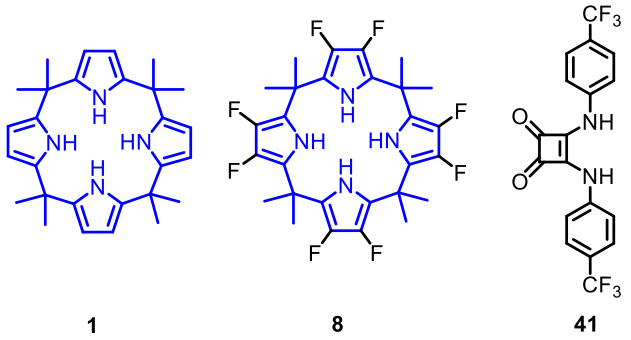

Fig. 38 Molecular structure of component **41** (structures of **1** and **8** are redrawn for convenience).

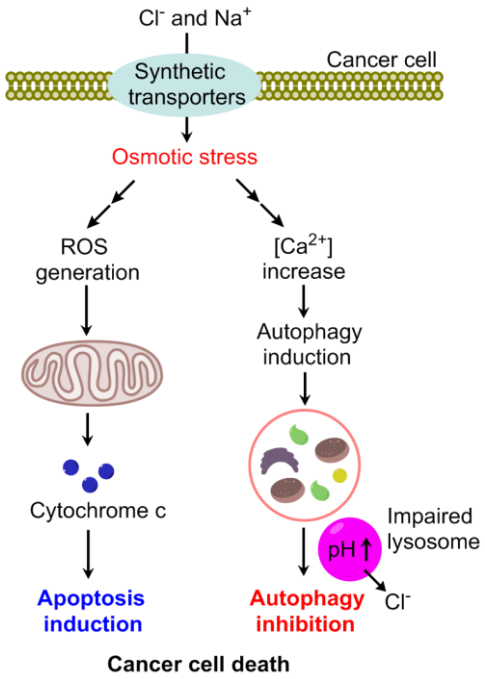

Fig. 39 Proposed mechanism of cancer cell death induced by the synthetic ion transporters **8**, **38**, and **41**.

Simple strapped calix[4]pyrroles can also function as "smart" molecular receptors in the case of appropriate structure design. Support for this general contention is provided by a set of strapped calix[4]pyrroles, *i.e.*, (*R*)-**42** and (*S*)-**42** bearing built-in chiral-recognition moieties, reported by Lee and co-workers.[105] In these systems, a binol group within the strap served as the asymmetry-defining element. Chiral carboxylate anions, specifically (*R*)-2-phenylbutyrate ((*R*)-PB) and (*S*)-2-phenylbutyrate ((*S*)-PB) (as their TBA^+ salts), were employed as

the anionic guests. (*S*)-**42** was found to complex (*S*)-PB with higher affinity than (*R*)-PB, as inferred from ^{1}H NMR spectroscopic analyses carried out in deuterated chloroform. An analogous conclusion was drawn from ITC analyses carried out in anhydrous acetonitrile, from which the corresponding 1:1 binding affinities corresponding to the interactions of (*S*)-**42** with (*S*)-PB and (*R*)-PB were determined to be 1.0×10^5 M^{-1} and 9.8×10^3 M^{-1}, respectively. The authors speculated that π–π interactions between the phenyl group of (*S*)-PB and one of the naphthyl groups of (*S*)-**42** play a role in stabilizing the complex (*S*)-**42**·(*S*)-PB. Conversely, unfavourable steric interactions between the corresponding groups in (*S*)-**42**·(*R*)-PB serve to relatively destabilize the latter complex (Fig. 40). Support for these conclusions came from DFT calculations.

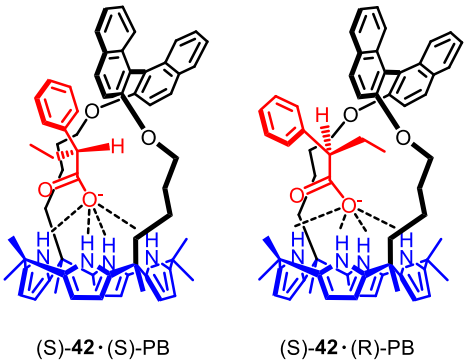

Fig. 40 Proposed binding modes of (S)-**42** with (S)-/(R)-PB.

3 Crown-ether-strapped calix[4]pyrroles

In this section, we review the synthesis and binding properties of crown-ether-strapped calix[4]pyrroles, including oligoether-strapped calix[4]pyrroles. These systems contain at least two disparate ion binding sites, allowing for the concurrent complexation of an anion and a cation.

In an effort to design an ion pair receptor capable of concurrent complexation with an anion and a cation a crown ether moiety was covalently linked in close proximity to the *meso*-carbon atoms of a calix[4]pyrrole backbone to give receptor **46**.[106] The synthesis of receptor **46**, reported by the Lee, Sessler, and Gale groups in 2012, is shown in Scheme 1. Briefly, the reaction of ditosylated pentaethylene glycol **44** with *meso*-(*p*-hydroxyphenyl-methyl)dipyrromethane **43** in the presence of K_2CO_3 in acetonitrile under reflux afforded the corresponding dipyrromethane **45** in 74% yield. Condensation of **45** with acetone in the presence of BF_3·OEt_2 at room temperature gave receptor **46** in 10% yield.

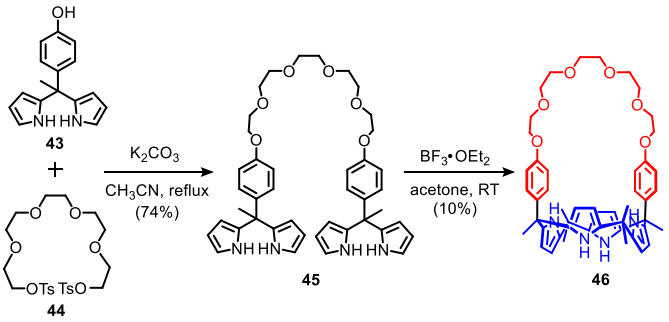

Scheme 1 Synthesis of receptor **46**.

A single crystal X-ray diffraction analysis of the complex of **46**·CsCl revealed that the chloride anions were hydrogen bonded to the four pyrrolic NH protons (Fig. 41). Two different complexation modes were seen for the caesium cations. One was captured within the cone-like calix[4]pyrrole "cup" while the other one was complexed by four oxygen atoms of the crown ether ring, as well as by two oxygen atoms from a different molecule. The separation distance between the oxygen-complexed Cs^+ cation and the Cl^- anion was 5.41 Å.

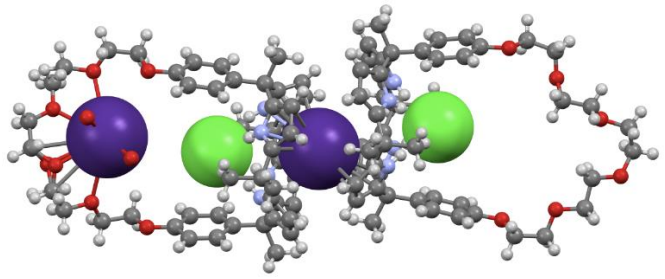

Fig. 41 Single crystal X-ray diffraction structure of the CsCl complex of receptor **46**. This figure was reproduced using data downloaded from the Cambridge Crystallographic Data Centre. These figures were generated using data downloaded from the Cambridge Crystallographic Data Centre (CSD Nos. 821894). The ion pairs are shown in space-filling form. Solvent molecules are omitted for clarity.

Varying binding behaviour was seen depending on both the choice of the added cation and the precomplexed anion. Receptor **46** was found capable of binding several alkali metal fluoride and chloride salts as inferred from ^{1}H NMR spectroscopic studies carried out in CD_3CN/CD_3OD (9:1 v/v). Addition of Li^+ or Na^+ cations (as their respective perchlorate salts) to the preformed complex **46**·F^- led to decomplexation of the fluoride anion (Fig. 42). In contrast, treatment of **46**·F^- with K^+ or Cs^+ (as the perchlorate salts) led to formation of the corresponding ion pair complexes. The potassium cation was found complexed within the crown ether ring of the host, while the caesium cation resided within the cone-shaped calix[4]pyrrole cavity. In contrast, when Na^+ or K^+ cations (as the perchlorate salts) were added to the chloride anion complex of receptor **46** (**46**·Cl^-), partial decomplexation of the bound chloride anion was observed (Fig. 43). In this case, the addition of Li^+ or Cs^+ cations (again as the perchlorate salts) led to the formation of the corresponding ion pair complexes. The lithium cation was bound to the crown ether moiety, while the caesium cation was complexed by the calix[4]pyrrole "cup".

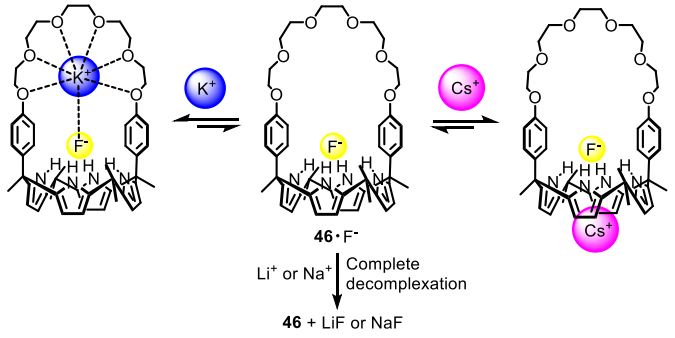

Fig. 42 Schematic representation of the varying complexation behaviour seen for the fluoride complex **46**·F^- (as the TBA^+ salt) upon exposure to various metal perchlorate salts in CD_3CN/CD_3OD (9:1 v/v).

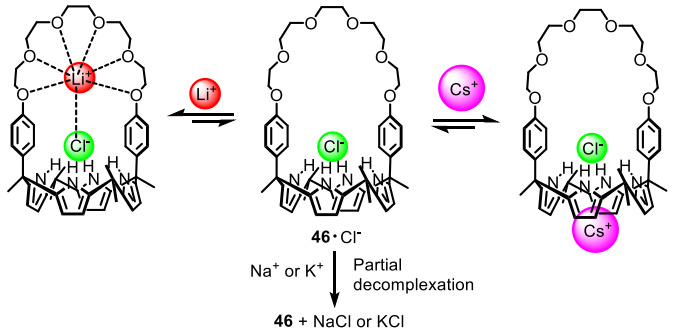

Fig. 43 Schematic view of the complexation and decomplexation events seen for the chloride complex **46**·Cl^- (TBA^+ salt) upon exposure to various alkali cations (as the respective perchlorate salts) in CD_3CN/CD_3OD (9:1 v/v).

Liposome model membrane transport studies using unilamellar POPC vesicles with external solutions of Na_2SO_4 and $NaNO_3$ revealed that receptor **46** is capable of transporting alkali metal chloride salts, including NaCl, KCl, RbCl, and CsCl (Fig. 44). Higher transport activities were observed in proportion to lipophilicity of cations ($Cs^+ > Rb^+ > K^+ > Na^+$). The inferred cotransport mechanism was supported by a U-tube bulk transport experiment wherein a dichloromethane solution of receptor **46** served as an intervening layer between aqueous source and receiving phases. On the basis of these transmembrane ion transport studies, it was concluded that receptor **46** could act as a co-transporter for KCl and CsCl, as well as an ion exchanger for Cl^-/NO_3^- (as its sodium salt).

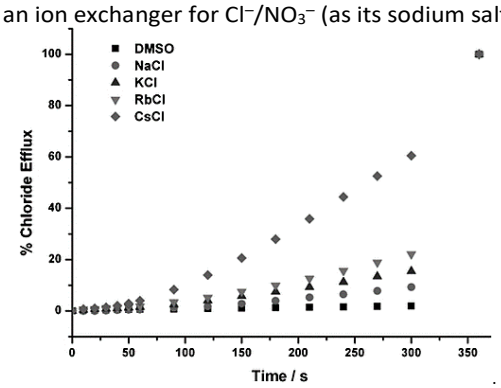

Fig. 44 Cl^- efflux promoted by receptor **46** (4 mol % with respect to lipid) from unilamellar POPC vesicles loaded with 489 mM MCl buffered to pH 7.2 with sodium phosphate salts (M = Na, K, Rb, or Cs). The vesicles were dispersed in 167 mM Na_2SO_4 buffered to pH 7.2 with 5 mM sodium phosphate salts. Each point represents the average of three trials. Reprinted with permission from ref. 106 Copyright 2012 Wiley-VCH Verlag GMbH & Co. KGaA.

Later, a benzocrown-ether-capped calix[4]pyrrole **51** was also reported by the same group.[107] Receptor **51** consists of a *m*-dibenzo-[26]crown-8 subunit and a parent calix[4]pyrrole motif, as well as phenyl spacers. Its synthesis is summarized in Scheme 2. Briefly, the reaction of ditosylated triethylene glycol **48** with 3,5-dihydroxy acetophenone **47** in the presence of K_2CO_3 in acetonitrile under reflux gave the macrocyclic bisketone **49** in 26% yield; subsequent condensation with pyrrole in the presence of trifluoroacetic acid at 60 °C gave the corresponding dipyrromethane **50** in 49% yield. Compound **50** was further condensed with acetone in the presence of $Bi(NO_3)_3$ at room temperature to afford receptor **51** in 5% yield.

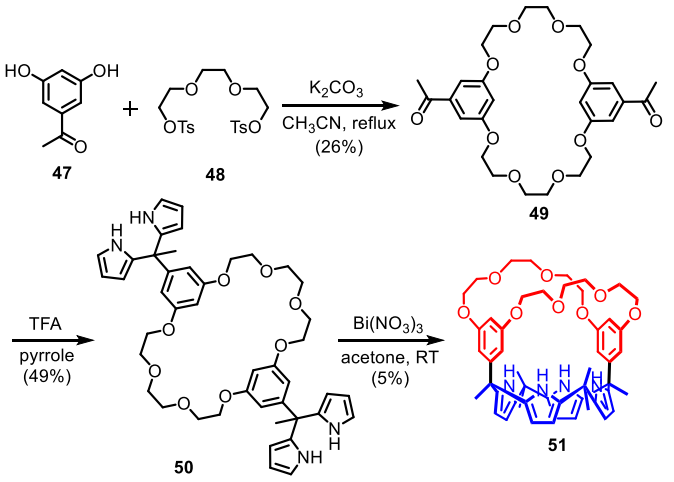

Scheme 2 Synthesis of receptor **51**.

A single crystal X-ray structural analysis revealed that receptor **51** formed stable ion pair complexes with CsF and LiCl in the solid state (Fig. 45). In complex **51**·CsF, the fluoride anion was found to be hydrogen-bonded to the pyrrolic NH protons. The Cs^+ cations was seen to be complexed within the cone-shaped calix[4]pyrrole "cup" and to interact with two oxygen atoms of a neighbouring crown ether ring. In the case of complex **51**·LiCl, the LiCl salt was found bound to the receptor in a 2:2 manner. While the chloride anion was bound by the calix[4]pyrrole NH protons, the two lithium cations were seen to interact with the oxygen atoms of the crown ether rings of two different receptor molecules. A water molecule was observed to bridge between the lithium cation and the chloride anion with a $Li^+\cdots Cl^-$ distance of 4.7 Å.

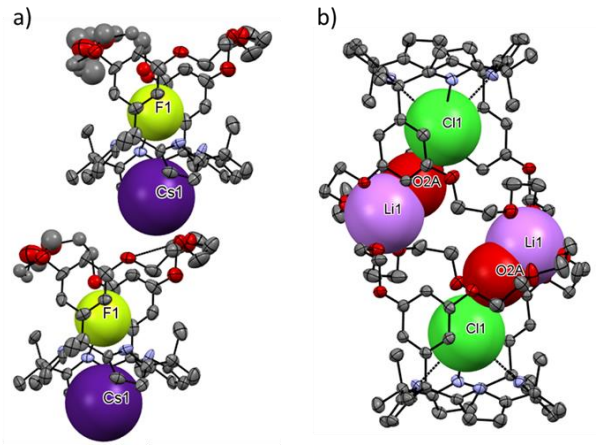

Fig. 45 Single crystal X-ray diffraction structures of (a) CsF complex and (b) LiCl complex of receptor **51**. This figure was generated using data downloaded from the Cambridge Crystallographic Data Centre (CSD Nos. 876360 and 875553). The ion pairs are shown in space-filling form. Solvent molecules are omitted for clarity.

Subsequent ^{1}H NMR spectral studies provided support for the conclusion that receptor **51** is able to bind the fluoride and chloride ions (as their tetraalkylammonium salts) and form stable 1:1 complexes in $CDCl_3$ and CD_3CN. When the complex of **51**·F^- was treated with Li^+, Na^+, Ca^{2+}, and Mg^{2+} cations (as their respective perchlorate salts), decomplexation of the pre-bound fluoride anion was observed (Fig. 46). In contrast, treatment of **51**·F^- with K^+ or Cs^+ led to formation of the corresponding ion pair complexes. In these latter complexes, the K^+ cations were found bound within the crown ether of host **51**, while the Cs^+ cations were held within the calix[4]pyrrole cavity. The chloride anion complex **51**·Cl^- displayed different cation-binding behaviour compared to the analogous fluoride ion complex (Fig. 47). Addition of Na^+, Mg^{2+}, or Ca^{2+} cations to the preformed complex **51**·Cl^- resulted in decomplexation of the pre-bound chloride anion. In contrast, addition of Li^+, K^+, or Cs^+ led to formation of ion pair complexes.

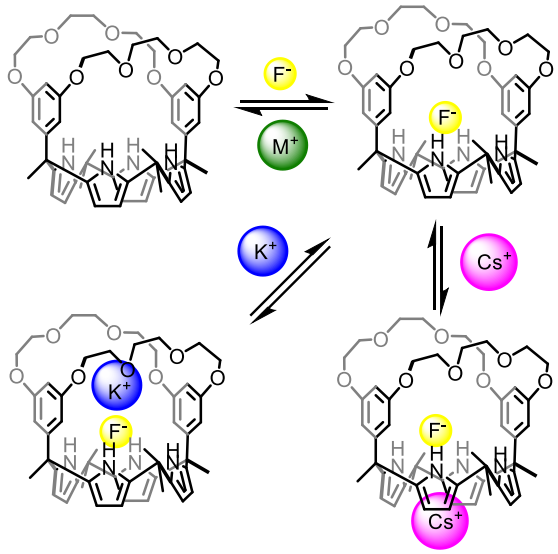

Fig. 46 Schematic representation of the proposed complexation behaviour exhibited by the fluoride complex **51**·F^- (TBA$^+$ salt) when exposed to the various metal cation perchlorate salts in CD_3CN. M^+ = Li^+, Na^+, Mg^{2+}, and Ca^{2+}.

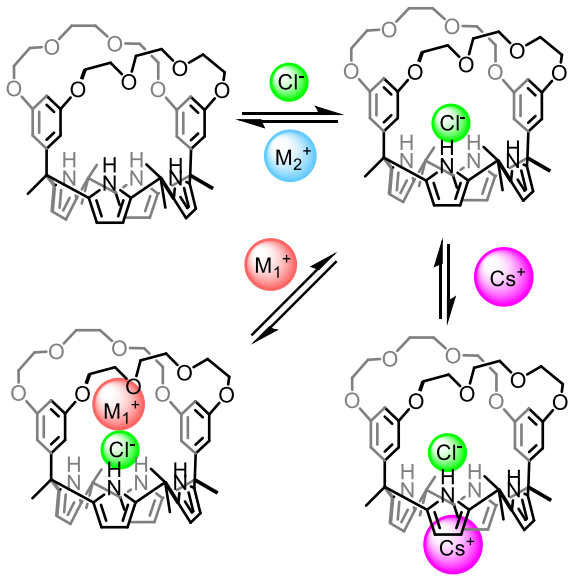

Fig. 47 Schematic view of the proposed binding modes of anion complex **51**·Cl^- (TBA$^+$ salt) upon exposure to perchlorate salts of various metal cations in CD_3CN. M_1^+ = Li^+ and K^+; M_2^+= Na^+, Mg^{2+}, and Ca^{2+}.

In 2014, Sessler and co-workers described the synthesis and self-assembly behaviour of a naphthocrown-strapped calix[4]pyrrole **55**. The synthesis started with functionalized dipyrromethane **52**, which was reacted with excess dibromoethane in the presence of K_2CO_3 in CH_3CN to yield the bromoethyl dipyrromethane **53** in 61% yield. The reaction of intermediate **53** with 2,3-dihydroxynaphthalene in acetonitrile at reflux using K_2CO_3 as the base gave compound **54** in 64% yield. Finally, the desired product was obtained in 13% yield via the condensation of the dipyrromethane intermediate **54** with acetone in the presence of a catalytic quantity of BF_3·OEt_2 (Scheme 3).[108] Receptor **55**, which features a strapped crown ether unit as an extra cation recognition site, was studied for its potential ion pair recognition and self-assembly behaviour. A solid-state structural analysis revealed that the nature of the host-guest complexes formed from receptor **55** and their aggregation behaviour depends heavily on the residual solvent within the crystal lattice. For instance, a linear supramolecular polymer involving one water molecule per receptor unit was found in the case of the CsF complex of **55** (Fig. 48a). In contrast, but for the same ion pair, a cyclic hexamer was found for **55** when the single crystals used for analysis were grown in the presence of methanol (Fig. 48b). These observations were interpreted in terms of the torsional angles between the residual solvents being different in the case of **55**·CsF·CH_3OH (top portion of Fig. 48c) and **55**·CsF·H_2O (Fig. 48c, bottom).

The solvent also has a great impact on the nature of the ion pair complex. Receptor **55** was found to bind M^+Cl^- (M = Li^+, Na^+, K^+, Cs^+ and TBA$^+$) to produce a so-called host–separated complex in DMSO–d_6. In sharp contrast, the strapped crown ether unit in receptor **55** was found to participate in cation

binding when LiCl, CsCl, or CsF were tested as substrates in 10% $CD_3OD/CDCl_3$ (Fig. 49).

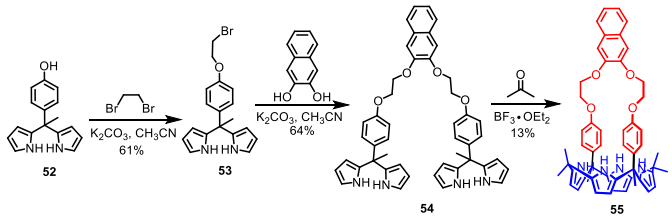

Scheme 3 Synthesis of receptor naphthocrown-strapped calix[4]pyrrole **55**.

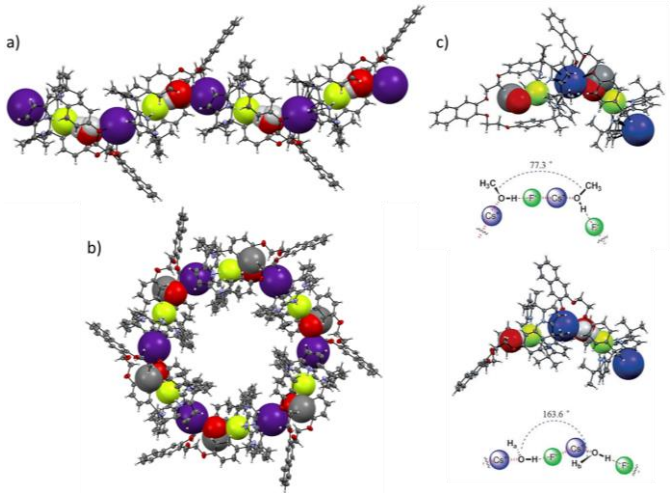

Fig. 48 Single crystal X-ray structure of complex formed from **55** with CsF with residual solvent of (a) H_2O and (b) CH_3OH. This figure was generated using data downloaded from the Cambridge Crystallographic Data Centre (CSD Nos. 980089 and 980088), (c) the torsional angles between the residual solvents in dimeric subunits in **55**·CsF·CH_3OH (top) and **55**·CsF·H_2O (bottom). Reprinted with permission from ref. 108. Copyright 2014 Wiley-VCH Verlag Publications.

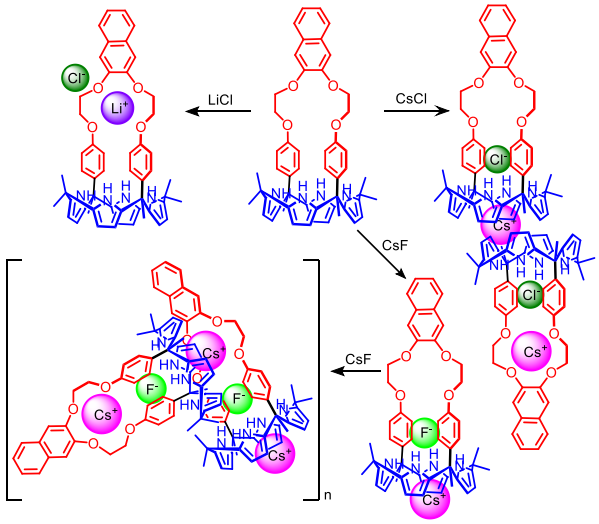

Fig. 49 Proposed binding modes of receptor **55** towards LiCl, CsCl, and CsF.

Based on the recognition of CsCl, a simplified version of **55** was prepared and incorporated into a diblock copolymer to give **57** containing hydrophobic poly(methyl methacrylate) (PMMA) domains (Scheme 4 and Fig. 50).[109] No evidence that copolymer **57** had amphiphilic character was found when it was studied in dichloromethane solution. However, it was found to generate reversed micelles upon treatment with caesium halide anion salts (e.g., CsCl or CsF) in dichloromethane, as inferred from dynamic light scattering (DLS), transmission electron microscopy (TEM), and energy-dispersive X-ray analyses (EDX). Changes in the conductivity of aqueous CsF, CsCl, CsBr, KF, and NaF solutions were monitored under conditions of liquid-liquid extraction (from aqueous to dichloromethane solution) using copolymer **57**, the control system **58** (Fig. 50), and PMMA as the putative extractants (Figs. 51 and 52). Copolymer **57** proved much more effective as an extractant than **58**, with no evidence of extraction being seen in the case of PMMA. Copolymer **57** was found to extract caesium fluoride more efficiently than other fluoride salts. In addition, caesium chloride was extracted more effectively than caesium fluoride by copolymer **57**. These results were interpreted in terms of copolymer **57** being more effective at extracting appropriately chosen ion pairs from aqueous source phases than the corresponding ion pair receptor **58**.

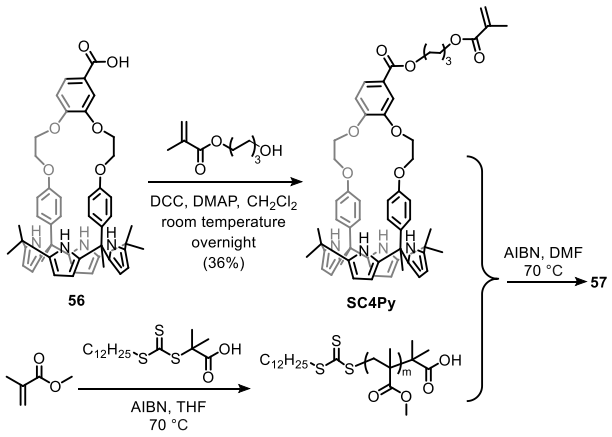

Scheme 4 Synthesis of the strapped calix[4]pyrrole-bearing diblock copolymer **57**.

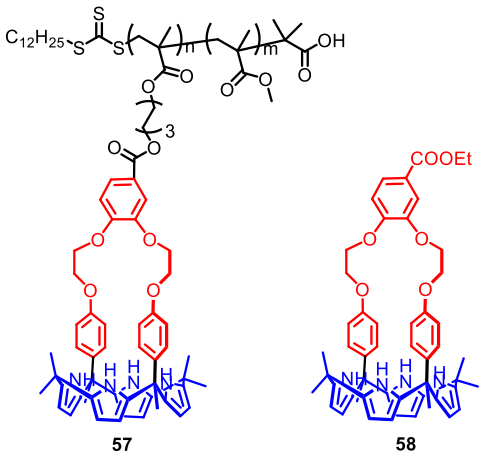

Fig. 50 Molecular structures of copolymer **57** and control **58**.

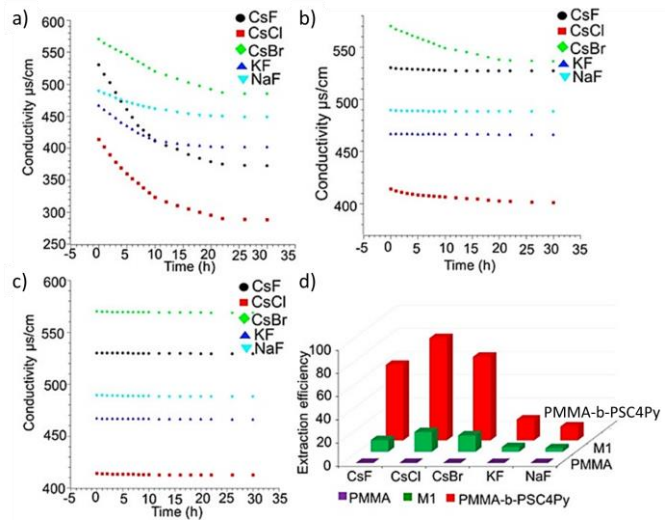

Fig. 51 Conductivity of aqueous inorganic salt solutions (5 mL each at an initial concentration of 5 mM) after liquid-liquid extraction with various extractants (effective calix[4]pyrrole concentration: 2 mM) at different analysis time. (a) **57**, (b) **58**, (c) PMMA. (d) Extraction efficiency recorded after 30 h using the conditions of studies (a–c). Reprinted with permission from ref. 109. Copyright 2018 ACS Publications.

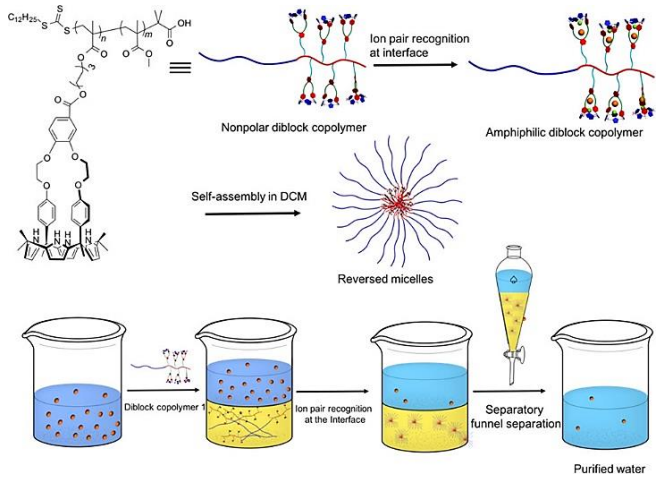

Fig. 52 Illustration of the self-assembly behaviour for diblock copolymer **57** that can create multi-aggregated reversed micelles. Reprinted with permission from ref. 109. Copyright 2018 ACS Publications.

4 Calixarene-strapped calix[4]pyrroles

Because of their facile functionalization at both their upper and the lower rims and the ease with which they may be subject to conformational modulation, calixarenes have been widely used as frameworks for the construction of ion receptors.[12, 110] In particular their ability to provide four or more oxygen donor atoms along the lower rim has made calixarene derivatives attractive as cations receptors.[12, 110] Not surprisingly, therefore, it was considered likely that the use of calix[4]arene subunits as a straps would produce calix[4]pyrrole derivatives capable of recognizing certain ion pairs effectively. Indeed, this paradigm was expressed in the context of various ion pair receptors that proved capable of binding both an anion and a cation.[9, 40] In this section we review such systems.

The earliest example of a calix[4]arene-strapped calix[4]pyrrole hybrid was reported by Sessler and co-workers.[111] Using the cone-*p*-*tert*-butylcalix[4]arene **59** as a template, the calix[4]arene-capped calix[4]pyrrole (**60**) was synthesized in 32% yield via the condensation of the calix[4]arene tetramethyl ketone with pyrrole in the presence of methanesulfonic acid (Fig. 53). Compound **60** was characterized by ^{1}H NMR spectroscopy and a single crystal X-ray diffraction analysis. In CD_2Cl_2, the proton signal corresponding to the pyrrolic NHs of compound **60** (at 11.22 ppm) were found to be significantly downfield-shifted relative to what was seen for simple calix[4]pyrroles, such as **1**. This finding was attributed to the formation of intramolecular hydrogen bonds between the pyrrolic NHs and the oxygen atoms of the calix[4]arene unit. A single crystal X-ray diffraction structure of compound **60** revealed that both the calix[4]arene and the calix[4]pyrrole subunits of **60** are fixed in the cone conformation (Fig. 54) in the solid state, presumably as a result of the strong intramolecular hydrogen bonds between the pyrrolic NHs and the oxygen atoms of the lower rim of the calix[4]arene. When compound **60** was treated with 10 equiv. of TBAF, no chemical shift changes in the ^{1}H NMR spectrum were observed. This finding was interpreted in terms of there being little appreciable interaction between receptor **60** and the fluoride anion, presumably reflecting the strong intramolecular hydrogen bonds.[111]

A similar strategy was adopted for the synthesis of an expanded calixpyrrole. Specifically, using a calix[5]arene as a template, the calix[5]arene-capped calix[5]pyrrole (**61**) could be synthesized in 10% yield via the condensation reaction of the calix[5]arene pentaketone with pyrrole in the presence of $BF_3{\cdot}OEt_2$.[112] In analogy to what was seen with the calix[4]arene-capped calix[4]pyrrole system **60**, ^{1}H NMR spectroscopic analyses in dichloromethane–d_2 revealed that the protons of the pyrrolic NHs of compound **61** resonated at relatively low field (at 9.88 ppm). Although the effect was less dramatic than in the case of compound **60**, this finding was again interpreted in terms of the pyrrolic NHs of **61** forming intramolecular hydrogen bonds with the oxygen atoms of the calix[5]arene moiety. However, in contrast to what was seen with compound **60**, receptor **61** proved capable of recognizing the chloride anion in dichloromethane–d_2 as inferred from ^{1}H NMR spectroscopic studies.[112]

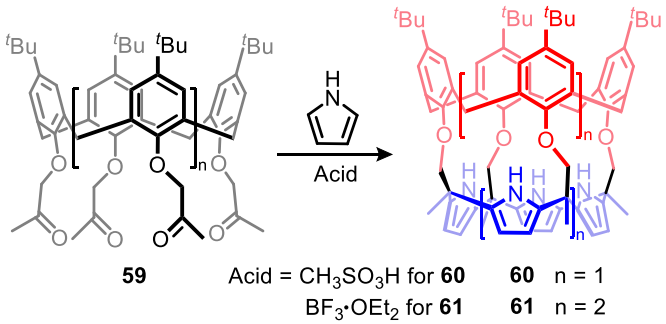

Fig. 53 Synthesis of calixarene-capped calix[4]- and calix[5]pyrroles **60** and **61**.

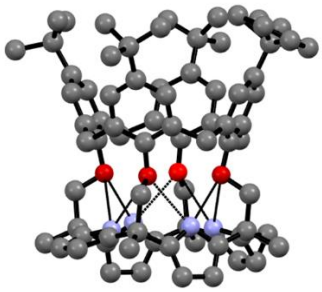

Fig. 54 Single crystal structure of **60**. This figure was generated using data downloaded from the Cambridge Crystallographic Data Centre (CSD Nos. 1247391). Solvent molecules and hydrogen atoms are omitted for clarity and hydrogen bonds are presented as dashed lines.

By coupling a calix[4]arene as a cation binding site with a calix[4]pyrrole as an anion binding motif, Sessler and co-workers created a number of ion pair receptors.[53] An early example of this class of ion pair receptors, namely the 1,3-*alternate* calix[4]arene-crown-6 strapped calix[4]pyrrole **62**, was reported in 2008. At the time, the 1,3-*alternate* calix[4]arene-crown-6 subunit was already well known for its high affinity and selectivity for the caesium cation.[113-116] Thus, compound **62** was expected to act as an ion pair receptor selective for caesium salts. Initial evidence that receptor **62** forms a stable 1:1 complex with CsF came from a single crystal X-ray diffraction analysis. The resulting crystal structure revealed that the caesium cation was coordinated to the calix[4]arene crown-6 ring while the fluoride anion was bound to the calix[4]pyrrole subunit *via* hydrogen bonding interactions with the pyrrolic NH protons (Fig. 55).[53] The co-bound caesium cation and fluoride anion were separated by a relatively large distance of 10.92 Å with a methanol molecule being seen to interact with the bound fluoride anion in the solid state (Fig. 55).

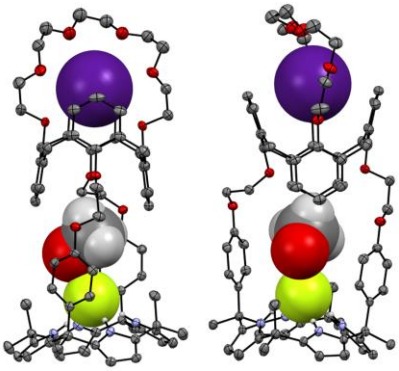

Fig. 55 Two different views of the single crystal X-ray diffraction structure of the CsF ion pair complex of receptor **62**, **62**·CsF·CH_3OH. These figures were generated using data downloaded from the Cambridge Crystallographic Data Centre (CSD Nos. 709924). The encapsulated ion species and solvent molecules are shown in space-filling model. Most solvent molecules and hydrogen atoms are omitted for clarity.

^{1}H NMR spectroscopic analyses carried out in chloroform–*d* containing 10% methanol-d_4 revealed that the caesium cation was complexed by the calix[4]arene crown-6 subunit and led to the suggestion that this initial interaction then served to facilitate fluoride binding by the calix[4]pyrrole subunit. Support for this notion came from the finding that when receptor **62** was treated with $CsClO_4$, the caesium cation was bound to the calix[4]arene-crown-6 subunit (Fig. 56).[53] Addition of TBAF to this Cs^+ complex led to formation of a stable CsF ion pair complex wherein the fluoride anion was bound to the calix[4]pyrrole macrocycle via hydrogen bonds to the pyrrolic NH protons (Fig. 56). Similarly, when receptor **62** was titrated with the CsF ion pair, the caesium cation was seen to interact with the calix[4]arene crown-6 ring before the fluoride anion began to bind to the calix[4]pyrrole subunit as inferred from ^{1}H NMR spectroscopic studies. Moreover, in the absence of Cs^+, no evidence of fluoride binding was seen when receptor **62** was exposed to TBAF. This latter finding was taken as additional evidence that the Cs^+ cation plays a crucial role in mediating anion recognition in the case of receptor **62**.[53]

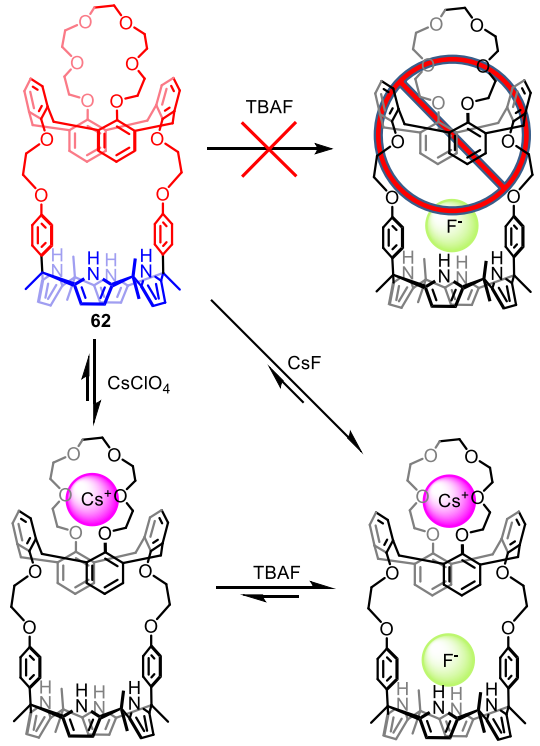

Fig. 56 Binding modes of receptor **62** with various salts of the Cs^+ cation and the F^- anion that are presumed to be operative in 10% CD_3OD in $CDCl_3$.

Receptor **63**, a calix[4]arene-calix[4]pyrrole hybrid that lacks a crown ether, was also synthesized.[117] Receptor **63** was functionalized with propyl groups so as to enforce a 1,3-*alternate* conformation within the calix[4]arene moiety thereby providing a structural analogue of **62** (Fig. 57). In contrast to what was seen in the case of **62**, receptor **63** was unable to recognize either the Cs^+ or F^- ions when treated with noncoordinating salts containing these ions (e.g., $CsClO_4$ or TBAF) in the absence of one another (Fig. 57), as inferred from ^{1}H NMR spectroscopic analysis performed in $CDCl_3/CD_3OD$ (1/9, v/v). However, in the presence of CsF or a mixture of salts that produce a source of CsF *in situ*, receptor **63** was found to bind both the Cs^+ cation and the F^- anion to form a stable 1:1 CsF ion pair complex (Fig. 57). Because it depends on the presence of both ions, this CsF recognition behaviour follows the rules of an AND logic gate.[117]

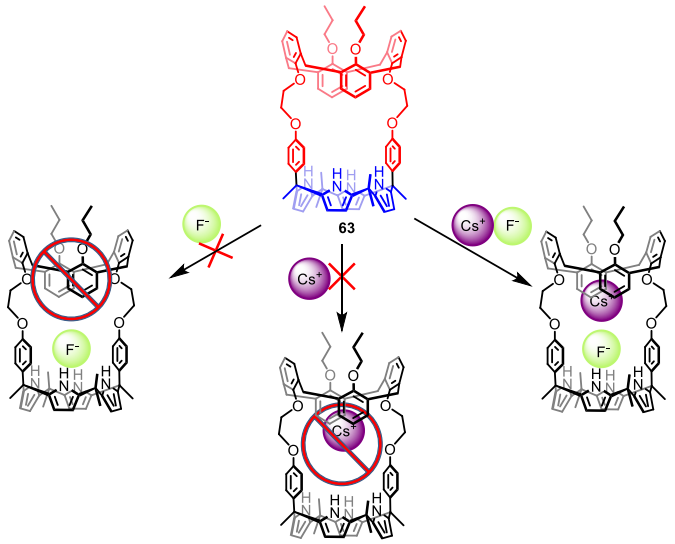

Fig. 57 Putative binding behaviour of receptor **63** following the AND logic gate when treated with the Cs^+, the F^-, and mixtures thereof in 10% CD_3OD in $CDCl_3$. In addition to the CsF ion pair, TBAF and $CsClO_4$ were used as the sources of the ions.

It was also revealed through ^1H NMR spectroscopic analyses and single crystal X-ray diffraction studies that ion pair receptor **63** was capable of binding other caesium salts, including CsCl, CsBr, and $CsNO_3$, in solution as well as in the solid state. In these cases, the crown-free calix[4]arene moiety acts as an effective binding site for the caesium cation. The actual nature of the ion pair complexes was found to differ dramatically with a strong dependence on the specific choice of anion of the caesium salts being found. For instance, receptor **63** proved capable of stabilizing a solvent-bridged ion pair complex with CsF wherein the cation and the anion are separated by a water molecule (Fig. 58). In contrast, $CsNO_3$ was complexed as a close contact ion pair within the cavity of the receptor. In addition, receptor **63** was found to form an unusual 2:2 ion pair complex with CsCl characterized by two different ion pair binding modes. In one mode, the caesium cation is complexed within the calix[4]arene cavity and contacts directly the chloride anion that, in turn, is hydrogen-bonded to the pyrrolic NH protons of an adjacent calix[4]pyrrole subunit. In contrast, the other caesium cation was found sandwiched within the capsule-like cavity formed by two cone-shaped, chloride bound calix[4]pyrrole subunits. The net result is formation of a host-separated ion pair complex (Fig. 58).[117]

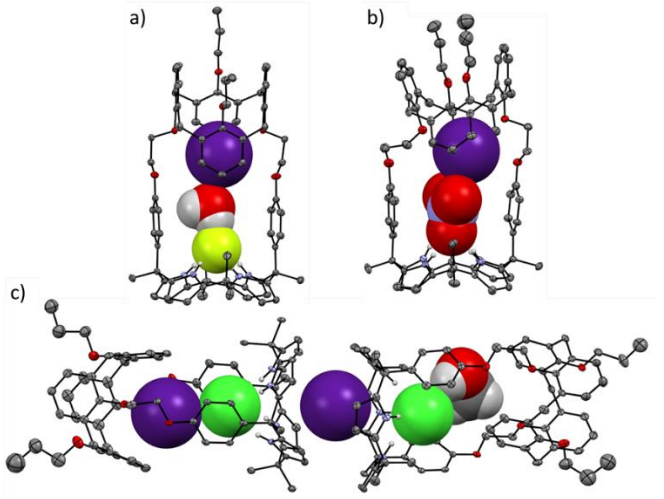

Fig. 58 Single crystal X-ray diffraction structures of the ion pair complexes of receptor **63** with (a) CsF, (b) $CsNO_3$ and (c) CsCl. This figure was generated using data downloaded from the Cambridge Crystallographic Data Centre (CSD Nos. 709925, 753420 and 753421, respectively). Most hydrogen atoms and solvent molecules are omitted for clarity.

The multitopic ion pair receptor **64** was also synthesized in an effort to control the binding and release of the caesium cation by cation metathesis (Fig. 59). Receptor **64** is comprised of one anion recognition site and three cation binding sites having different affinities and selectivities towards the Cs^+ and K^+ cations (Fig. 59). For instance, the 1,3-*alternate* calix[4]arene crown-5 subunit has an inherently high affinity for the K^+ cation relative to the Cs^+ cation. This high affinity holds for other cation binding sites within receptor **64**. Consequently, receptor **64** was expected to bind the Cs^+ cation in the absence of the K^+ cation but to release the Cs^+ cation when the Cs^+ complex of receptor **64** was treated with a K^+ cation source (Fig. 59).[118]

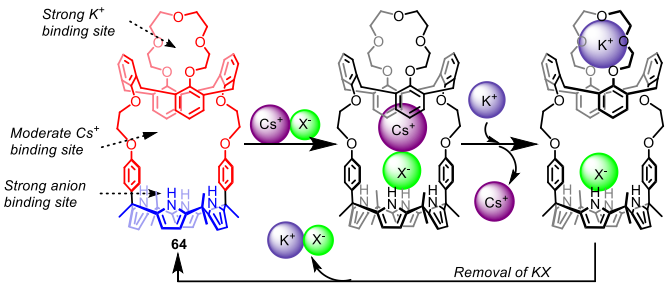

Fig. 59 Design concept underlying receptor **64** and its proposed mode of action involving the binding and release of the Cs^+ cation via cation metathesis.

It was demonstrated by means of ^1H NMR spectroscopic analyses and single crystal X-ray diffraction studies that receptor **64** could bind cations, anions, and various ion pairs containing the K^+ and Cs^+ cations, both in solution and in the solid state (Fig. 60).[118, 119] In this case, ion pair recognition was found to take place via various binding modes (Fig. 60). For instance, receptor **64** interacts with KF, KNO_3, $CsNO_3$, CsF, and CsCl to form stable 1:1 complexes in which the cations are encapsulated by the 1,3-*alternate* calix[4]arene crown-5 subunit and the counter anions are bound to the calix[4]pyrrole subunit. While the overall geometries of these ion pair complexes are similar in all cases, their binding kinetics and

physical properties were found to differ significantly.[118, 119] For example, in the cases of KF, KCl, and KNO_3, receptor **64** was found to bind the K^+ cation and the anions in a stepwise manner when studied in $CD_3OD/CDCl_3$ (1/9, v/v) as shown in Figs. 60 and 61. Ultimately, this results in precipitation of the complexes[118, 119]

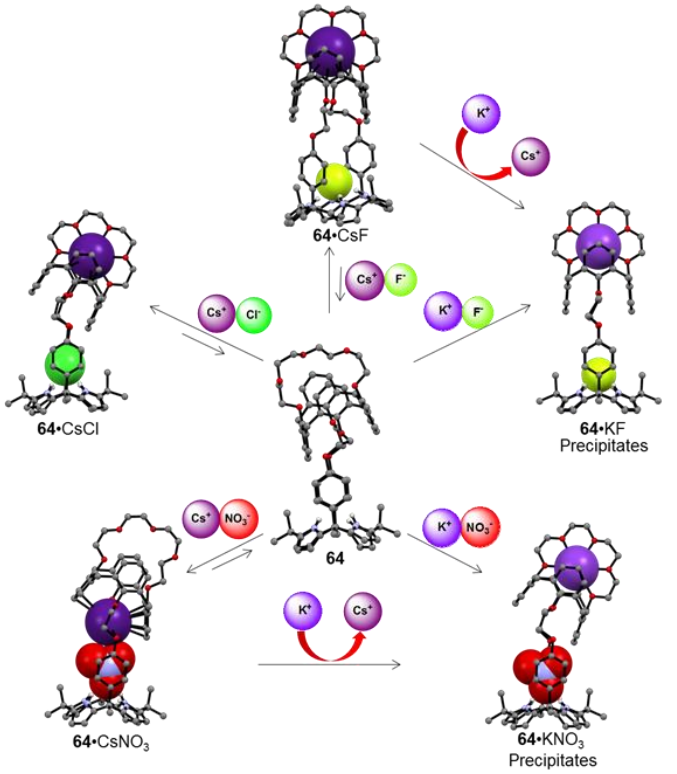

Fig. 60 Proposed binding modes of receptor **64** with various Cs^+ and K^+ ion pairs as inferred from ^1H NMR spectroscopic analysis performed in 10% CD_3OD in $CDCl_3$. Also shown are single crystal X-ray diffraction structures of the ion pair complexes in question. Most hydrogen atoms and solvent molecules are omitted for clarity. Reprinted with permission from ref. 40. Copyright 2014 ACS Publications.

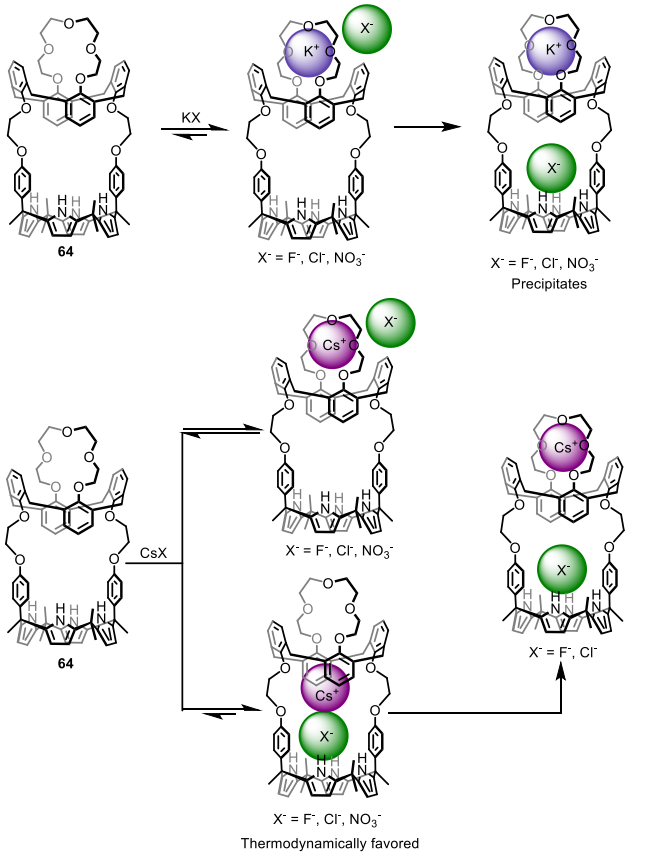

Fig. 61 Proposed binding interactions of receptor **64** with various K^+ and Cs^+ salts as inferred from ^1H NMR spectroscopic studies carried out in 10% CD_3OD in $CDCl_3$ as well as from single crystal X-ray diffraction structures of the corresponding ion pair complexes.

Under the same solution phase conditions ($CD_3OD/CDCl_3$ (1/9, v/v)) as used in the initial studies, receptor **64** was found to interact with CsF and CsCl to form ion pair complexes via two different binding modes. In one binding mode, the Cs^+ cation, but not the anion, was weakly bound to the calix[4]arene crown-5 subunit to give a Cs^+ cation complex ([**64**·Cs^+]X^-, X^- = F^- or Cl^-) without a counter anion being co-bound (Fig. 61). These latter Cs^+ complexes proved labile and were found to exist in fast equilibrium with the cation-free form of the receptor on the NMR time scale. In the other recognizable binding mode, the Cs^+ cation and the anions (either F^- and Cl^-) were concurrently bound to the receptor (Fig. 61). On the basis of the detailed ^1H NMR spectral titration experiments it was further concluded that the Cs^+ cation was bound first to the ethylene glycol linkers and then moved to the crown-5 ring to form what were deemed to be more thermodynamically stable ion pair complexes, namely **64**·CsF and **64**·CsCl, wherein the cation and the anion are spatially separated from one another (Fig. 61).[118, 119]

In analogy to what was seen with CsF and CsCl, receptor **64** was also found to bind the $CsNO_3$ ion pair via two different binding modes. However, in this case, the Cs^+ cation remained bound to the ethylene glycol moieties to form a contact ion pair with the NO_3^- anion, which in turn was hydrogen-bonded to the calix[4]pyrrole subunit (Fig. 61). No evidence in support of the Cs^+ cation being coordinated to the calix[4]arene crown-5

moiety was seen. Support for these conclusions came from a theoretical study based on the DFT calculations.[120]

In sharp contrast to what was seen for the Cs^+ complexes, in the case of KNO_3, the K^+ cation was found complexed within the calix[4]arene crown-5 ring. This difference was ascribed to the fact that the crown-5 ring of receptor **64** has a higher affinity for the K^+ cation than the Cs^+ cation (Fig. 60 and 61). Perhaps as a consequence of this change in the cation binding mode, in the KNO_3 complex of receptor **64**, the NO_3^- anion was found to be separated spatially from the K^+ cation and to form hydrogen bonds with the calix[4]pyrrole NH protons (Fig. 60 and 61).[118, 119]

In accord with the underlying design concept, receptor **64** was found to release the Cs^+ cation via cation metathesis when one of the preformed Cs^+ cation complexes was exposed to the K^+ cation. For example, when a $KClO_4$ solution in $CD_3OD/CDCl_3$ (1/9, v/v) was added to either the CsF or $CsNO_3$ complex of receptor **64** in the same solvent system, the formation of white precipitates was observed (Fig. 60). This phase change is ascribed to the formation of insoluble ion pair complexes with KF and KNO_3 as a result of cation metathesis. In other words, replacement of the pre-bound Cs^+ cation by the K^+ cation produces species that are more strongly bound to the receptor and less soluble (Fig. 60 and eqns. 1 and 2).[118, 119]

[**64**] + CsX → [**64**·CsX] (1)

[**64**·CsX] + $KClO_4$ →[**64**·KX] + $CsClO_4$, X = F or NO_3 (2)

Receptor **64** was also found to be able to extract the Cs^+ cation (as its nitrate ion pair) from an aqueous phase into an organic phase of nitrobenzene.[118] The Cs^+ cation extracted in this way could be released and recovered by exposure of the organic phase containing the $CsNO_3$ complex to an aqueous phase containing the K^+ cation (ClO_4^- salt) as shown schematically in Fig. 62. In actual experiments, receptor **64** dissolved in nitrobenzene–d_5 was exposed to an aqueous D_2O solution of $CsNO_3$ containing excess $NaNO_3$.[118] The resulting ^1H NMR spectral change of the organic phase was consistent with the formation of the $CsNO_3$ complex of receptor **64**. This finding was taken as evidence that the receptor is capable of extracting $CsNO_3$ from an aqueous source phase to form a stable $CsNO_3$ complex within the organic receiving phase. Contacting the organic phase containing the $CsNO_3$ complex of receptor **64** with an aqueous D_2O solution of $KClO_4$ led to release of the $CsNO_3$ complexed by the receptor into the aqueous phase (Fig. 62). This process gave rise to a new cation complex, [**64**·K^+]ClO_4^-, in the organic phase, as supported by ^1H NMR spectroscopic analyses. Washing the nitrobenzene phase containing this latter K^+ complex with excess chloroform and D_2O (twice) enabled regeneration of the ion-free receptor **64** in the organic layer (Fig. 62).[118] By contrast, under the same two phase extraction conditions, binding and release of these ions or ion pairs could not be achieved using either the unsubstituted calix[4]pyrrole or a simple 1,3-*alternate* calix[4]arene crown-5 derivative lacking an anion binding site, or an equimolecular mixture of these two receptors.[118]

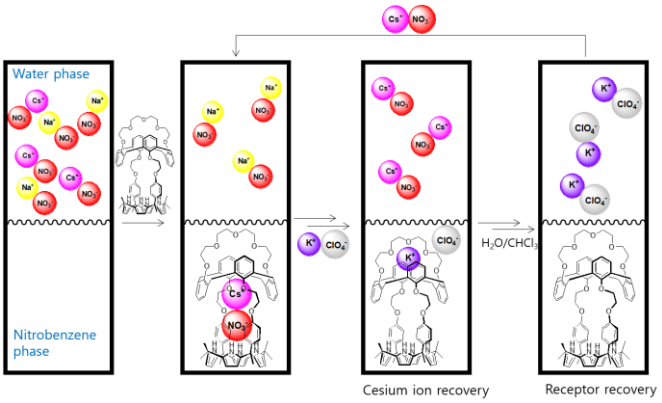

Fig. 62 Schematic representation of a process for two phase extraction and recovery of $CsNO_3$ using ion pair receptor **64**. Cation metathesis enables controlled removal of the caesium cation while subsequent contacting steps with chloroform and water allow the receptor to be recycled. Reprinted with permission from ref. 118. Copyright 2012 ACS Publications.

In a similar way, the more hydrophilic KNO_3 ion pair could be extracted and recovered using ion pair receptor **62** containing the 1,3-*alternate* calix[4]arene crown-6. Receptor **62**, in contrast to receptor **64**, contains a relatively large calix[4]crown-6 ring.[121] When exposed to an aqueous D_2O solution containing KNO_3, receptor **62** was found to bind and extract KNO_3 into a nitrobenzene organic phase (Fig. 63). Subsequent washing of the nitrobenzene layer containing the KNO_3 complex of receptor **62** with an aqueous solution containing $CsClO_4$ led to the release of the receptor-complexed KNO_3 into the aqueous phase leaving a new cation complex, [**62**·Cs^+]ClO_4^-, in the organic phase (Fig. 63).[121]

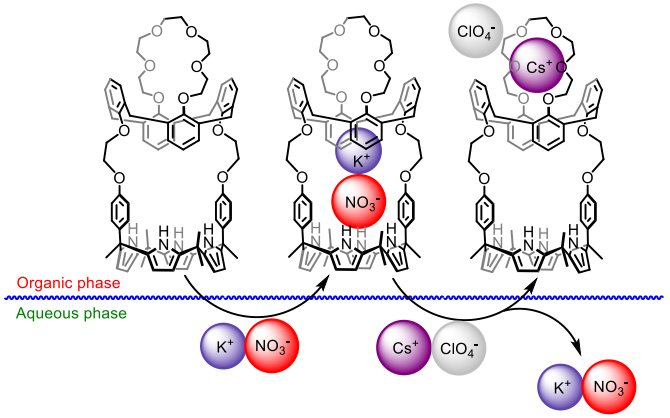

Fig. 63 Schematic representation showing a two-phase extraction and recovery process for KNO_3 that relies on ion pair receptor **62**.

The ion pair receptor **65** contains linkers that are relatively more flexible than those present in receptor **64**. Its preparation and ion binding properties were investigated by Lee and co-workers.[122] In analogy to receptor **64**, receptor **65** contains a 1,3-*alternate* calix[4]arene crown-5 linked to a calix[4]pyrrole core. However, it incorporates more flexible pentyl chains (Fig. 64). On the basis of ^1H NMR spectroscopic analysis it was concluded that receptor **65** fails to form a complex with the Cs^+ cation or the K^+ cation when exposed to their ClO_4^- salts in 10% CD_3OD in $CDCl_3$ (Fig. 64). These findings stand in sharp contrast

to what was seen in the case of receptor **64**. However, when the initial counter anion (ClO_4^-) was replaced by the F^- anion, receptor **65** was found to form complexes with both KF or CsF, albeit via different binding modes.[122] Specifically, in the presence of KF, receptor **65** was found to stabilize a K^+ cation complex, [**65**·K^+]F^-, wherein the F^- anion is not directly bound to the receptor (Fig. 64). In contrast, when exposed to CsF under the same solution condition, both the Cs^+ cation and the F^- anion were found to be bound concurrently to form an ion pair complex, [**65**·CsF]. In this complex, the Cs^+ cation is coordinated to the calix[4]crown-5 subunit while the F^- anion is bound to the calix[4]pyrrole moiety. In contrast to what was seen with receptor **64**, receptor **65** was found to bind the CsF ion pair more strongly than the corresponding KF ion pair. As a consequence, when the K^+ complex of receptor **65**, [**65**·K^+]F^-, was treated with CsF in 10% CD_3OD in $CDCl_3$, the pre-complexed K^+ cation was replaced by the Cs^+ cation to give a stable CsF ion pair complex, **65**·CsF (Fig. 64). These findings led to the suggestion that the selectivity and affinity of ion pair receptors could be fine-tuned to favour specific ionic targets via the choice of linkers between the cation and an anion binding sites.[122]

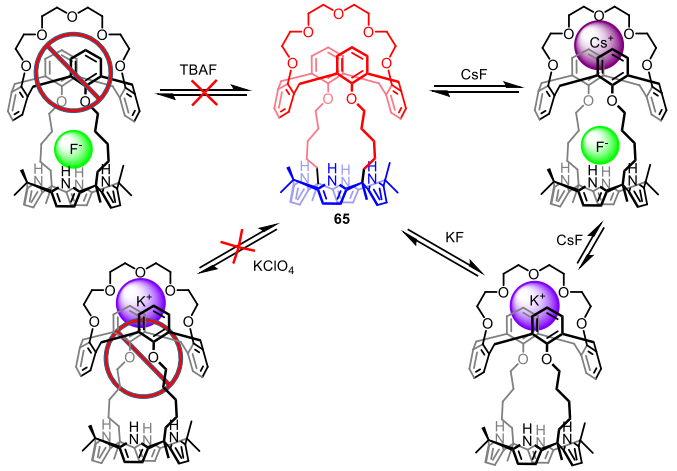

Fig. 64 Proposed binding modes corresponding to the interactions between receptor **65** and KF and CsF as inferred from ^{1}H NMR spectroscopic studies carried out in 10% CD_3OD in $CDCl_3$.

To understand the interplay between calix[4]arene conformations and anion/cation recognition in multicomponent systems, the 1,3-dihydroxycalix[4]arene- and 1,3-dimethoxycalix[4]arene-strapped calix[4]pyrroles (**66** and **67**) were synthesized by Sessler, *et al*.[123] In solution as well as in the solid state, the calix[4]arene subunit of receptor **66** adopts a cone conformation as the presumed result of intramolecular hydrogen bonding interactions between the hydroxy OH protons and the adjacent phenoxy oxygen atoms. In contrast, receptor **67** proved to be conformationally mobile and to interconvert between the cone and the partial cone conformations in solution (Fig. 65).[123] The conformational mobility of receptor **67** stands in stark contrast to what was seen in the case of receptor **63** wherein the calix[4]arene subunit is locked in the 1,3-*alternate* conformation as the result of steric effects. Both receptors **66** and **67** proved capable of binding the F^- and Cl^- anions. The nature of the binding interactions was found to be highly dependent on the choice of counter cations. For example, these receptors were found to bind only the F^- anion when it and various other anions were studied in the forms of their tetrabutylammonium salts in $CDCl_3$. In contrast, the corresponding Cs^+ salts were used, both the F^- and Cl^- anions were bound by both receptors **66** and **67**.[123] However, neither receptor **66** nor receptor **67** was found to recognize appreciably either CsBr or $CsNO_3$ in 10% CD_3OD in $CDCl_3$. This latter finding stands in contrast to what was seen in the case of receptor **63**.[117, 123]

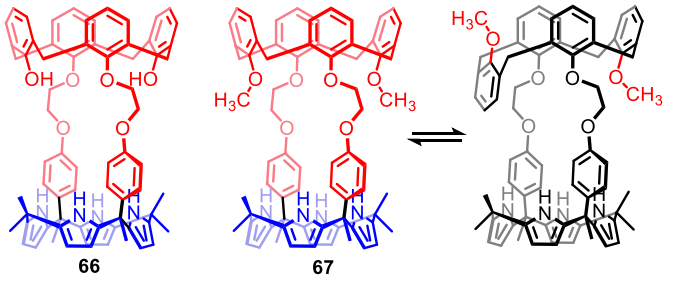

Fig. 65 Chemical structures of receptors **66** and **67**.

Even in the case of CsF and CsCl, the complexation modes with **66** were found to vary with the conditions. For example, when one molar equivalent of CsF was present, receptor **66** was found to stabilize a 1:1 ion pair complex wherein the Cs^+ cation was complexed within the cone-shaped calix[4]pyrrole cavity with the F^- anion being hydrogen bonded concurrently to the calix[4]pyrrole NH protons (Figs. 66 and 67). The addition of excess CsF to this 1:1 CsF complex gave rise to the formation of a coordination polymer (Figs. 66 and 67). In contrast, the CsCl ion pair was found to interact with receptor **66** with a 2:3 stoichiometry (**66** : CsCl) in the solid state. In the resulting multicomponent ion pair complex, [**66**$_2$·$(Cs^+)_3$·$(Cl^-)_2$]Cl^-, two Cs^+ cations were found coordinated to the oxygen atoms of the calix[4]arene in the cone conformation, as well as to the oxygen atoms of the ether linkages. The other Cs^+ cation was found sandwiched between two cone-shaped calix[4]pyrrole subunits (Fig. 68). Two of the three Cl^- anions were bound to the calix[4]pyrrole subunits forming contact ion pairs with the Cs^+ cations complexed by the calix[4]arene constituent (Fig. 68). The other Cl^- anion was positioned outside the receptor and separated from the receptor-complexed Cs^+ cation by an ethanol molecule (Figs. 67 and 68).[123]

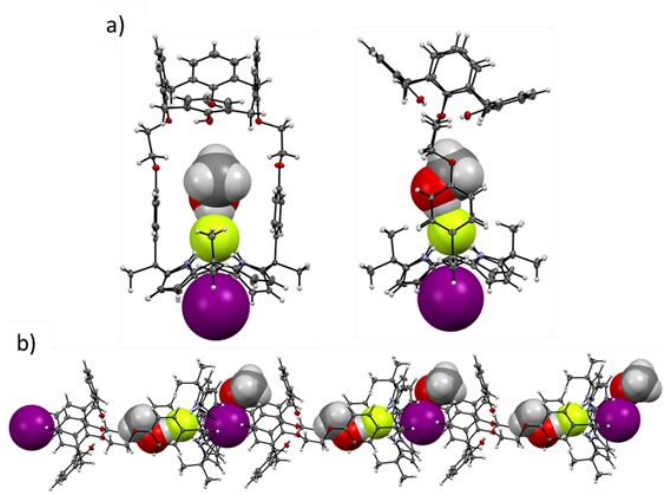

Fig. 66 (a) Different views of the single crystal X-ray diffraction structure of the CsF complex of receptor **66**. The bound F^- anion is solvated by a methanol molecule. (b) Truncated views of the extended structure seen in the crystal lattice. Most hydrogen atoms and solvent molecules have been removed for clarity. This figure was generated using data downloaded from the Cambridge Crystallographic Data Centre (CSD Nos. 1025274).

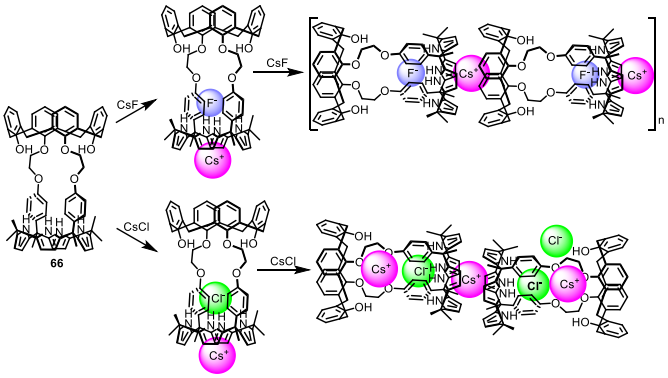

Fig. 67 Suggested binding modes corresponding to the interaction between receptor **66** and either CsF and CsCl as inferred from ^{1}H NMR spectroscopic studies performed in 10% CD_3OD in $CDCl_3$.

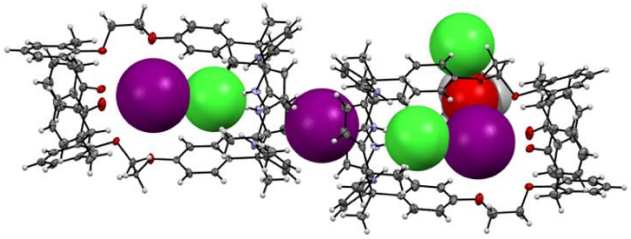

Fig. 68 Single crystal X-ray diffraction structure of $[\mathbf{66}_2{\cdot}(Cs^+)_3{\cdot}(Cl^-)_2]Cl^-{\cdot}CH_3CH_2OH$. Most hydrogen atoms and solvent molecules not involved in ion pair complexation have been omitted for clarity. This figure was generated using data downloaded from the Cambridge Crystallographic Data Centre (CSD Nos. 1025273).

In contrast to what was seen with receptor **66**, the calix[4]arene constituent of receptor **67** was found to retain its conformational mobility and to interconvert between the partial cone and the cone conformation on the NMR time scale in the presence of CsF (Fig. 69).[123] When excess CsF was present in 10% CD_3OD in $CDCl_3$ relative to **67**, the calix[4]arene subunit was found to exist in the form of a single conformer that is locked in the pinched cone conformation (Fig. 69). Under the latter conditions, the Cs^+ cation is complexed by the cone-shaped calix[4]pyrrole cavity while also interacting with the aromatic rings of the calix[4]arene subunit of a different molecule. As evidenced by DOSY (diffusion ordered spectroscopy) NMR and single crystal X-ray diffraction analyses, the net result of these interactions was the formation of a linear supramolecular polymer in the solid state as well as in solution (Fig. 69). In contrast, in the presence of CsCl, receptor **67** was found to exist in the form of a 1:1 ion pair complex with the calix[4]arene subunit adopting a partial cone conformation. In this latter conformation, the Cl^- anion is bound to the calix[4]pyrrole NH protons and further stabilized by presumed aryl CH···Cl^- hydrogen bond interactions involving the inverted aromatic proton of the calix[4]arene methoxy phenyl group (Figs. 69 and 70).[123]

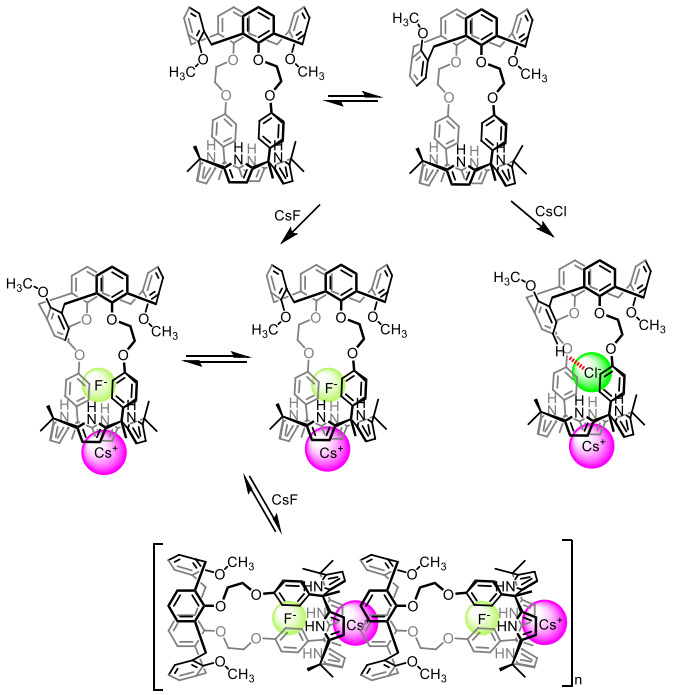

Fig. 69 Proposed binding modes corresponding to the interaction of receptor **67** with CsF and CsCl as inferred from ^{1}H NMR spectroscopic studies carried out in 10% CD_3OD in $CDCl_3$ and single crystal X-ray diffraction analyses.

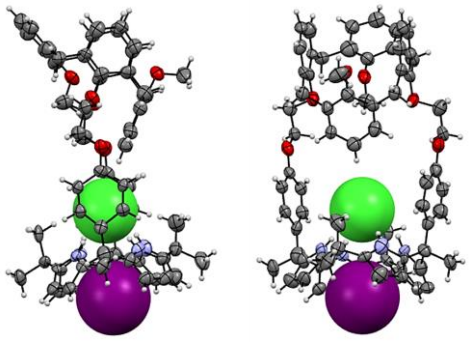

Fig. 70 Different views of the single crystal X-ray diffraction structure of the CsCl complex of receptor **67**. Most hydrogen atoms and solvent molecules not involved in ion pair complexation have been removed for clarity. This figure was generated using data downloaded from the Cambridge Crystallographic Data Centre (CSD

Nos. 1025279).

The Sessler group also synthesized a calix[4]pyrrole (**68**) strapped via rigid phenoxy linkers to a relatively bulky calix[4]arene diethyl ester.[124] It was revealed through ^{1}H NMR spectroscopic studies that receptor **68** binds the F^- anion (as its TBA^+ or TEA^+ salt) with essentially complete selectivity and high affinity in the presence of an excess of various potentially competing anions, including Cl^-, Br^-, I^-, OAc^-, NO_3^-, SO_4^{2-}, $H_2PO_4^-$, and $HP_2O_7^{3-}$. This selectivity for F^- anion was attributed to the small rigid cavity provided by receptor **68**, which is based on a calix[4]arene locked in the cone conformation. As inferred from the single crystal X-ray diffraction structure of the TEAF complex of receptor **68**, the F^- anion is hydrogen bonded to the calix[4]pyrrole NH protons but is also monohydrated by a water molecule co-encapsulated within the receptor cavity (Fig. 71).[124] The high F^- anion selectivity of receptor **68** was retained when the TBA^+ counter cation was replaced by the Cs^+ cation. This finding stands in contrast to what were seen with most of the calix[4]arene strapped calix[4]pyrroles that were known at the time, including receptors **66** and **67** (*vide supra*). A single crystal X-ray diffraction structure of the CsF complex of receptor **68** revealed that the caesium cation was bound within the cone-shaped calix[4]pyrrole cavity formed as the result of fluoride anion binding to the pyrrolic NH protons (Fig. 72). The distances between the caesium cation and the centroids of the pyrrole rings were found to fall between 3.37 and 3.69 Å. The caesium cation bound to the calix[4]pyrrole cavity was also found to interact with the carbonyl oxygen atom of the ester group present on a separate molecule of **68**. As a result, a coordination polymer is stabilized in the solid state (Fig. 72).[124]

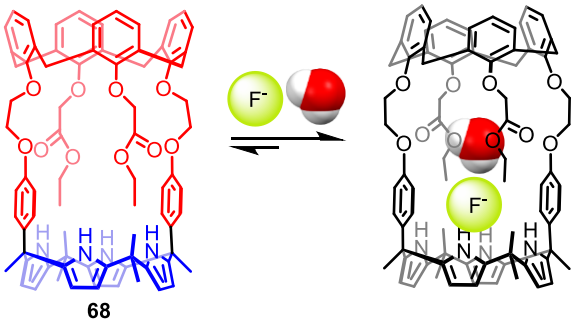

Fig. 71 Proposed binding mode corresponding to the interaction of receptor **68** with a mono-hydrated F^- anion as inferred from ^{1}H NMR spectroscopic studies carried out in $CDCl_3$ and a single crystal X-ray diffraction analysis.

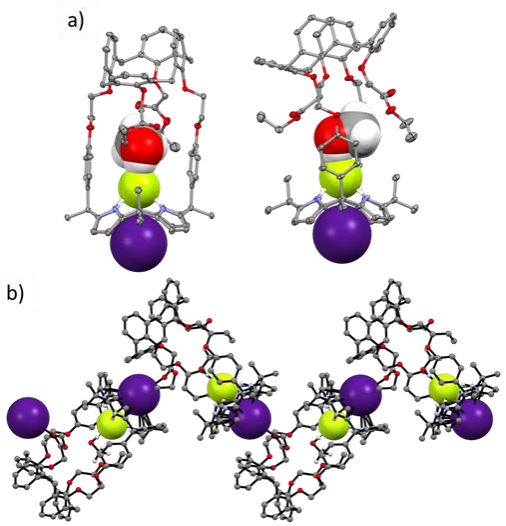

Fig. 72 (a) Two different views of the single crystal structure of **68**·CsF·CH_3OH. (b) Partial view of the extended structure seen in the crystal lattice. Most hydrogen atoms and solvent molecules not involved in stabilization of the ion pair complex have been removed for clarity. This figure was generated using data downloaded from the Cambridge Crystallographic Data Centre (CSD Nos. 1026516).

A chromogenic fluoride sensor **74** (Fig. 73), featuring an azocalix[4]arene as the strap, was designed and synthesized by Thiampanya, *et al.*[125] This receptor was obtained following the synthetic route shown in Fig. 73. After obtaining the key precursor 1,3–calix[4]arene-bisdipyrromethane (**73**), catalytic condensation of **73** with dry acetone in the presence of BF_3·OEt_2 afforded the desired component **74** in 13% yield. Colour changes were observed upon the addition of different anions into CH_3CN solutions of **74**. The original colour of **74** in acetonitrile was light orange. After titration with F^-, $CH_3CO_2^-$, $PhCO_2^-$, and $H_2PO_4^-$ (as the respective TBA^+ salts), the colour changed to blue, light blue, light pink and light yellow, respectively. Specificity for the F^- anion was seen. Nevertheless, the original orange colour of the free receptor **74** could be obtained from blue coloured acetonitrile solutions of **74**·F^- by treatment with $Ca(NO_3)_2$ (Fig. 74). On this basis, it was suggested that **74** could serve as a reversible fluoride anion sensor.

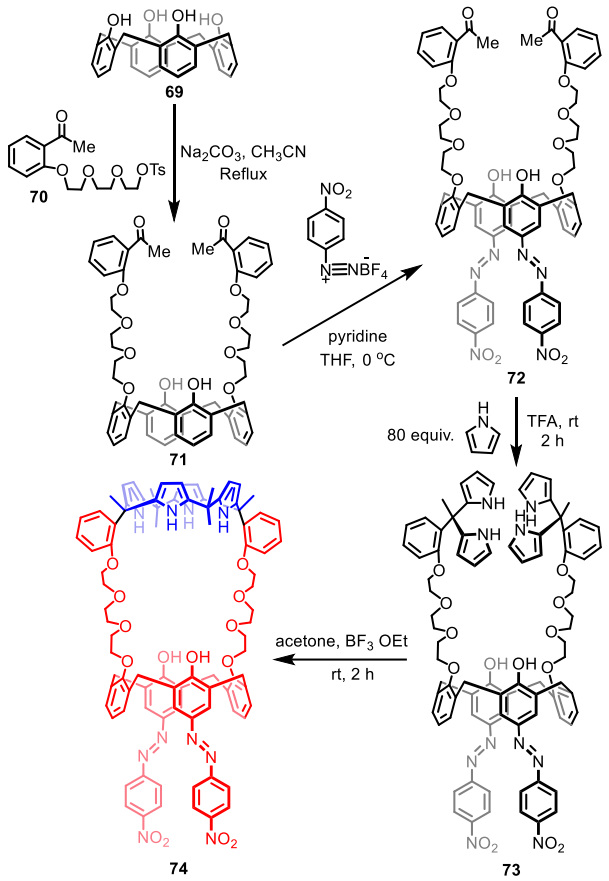

Fig. 73 Preparation and molecular structure of receptor **74**.

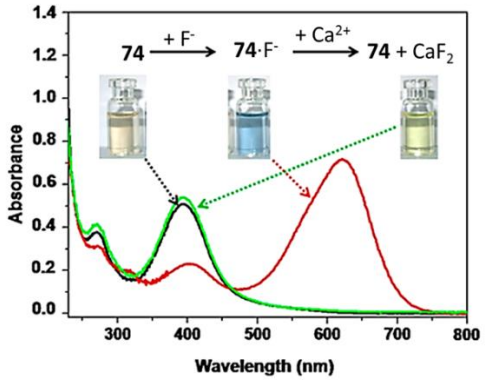

Fig. 74 Reversible coordination of **74** with F^- promoted by the addition of $Ca(NO_3)_2$ (acetonitrile solution). Reproduced with permission from ref. 125. Copyright 2012 American Chemical Society.

By introducing a 3-(dicyanomethylidene)indan-1-one chromophore into the known ion pair receptor (**63**) at a calix[4]pyrrole *β*-position (Fig. 75), Sessler, *et al.*[126] synthesized a colorimetric sensor (**75**) for various caesium salts (CsF, CsCl, and $CsNO_3$). UV-Vis and ^1H NMR spectroscopic studies performed in 10% methanol in chloroform revealed that receptor **75** was, as expected, capable of binding only caesium ion pairs (e.g., CsF, CsCl, and $CsNO_3$) but not the constituent caesium cation (as its perchlorate salt) or the F^-, Cl^-, or NO_3^- anions (as their TBA^+ salts). This system thus shows AND logic gate behaviour. In the presence of CsCl, and $CsNO_3$, the absorption peak of **75**, originally appearing around 500 nm in the UV-Vis spectrum, was found to undergo a bathochromic shift to 520 nm with a shoulder around 430 nm (Fig. 76).[126] These absorption spectral change accompany a noticeable colour change and are attributed to anion binding to the calix[4]pyrrole moiety covalently linked to the chromophore (Fig. 76). In the case of CsF, an association constant of 1.1×10^4 M^{-1} in 10% methanol in chloroform could be calculated for **75** for CsF on the basis of a UV-Vis spectral titration. Receptor **75** also showed a selective colorimetric response to caesium ion pairs under conditions of solid-liquid extraction when nitrobenzene was used as the receiving organic phase. Extractions of caesium salts could be achieved using nitrobenzene–d_5 and D_2O as the two phases.[126]

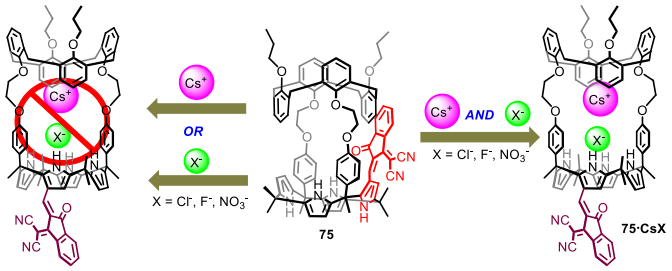

Fig. 75 Chemical structure of ion pair sensor **75** and its proposed ion or ion pair binding behaviour that proved consistent with that of an AND logic gate.

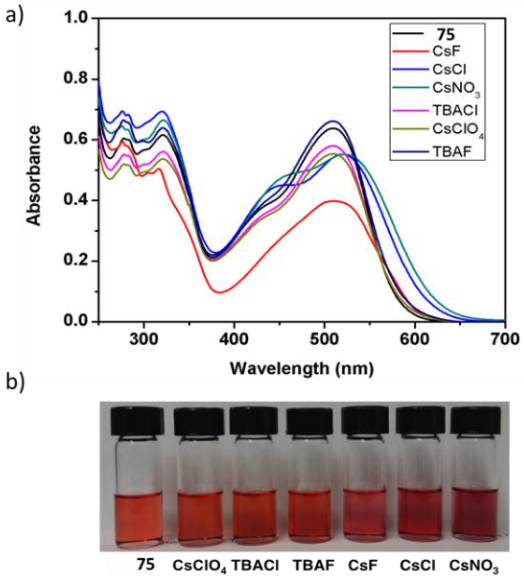

Fig. 76 (a) UV-Vis absorption spectra of receptor **75** in 10% methanol in chloroform recorded in the presence and absence of 5 equiv. of various salts. (b) Colour changes of solutions of **75** induced by the indicated ion pairs (5 equiv.). Reproduced with permission from ref. 126. Copyright 2016 American Chemical Society.

5 Hemispherand-strapped calix[4]pyrroles

Recent work has established that hemispherand-strapped calix[4]pyrroles are effective receptors for lithium salts, *e.g.*, $LiNO_2$ and LiCl. Such systems also show promise for recognizing

and extracting relatively "hard" ion pairs, such as CsOH. The design strategy, synthesis, and applications of such receptors will be discussed in detail in this section.

Recognition and extraction of the lithium cation is regarded as a challenge because of the high hydration energy (–473 kJ mol^{-1}) of this hard ion.[73] Given the importance of lithium cations in modern life,[127-129] Sessler and co-workers recently synthesized a new calix[4]pyrrole **76** in an effort to extract and recycle lithium salts. The hemispherand-containing strap (Fig. 77a) in receptor **76** was designed to serve as a lithium cation recognition site.[130] As true for the majority of strapped calix[4]pyrroles, the desired receptor, as well as other hemispherand-strapped calix[4]pyrroles mentioned in this section, were obtained via the condensation of a hemispherand-containing bis-dipyrromethane and excess acetone in the presence of $BF_3{\cdot}OEt_2$ as a catalyst. According to a single-crystal X-ray diffraction analysis, receptor **76** is capable of complexing several lithium salts (e.g., LiCl, LiBr, LiI, $LiNO_2$, and $LiNO_3$) with 1:1 stoichiometry (Fig. 77b). ^{1}H NMR spectral analyses in CD_2Cl_2/CD_3OD (9:1, v/v) solution revealed a high selectivity towards lithium salts over the corresponding Na^+, K^+, and Rb^+ salts. This observed selectivity was supported by DFT calculations. When employed as an ion pair extractant under both solid-liquid extraction (SLE) into CD_2Cl_2 and liquid-liquid extraction (LLE), from D_2O to $CDCl_3$, conditions, receptor **76** proved capable of extracting $LiNO_2$ efficiently into the organic phase. High selectivity over $NaNO_2$ and KNO_2 was seen (Fig. 78).

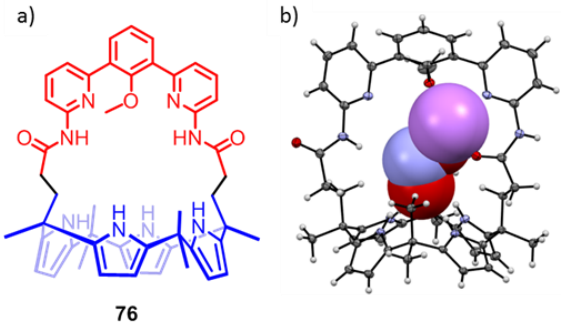

Fig. 77 (a) Structure of receptor **76** and (b) single crystal structure of **76**·$LiNO_2$. Solvents are omitted for clarity. The figure was generated using data downloaded from the Cambridge Crystallographic Data Centre (CSD Nos. 1483283).

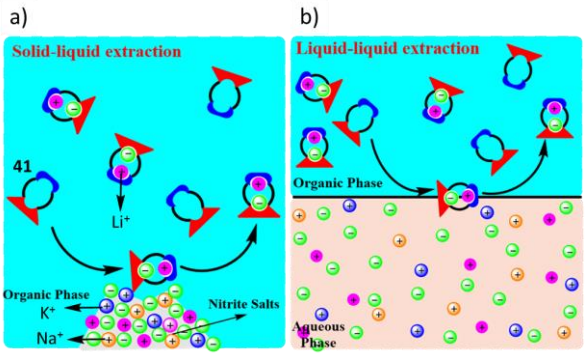

Fig. 78 Illustration of solid-liquid extraction and liquid-liquid extraction of $LiNO_2$ with **76** as the extractant. Adapted with permission from ref. 130. Copyright 2016 American Chemical Society.

Apart from serving as a ditopic ion pair receptor, **76** proved able to act as a M_2X-type tritopic ion pair receptor for charge-diffuse cations such as Cs^+. A M_2X-type ion pair complex was predicted based on an appreciation that calix[4]pyrrole is able to accommodate large cations in its cone conformation, whereas the defined cavity of the large hemispherand strap could fit well another Cs^+ cation. In fact, receptor **76** was found to bind Cs_2CO_3 in a 1:1 ratio. In the resulting complex, both tight-contact and host-separated binding modes were observed (Fig. 79a), as determined via a single crystal X-ray diffraction analysis, DFT calculations, as well as ^{1}H NMR spectroscopic analyses carried out in $CDCl_3$.[131] The ion pair CsOH was also captured by **76** as a tight contact pair (Fig. 79b), as evidenced from DFT calculations and ^{1}H NMR spectroscopic titrations carried out in acetone–d_6/D_2O (9:1, v/v). In liquid-liquid extraction experiments, **76** was found capable of extracting Cs_2CO_3 and CsOH from highly basic aqueous solutions into a $CDCl_3$ organic phase. Decent selectivity over CsF, CsCl, CsBr, and CsI was found (Fig. 80a). The results were even more impressive considering the high hydration energies of OH^- (–430 kJ mol^{-1}) and CO_3^{2-} (–1315 kJ mol^{-1}).[132] Further evidence of CsOH extraction by **76** came from a U-tube transport experiment (Fig. 80b), wherein the transport of CsOH through an intervening chloroform layer was promoted by **76**.

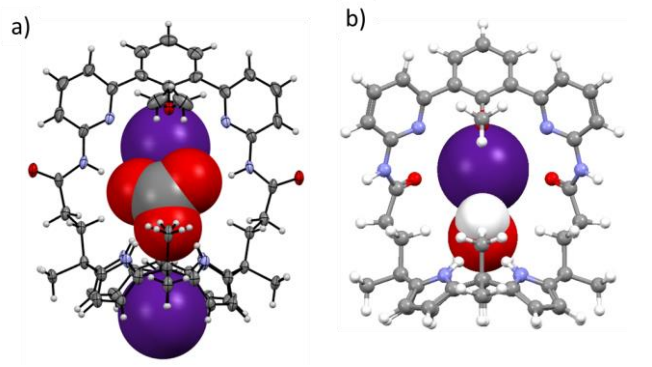

Fig. 79 (a) Single crystal structure of complex **76**·$CsCO_3$. The figure was generated using data downloaded from the Cambridge Crystallographic Data Centre (CSD Nos. 1549914). (b) DFT optimized structure of complex **76**·CsOH. Reproduced from ref. 131 with permission. Copyright 2017 Wiley-VCH Verlag GmbH & Co. KGaA.

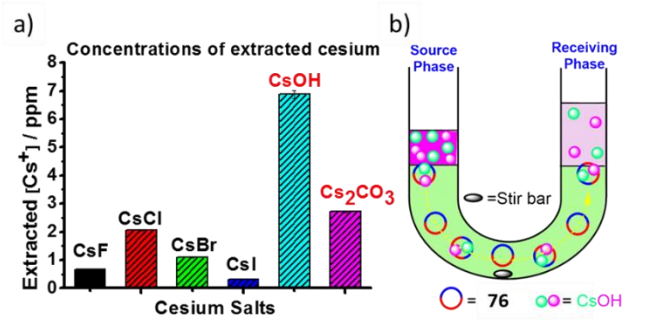

Fig. 80 (a) Concentrations of caesium salts extracted from aqueous solutions using **76** as the extractant. (b) Illustration of U-tube setup to test the ability of **76** to extract CsOH in liquid-liquid conditions. Reproduced from ref. 131 with permission. Copyright 2017 Wiley-VCH Verlag GmbH & Co. KGaA.

In order to isolate the classic hard salt LiCl from unconventional sources, such as brackish brines,[133] in 2018, Kim, Moyer, Sessler, *et al.* synthesized the two strapped calix[4]pyrroles **77** and **78** (Fig. 81). These systems, which contain, respectively, hemispherand and phenanthroline subunits on the straps, were found to promote the solid-liquid extraction and liquid-liquid extraction of LiCl.[134] Receptors **77** and **78** were found to complex LiCl with a 1:1 binding stoichiometry, as inferred from ^{1}H NMR spectral studies in $CDCl_3/CD_3OD$ (9:1, v/v), as well as a single crystal structure analysis (Fig. 82). As expected, the relatively small size of the strap-defined cavity favoured binding of the bound LiCl ion pair in a direct contact mode that maximized a coulombic interaction. These complexation features were thought to improve the selectivity and efficiency of the LiCl binding. process. Extraction experiments revealed that **77** is capable of extracting LiCl, NaCl, and KCl individually from the corresponding pure solid phases into an organic $C_6D_5NO_2$ phase, and with 100% receptor loading when the contact time exceeded 48 h. However, when a mixture of these three salts was tested as the solid phase, receptor **77** exhibited high selectivity towards LiCl over the other two salts (i.e., NaCl and KCl), even when the mass content of LiCl was as low as 1% (Fig. 83), as inferred from ^{1}H NMR spectroscopy analyses, flame tests, and inductively coupled mass spectrometric (ICP–MS) experiments. In the case of liquid-liquid extraction (from an aqueous source phase into a nitrobenzene solution), an extraction selectivity of KCl > NaCl > LiCl was seen for **77**; this is exactly opposite the order expected based on the hydration energies of the salts in question.[132, 135]

In contrast to **77**, receptor **78** was found to complex only LiCl under the conditions of both solid-liquid and liquid-liquid extraction. A selectivity of almost 100% in favour of LiCl over NaCl and KCl was thus inferred; this was true even when the LiCl content in the salt mixture was as low as 200 ppm. This remarkable selectivity was attributed to the relatively small cavity defined by the bridging strap. However, in spite its superior selectivity, the extent of LiCl loading achieved using **78** proved to be lower than that of **77**.

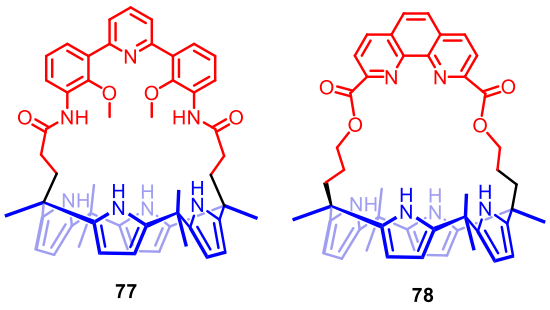

Fig. 81 Structures of receptors **77** and **78**.

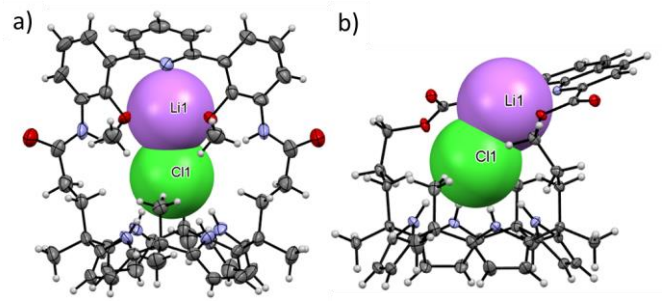

Fig. 82 Single crystal structures of complexes (a) **77**·LiCl and (b) **78**·LiCl. These figures were generated using data downloaded from the Cambridge Crystallographic Data Centre (CSD Nos. 1821811 and 1821810).

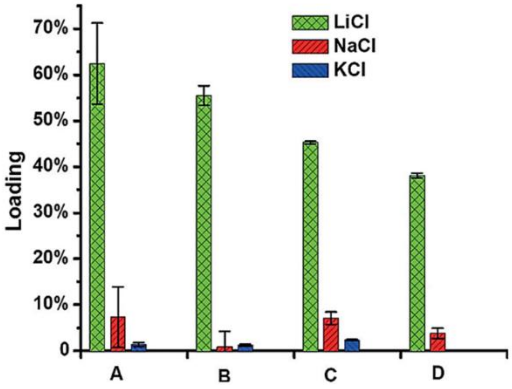

Fig. 83 Receptor loading percentage obtained from ICP–MS analyses made after solid-liquid extraction with different solid mixture A) LiCl, NaCl, and KCl (1:1:1 in molar ratio), B) NaCl and KCl containing 10% wt. of LiCl, C) NaCl and KCl containing 1% wt. of LiCl, and D) NaCl and KCl containing 200 ppm LiCl (by mass). A)–C) Results for receptor **77** (4 mM in nitrobenzene), and D) receptor **78** (3 mM in chloroform). Reproduced from ref. 134 with permission. Copyright 2018 Wiley-VCH Verlag GmbH & Co. KGaA.

6 Calix[4]pyrrole-strapped calix[4]pyrroles

In this section, calix[4]pyrrole-strapped calix[4]pyrroles, namely bis-calix[4]pyrroles, will be discussed. Typically, bis-calix[4]pyrroles contain larger inner cavities and a greater number of anion recognition sites than simple monomeric calix[4]pyrroles. As a consequence, they often display unexpected binding behaviour. For example, bis-calix[4]pyrroles are capable of capturing two anions, such as two fluoride anions, two chloride, two $H_2PO_4^-$ anions, or two SO_4^{2-} anions. In addition, they often function as effective complexants for ion pairs.

In 2012, a bis-calix[4]pyrrole macrocycle **80** (Fig. 84) was reported by Ballester and co-workers along with a new strategy for the construction of pseudorotaxanes via polyatomic anion assistance.[136] Hay coupling of calix[4]pyrrole **79** templated by one equivalent of 4,4'-bispyridine-1,1'-dioxide afforded macrocycle **80** (Fig. 84). Bis-calix[4]pyrrole **80** proved capable of recognizing ditopic linear bis-amidepyridyl-*N*-oxides (e.g., **81**) in ratio of 1:1, forming a noncovalent neutral ion pair complex **80·81** (Fig. 85), as evidenced by ^{1}H NMR spectroscopic analyses carried out in $CDCl_3$. The linear substrate **81** was found to thread through the receptor cavity, giving rise to a pseudorotaxane topology.

The addition of one equivalent of **83** to $CDCl_3$ solutions of **80**

and **81** produced four-particle threaded assemblies **83**⊃**80**·**81**, wherein the polyatomic anion resides in the cavity defined by the encapsulated **81** and a calix[4]pyrrole macrocycle. The TBA$^+$ counter cation is located in the external bowl-shaped calix[4]pyrrole cavity (Fig. 85). The pseudorotaxane topology proposed for **83**⊃**80**·**81** was supported by ^{1}H NMR spectroscopic studies carried out in $CDCl_3$, as well as by ROESY and DOSY experiments. Replacing **81** by **82** allowed for the formation of a similar pseudorotaxane at room temperature. This also held true when **83** was replaced by **85**.

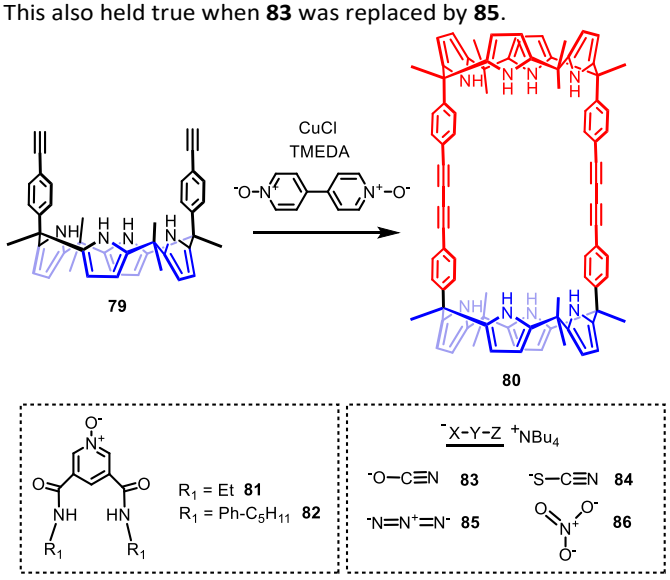

Fig. 84 Synthesis of **80**, structures of **81**, **82**, and ion pairs **83**–**86**.

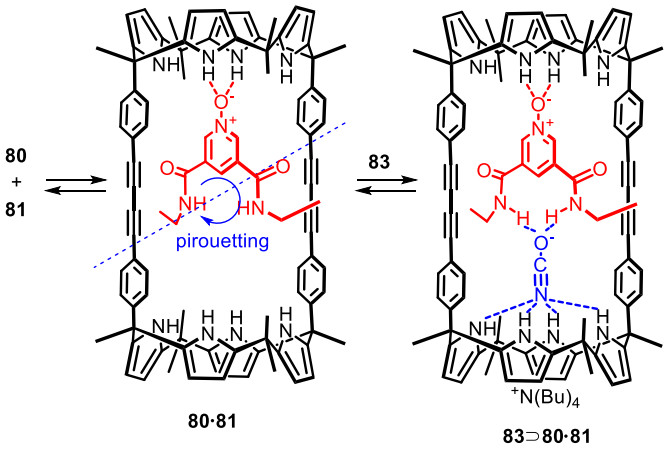

Fig. 85 Self–assembly of the [2]pseudorotaxane, **83**⊃**80**·**81**.

Soon after this finding was published, the same research group reported examples of cooperative aggregates containing ion pair dimers and ion quartets by using **80** as the host[137] in conjunction with guests **87**–**89** (Fig. 86). Upon the titration of **80** with TBACl or TBAOCN in $CDCl_3$, a 1:2 (receptor:ion pair) complex was formed. Importantly, the corresponding 1:1 complex was not observed under these experiment conditions. In the solid state a five-component cascade structure **87**$_2$⊂**80** (**88**$_2$⊂**80**) was seen as inferred from a single crystal structural analysis. In this structure, one ion pair is bound in a direct contact mode, while the other pair is bound in a host-separated fashion (as **87**$_2$⊂**80**; shown in Fig. 87a). The stability constant of **87**$_2$⊂**80**, defined as the square value of the binding constant, was determined to be $K_{2:1}$(**87**$_2$⊂**80**) = (1.5 ±0.3) x 10^{11} L^2 mol^{-2} in $CHCl_3$ via an ITC analysis. Setting the binding constant for the formation of **87**⊂**79** (K_{ref} = 33 L mol^{-1}) as the reference, the cooperativity factor was calculated as α = $K_{2:1}$(**87**$_2$⊂**80**)/K_{ref}^2 = 1.3 x 10^8, which defined this recognition process as one of the most cooperative binding events reported at the time.

In $CDCl_3$ solutions containing equimolar quantities of **87**, **88**, and **80**, the ion pair heterodimer complexes **87&88**⊂**80** could be obtained (Fig. 87b). Upon the addition of equimolar quantities of **89** to a $CDCl_3$ solution of **80**, a mixture consisting of free **80**, along with complexes **89**⊂**80** and **89**$_2$⊂**80** was obtained as inferred from ^{1}H NMR spectroscopic analyses. In this case, a host-separated ion pair binding mode was found to dominate, presumably because of the better fit provided by the methyl trioctylammonium (MTOA$^+$) cation than a TBA$^+$ cation within the external bowl-shaped calix[4]pyrrole "cup" (Fig. 88). In this case, the calculated cooperativity factor value was only 35 (Fig. 88).

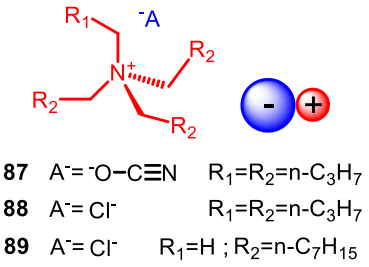

Fig. 86 Structure of ion pairs **87**, **88**, and **89**.

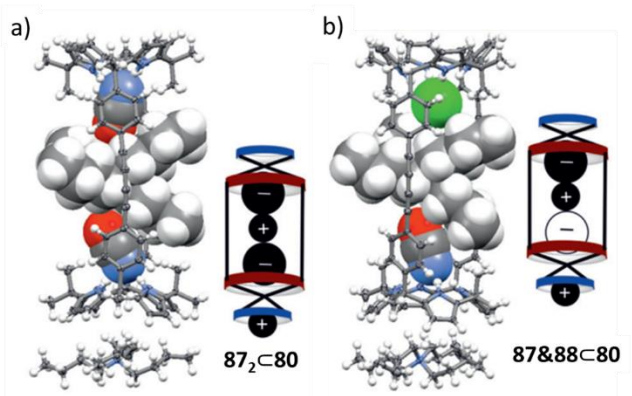

Fig. 87 Single crystal structures of **87**$_2$⊂**80** and **87&88**⊂**80**. Reproduced from ref. 137 with permission. Copyright 2018 Wiley-VCH Verlag GmbH & Co. KGaA.

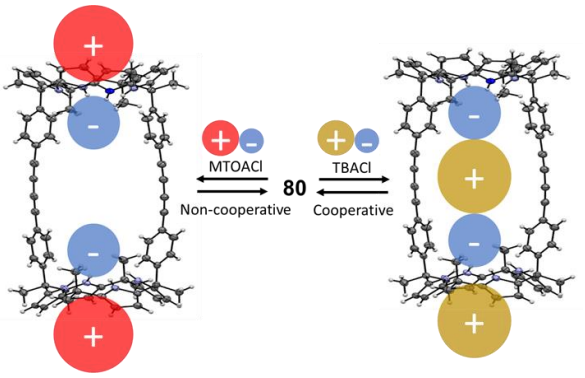

Fig. 88 Illustration of binding modes of complexes **89**$_2$⊂**80** (left) and **88**$_2$⊂**80** (right).

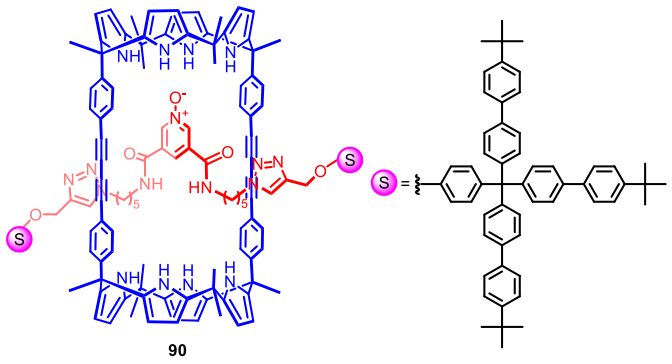

Fig. 89 Structure of the [2]rotaxane **90**.

In situ capping of the above **80**-derived [2]pseudorotaxane with tris(biphenyl) stoppers, allowed the [2]rotaxane **90** (Fig. 89) to be prepared, as demonstrated by Ballester and co-workers.[138] In $CDCl_3$ solution, hydrogen bonding interactions between the macrocycle, the threaded linear molecule, and the interlocked supramolecular structure were identified using ^{1}H NMR and DOSY NMR spectroscopy. The [2]rotaxane **90** was found to bind TBAOCN in a 1:1 host:guest ratio, wherein the ion pair was held in a host-separated fashion. When $TBANO_3$ and TBACl were tested as ion pair guests, similar results were obtained. Receptor **90** demonstrated high selectivity for TBAOCN over $TBANO_3$ and TBACl, as inferred from ITC studies carried out in chloroform solution. The selectivity observed was ascribed to the better shape and size match between the specific cavity of the [2]rotaxane and the TBAOCN ion pair. This conclusion was supported by simple molecular modelling studies. It was found that the size of the counter cation also played an important role in modulating the binding features. For instance, the association constant corresponding to the formation of MTOACl⊂**90** proved to be three orders of magnitude higher than that for the formation of TBACl⊂**90**. Again, this finding was rationalized in terms of a better fit of the $MTOA^+$ cations within the bowl-shaped calix[4]pyrrole cavity. In fact, under otherwise identical experimental conditions, ^{1}H NMR spectral studies revealed that the complex MTOACl⊂**80·91** completely disassembled upon the addition of 2 equiv. of MTOACl. In contrast, the proton signal of MTOACl⊂**90** was still observed even after adding 8 equiv. of MTOACl. The higher stability for MTOACl⊂**90** inferred on this basis was reflected in the corresponding stability values. Taken in concert, these findings led the authors to propose that the complexation events are guided by the mechanism shown in Fig. 90.

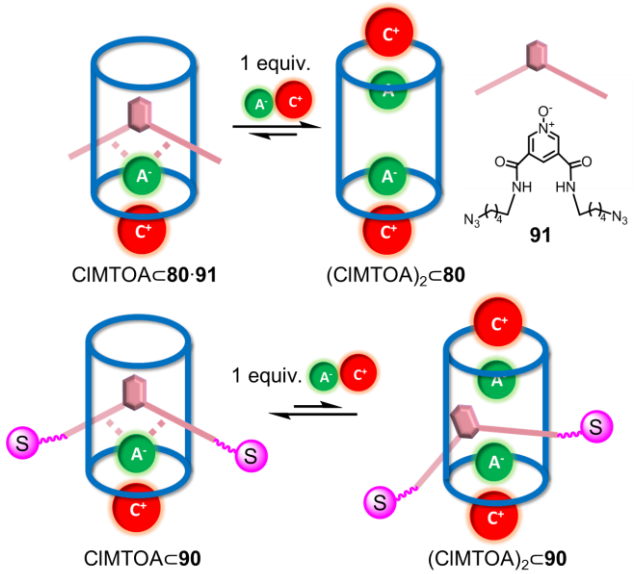

Fig. 90 Illustration of the plausible equilibria between 1:1 and 2:1 (ion pair:receptor) complex involving the [2]pseudorotaxane **80·91** and [2]rotaxane **90**.

In 2018, the same research group synthesized a bis-calix[4]-pyrrole macrocycle, **93**, that features a 1,4-diphenyl-triazole subunit as the spacer (Fig. 91).[139] This linker endowed **93** with a bent shape rather than the linear shape seen in the case of **80**. The presence of substituents within the 1,2,3-triazole spacers served to lower the symmetry of macrocycle **93** giving rise to two different calix[4]pyrrole binding sites. Supporting ^{1}H NMR spectral titrations with MTOACl carried out in $CDCl_3$ revealed the ion pair to be bound preferentially to the N–1 substituted hemisphere. This results in formation of a host-separated 1:1 complex. Incremental injection of MTOACl was found to give a 2:1 (ion pair:host) complex best described as involving a receptor-separated binding mode (Fig. 92a).

Taking the "two-wall" calix[4]pyrrole receptors **94** and **95** as references, ITC studies in $CHCl_3$ revealed a negative cooperativity for the binding of a second MTOACl ion pair. Plausible reasons for this behaviour include the electrostatic repulsion between the two bound chloride ions and the relatively low conformational flexibility of the system**.** In sharp contrast, complex $(TBACl)_2$·**93** proved to be characterized by a "cascade-like" structure (Fig. 92b), wherein one TBA^+ cation is

sandwiched between the two co-bound chloride ions. On the basis of ITC binding studies, it was proposed that the two binding sites do not interact in a cooperative fashion. The lack of cooperativity was thought to reflect the reduced size and the bent shape of the receptor and its cavity, which precludes formation of a perfect cascade arrangement as observed in the case of, e.g., $(TBACl)_2$·**80**.

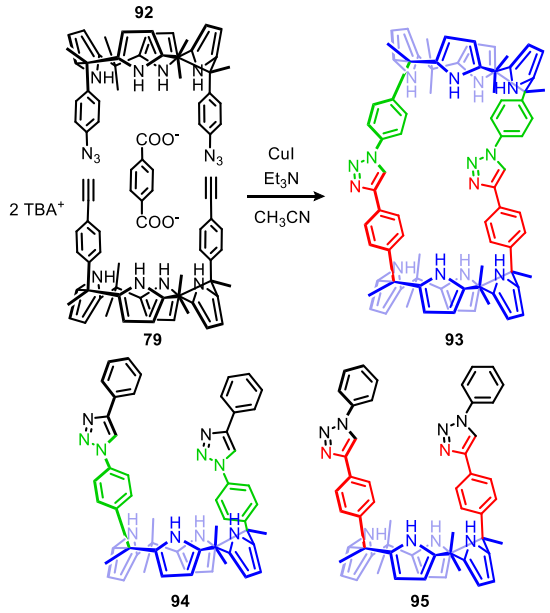

Fig. 91 Synthesis of **93** and structures of **94** and **95**.

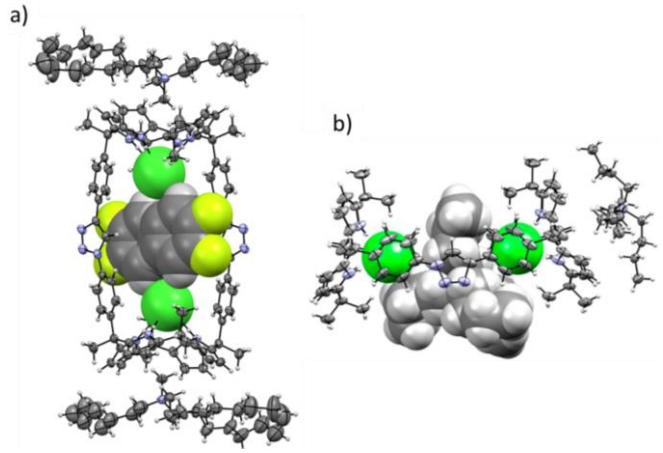

Fig. 92 (a) X-ray single crystal structure of $(MTOACl)_2$·**93** (two solvent molecules, 1,2–difluorobenzene, sandwiched by two chloride ions were displayed) and (b) $(TBACl)_2$·**93**. Reproduced from ref. 139 with permission. Copyright American Chemical Society, 2018.

In 2015, Lee and co-workers reported a tetracationic calix[4]pyrrole homodimer system, **96**, (Fig. 93a).[140] This receptor was obtained by coupling two *cis*-calix[4]pyrroles using a 9,10-bis(chloromethyl)anthracene subunit as the spacer. In **96**, the anthracene moiety was expected to serve as a fluorophore thus facilitating molecular recognition studies. As inferred from fluorescence spectroscopic titration analyses carried out in CH_3CN, receptor **96** exhibited a remarkable selectivity toward the fluoride ion (as its TBA^+ salt) over other anions (i.e., Cl^-, Br^-, I^-, $HP_2O_7^{3-}$, *etc.*), as inferred from the "turn on" fluorescence response that was seen only in the presence of a F^- anion source (Fig. 93b). Such high selectivity was attributed to the conformational restrictions imposed within receptor **96**. Non-linear sigmoidal binding isotherms were observed when the complexation events were monitored as a function of the F^- concentration. This was taken as evidence for a binding process subject to favourable cooperativity (i.e., positive homotropic allosterism). ITC studies proved consistent with the formation of 1:1 and 1:2 host:guest complexes at molar ratios of ~0.5 and ~1.0 in CH_3CN and in a cooperative fashion. For instance, the second binding constant was found to be ~311-fold greater than the first one. Further support for this conclusion came from ^1H NMR spectroscopic studies carried out in CD_3CN.

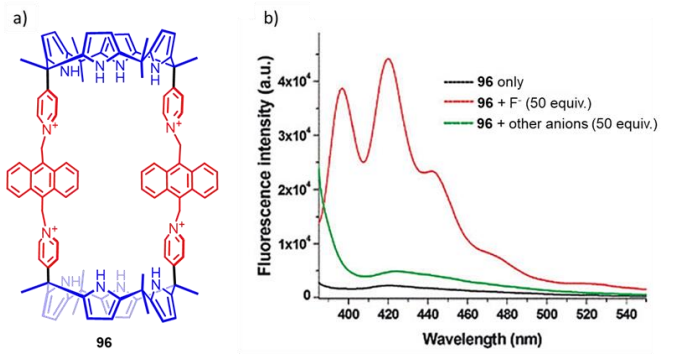

Fig. 93 (a) Structure of receptor **96** and (b) changes in the fluorescence intensity of **96** seen upon the addition of various anions. Reproduced from ref. 140 with permission. Copyright Royal Society of Chemistry, 2015.

Recently, the Sessler group reported a large capsule-like bis-calix[4]pyrrole **97** (Scheme 5).[141] Unlike Ballester's and Lee's work described above,[136-140] here a linked bis-dipyrromethane **98** serves as the key intermediate rather than a preformed disubstituted calix[4]pyrrole of generic structure **99** (Scheme 5). This strategy obviated the need to separate the two configurational isomers defined by **99**. Receptor **98** proved capable of accommodating large anions, *i.e.*, $H_2PO_4^-$, SO_4^{2-}, and $HP_2O_7^{3-}$ in a 1:2 host:guest ratio. The resulting system exhibited enzyme mimic-like features in that two oxoanions could be co-encapsulated and in close proximity. Evidence for these conclusions came from ^1H NMR and UV-vis spectroscopic studies, ITC titrations conducted in CD_2Cl_2/CH_3OD (9/1, v/v) or 1,2-dichloroethane, as well as a single crystal X-ray diffraction structure and DFT calculations (Fig. 94).

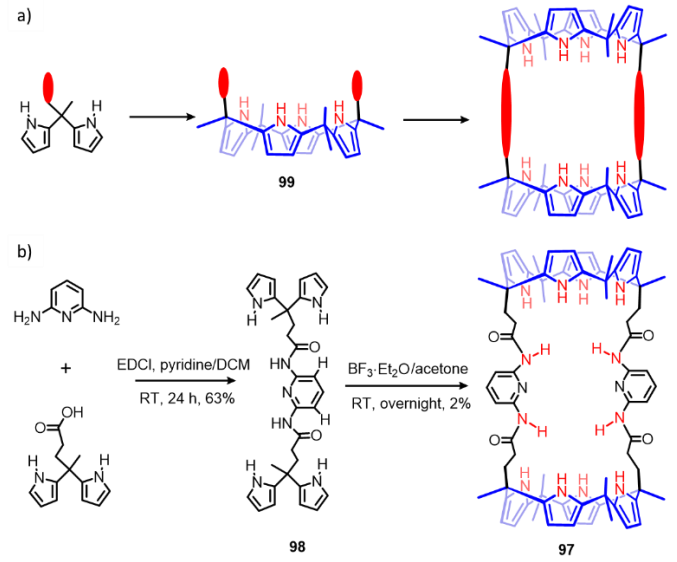

Scheme 5 Different strategies used to synthesize bis-calix[4]pyrroles (a) Ballester's and Lee's approach, and (b) that of Sessler. See ref. 141.

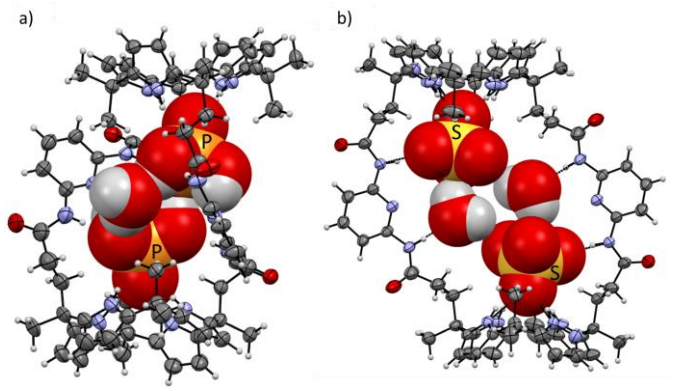

Fig. 94 Single crystal structure of (a) $(H_2PO_4^-)_2{\cdot}H_2O \subset$ **97** and (b) $(SO_4^{2-})_2{\cdot}(H_2O)_2 \subset$ **97** complex. These figures were generated using data downloaded from the Cambridge Crystallographic Data Centre (CSD Nos. 1535973 and 1535974).

7 Other types of strapped calix[4]pyrroles

In this section, strapped calix[4]pyrroles whose features make them difficult to be classified into one of the above categories will be reviewed. Examples include structurally complex 1,2-*meso*-*meso* mono strapped, doubly strapped calix[4]pyrroles, and quadruple strapped calix[4]pyrroles, among others.

In 2004, Lee and co-workers reported the synthesis and unique anion recognition characteristics of the metalloporphyrin strapped calix[4]pyrroles **100**–**105** (Fig. 95).[52, 142] It was expected that the combination of two noncovalent interactions (*i.e.*, the hydrogen bonding from calix[4]pyrroles NH protons and metal coordination-derived interactions stabilized by the metalloporphyrin) within one receptor would lead to a set of improved anion receptors. The syntheses involved condensation of metalloporphyrins bearing bis-dipyrromethane substituents with acetone. This afforded the desired macrocycles **100**–**102** and the unexpected isomers **103**–**105**. These latter isomers displayed distinct binding features, in particular, when tested in the context of halide anion recognition. In the case of **100**–**102**, host:ion pair complexes with a 1:1 binding ratio were formed upon the titration with the fluoride ion (as its TBA^+ salt) in $CDCl_3$. Selectivity for F^- over other halide anions was seen. Conversely, macrocycles **103**–**105** displayed minimal anion binding affinities, presumably as the result of their twisted nature that precluded facile accommodation of an anionic guest within their respective cavities.

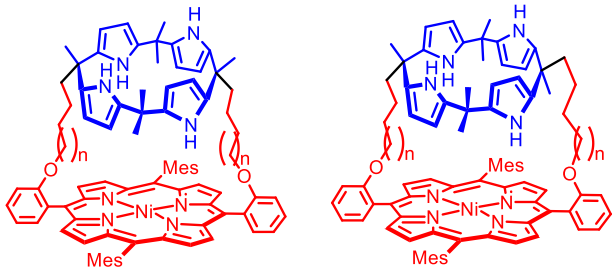

100 (n=1)
101 (n=2)
102 (n=3)

103 (n=1)
104 (n=2)
105 (n=3)

Fig. 95 Molecular structures of receptors **100**–**105**.

In 2007, the synthesis and qualitative anion binding features of calix[6]pyrroles **106**–**108** (Fig. 96) bearing 1,3,5-trisubstituted benzene caps were reported by the same group.[143] These large calixpyrrole derivatives were obtained via the intramolecular condensation of three dipyrromethane units appended to a 1,3,5-trisubstituted benzene platform. Qualitative anion binding studies revealed a high affinity towards the fluoride anion (studied as its TBA^+ salt) in the case of receptor **107** and the formation of a 1:1 host:guest complex in DMSO–d_6 solution. Similar analyses led to the conclusion that in the case of the chloride anion, only four out of six pyrrolic NH protons were involved in binding.

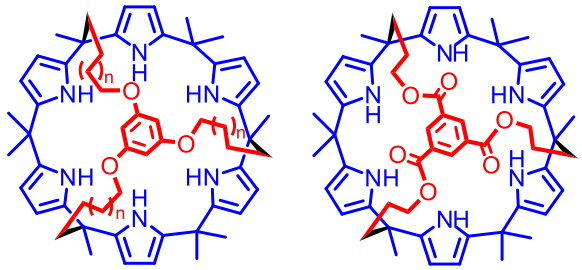

106 (n=1)
107 (n=2)

108

Fig. 96 Molecular structures of receptors **106**–**108**.

Urea functionalized calix[4]pyrrole and calix[4]arene derivatives are known to form heterodimeric capsular assembly in presence of suitable guest molecules.[144] In 2012, the Ballester group reported a mechanically interlocked calix[4]arene capped calix[4]pyrrole **115** designed to exploit this key self-assembly chemistry.[145] The synthetic route used to access **115** is summarized in Scheme 6. Firstly, the doubly-looped tetraurea

calix[4]arene **112** was synthesized from the alkenyl tetraurea **109** by employing the tetratosyl urea **110** as a template (Scheme 6 and Fig. 97). This approach was thought to preclude intermolecular polymerization through the alkenyl group (Step 1). Using **112** as both the template and the reaction partner, a heterodimeric pseudo-[2]rotaxane **111·112** could then be formed (Step 2). Guests (**113** or **114**) were then used to induce dimerization of **111·112** and to form the bis-catenated supramolecular capsule **115** (Step 3).

The asymmetrical mechanically interlocked structure embodied in **115** leads to the presence of two complementary binding domains at opposite ends of the construct; these consist of a calix[4]pyrrole designed to provide hydrogen bond donors for anion or N–oxide recognition and a calix[4]arene for cation complexation. Thus, it was expected that **115** would serve as a closed container for ion pairs of suitable size and shape. In fact, encapsulation of tetramethylammonium chloride and tetramethylphosphonium chloride was demonstrated inside the cavity of the interlocked assembly. The interlocked system **115** was also used as a molecular container to encapsulate highly reactive N,N-dimethyl-2-propyn-1-amine N-oxide. This encapsulation served to stabilize the N-oxide moiety, which otherwise undergoes decomposition through sigmatropic rearrangements.[146] The control tetraurea-bis-loop calix[4]pyrrole **116** (Fig. 98) was also reported by the same group.[147]

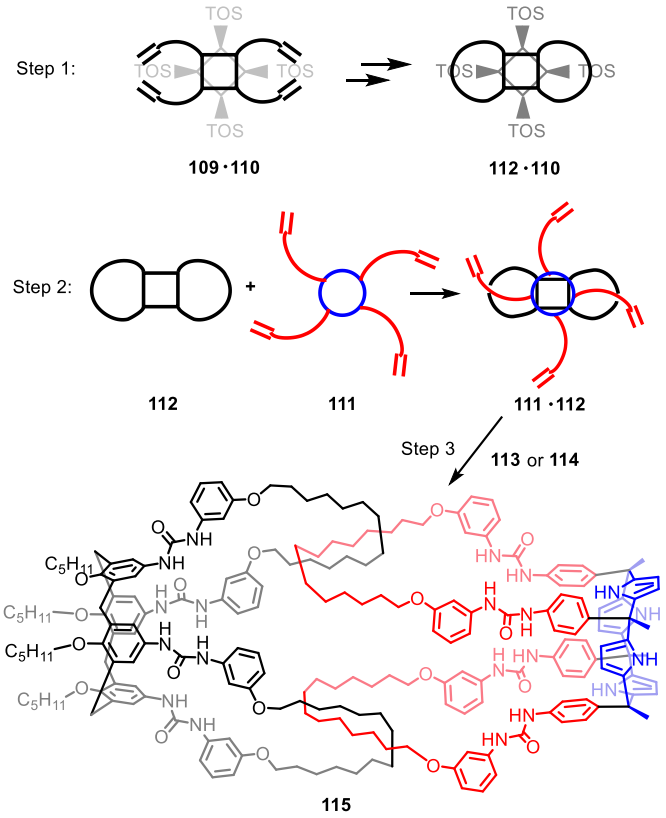

Scheme 6 Synthetic route used to access the interlocked receptor **115**.

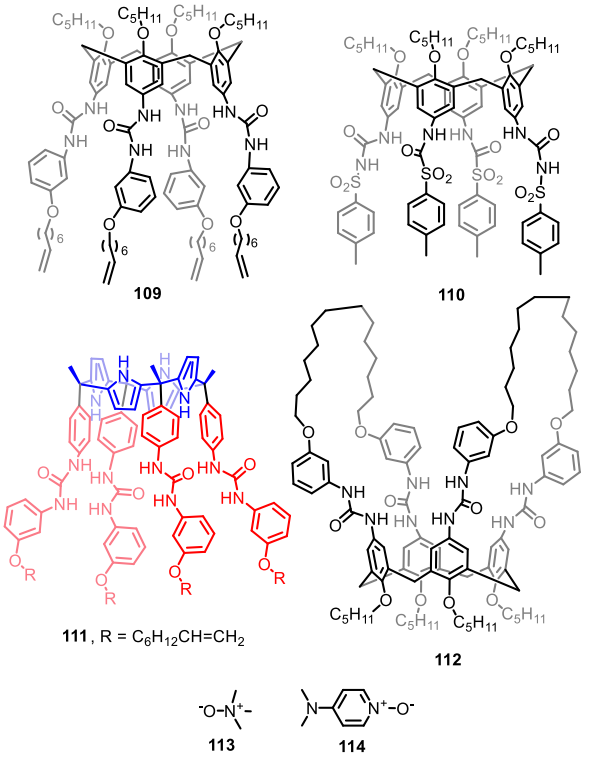

Fig. 97 Chemical structures of **109**–**114**.

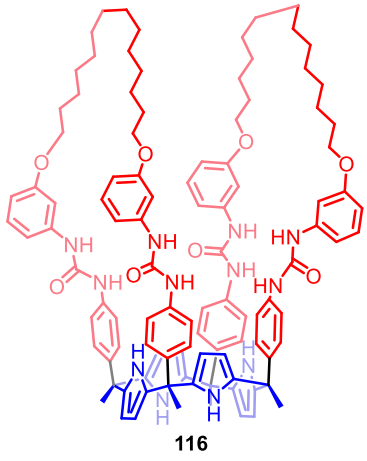

Fig. 98 Molecular structure of **116**.

Supramolecular hosts with deep cavities are of interest in the context of creating self-assembled molecular capsules and for the construction of covalent cages. They are appealing due to their ability to shield a bound guest from solvent and to control the structure of substrates through complexation.[148-151] A convenient synthetic strategy to access strapped calix[4]pyrroles with deep cavities involves the so-called intramolecular stitching of the *meso*-substituents present on aryl-extended calix[4]pyrroles.[152] A series of such strapped receptors (**118**–**121**) was generated from the calix[4]pyrrole-resorcinarene hybrid **117** bearing lipophilic $C_{12}H_{25}$ groups (Scheme 7). This cavitand-type system bears aromatic walls that can adopt two limiting conformations, a so-called kite form

where all the brim aromatic and heteroaromatic rings adopt equatorial orientations, and a vase form where the corresponding units are found in axial orientations. The ^{1}H NMR spectra of receptors **118**–**121** recorded in $CDCl_3$ led to the suggestion that the kite conformation was favoured over the vase form in all cases (Fig. 100a, b). X-ray diffraction analyses of single crystals of **118**, **119** and **120** obtained from acetonitrile solutions or acetonitrile/dichloromethane mixtures supported this conclusion and revealed the presence of a solvent molecule bound within the cavity.

Pyridine N-oxide derivatives (specifically **114** and **122–124**, Fig. 99) were employed as guest molecules in an effort to change the relative thermodynamic stabilities of the vase and the kite forms. Inclusion complexes with 1:1 host:guest stoichiometry were formed upon the titration of **114** into $CDCl_3$ solutions of **118** or **119**. Upfield shifts for the aryl proton signals were seen in the corresponding ^{1}H NMR spectra upon treatment of these receptors with **114**. This was taken as evidence that the guest is bound within the receptor cavity. As inferred from both solution phase studies and solid state structural analyses, the N-oxide complex also favours the kite form (Fig. 100c). In the resulting complex, the oxygen atom of the guest is bound to the four pyrrolic NH protons via hydrogen bonds, whereas the pyridyl unit interacts with the aromatic wall through presumed π–π or CH–π interactions.

A 1:1 complex was also observed in the system consisting of **114** and **120**. In this case, an ^{1}H NMR spectral analysis ($CDCl_3$) led to the suggestion that the vase and kite forms of the complex might coexist. The N-oxides **122–124** were used to probe this possibility and to test whether guest binding could be used to induce changes in the receptor conformation. In fact, structural analyses revealed that all of the N–oxide inclusion complexes existed exclusively in the kite form, at least in the solid state. Experiments performed a higher-temperatures (398 K) using tetrachloroethane–d_2 as the solvent, revealed that the vase form of the inclusion complexes generated from **120** are favoured under these specific solution phase conditions. Unfortunately, the percentages of the two limiting conformers proved difficult to quantify.

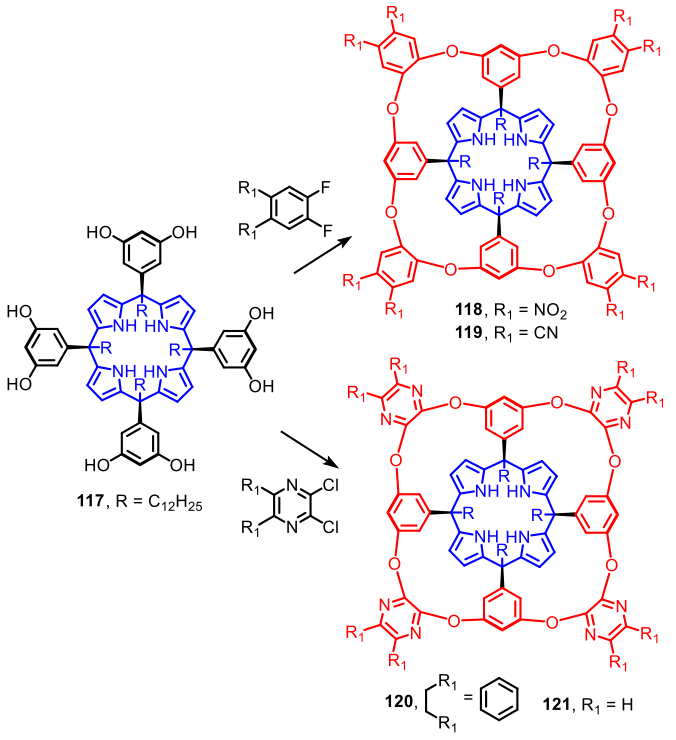

Scheme 7 Synthesis of **118**–**121** from **117**.

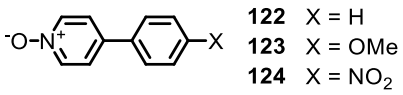

Fig. 99 Structure of pyridine N-oxide derivatives **122**–**124**.

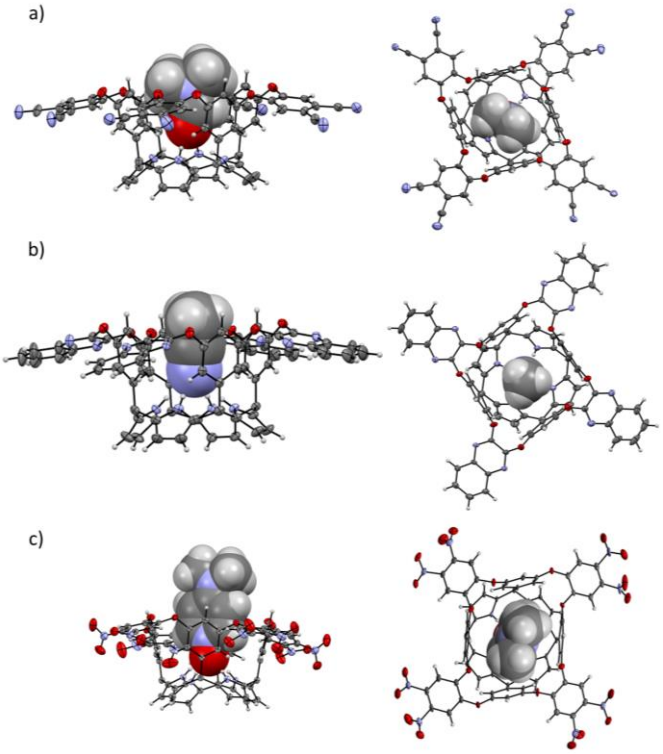

Fig. 100 Side and top views of the single crystal X-ray structures of (a) DMF⊂**119** and (b) CH_3CN⊂**120** and (c) **114**⊂**118**. Disordered solvent molecules and *meso*-alkyl chains are omitted for clarity. These figures were generated using data

downloaded from the Cambridge Crystallographic Data Centre (CSD Nos. 1009754, 1009753 and 1009752).

Efforts to create calix[4]pyrrole capped calix[4]pyrrole dimers were reported by Ballester in 2012.[136] Here, a *meso*-bis-aryl calix[4]pyrrole bearing terminal alkyne functionality (**125**) was tested as the key precursor. Intermediate **125** was then tested in conjunction with **128** and **129** as putative cyclization templates.[153] Unfortunately, in the case of the shorter putative template **128**, the products of the 'macrocyclization' reaction turned out to be an insoluble mixture of oligomers and polymers. On the other hand, Hay coupling of calix[4]pyrrole **125** in presence of the elongated template **129** afforded two soluble, but also undesired products, which were assigned as the partially connected homodimer **126** and a chiral tetrameric calix[4]pyrrole **127** (Fig. 101). A single-crystal X-ray diffraction analysis revealed that the calix[4]pyrrole tetramer **127** adopts a helical-like conformation upon encapsulation of two bis-N-oxide **129** (Fig. 102). This helical complex is chiral and mimics the structural features of a "Siamese-Twin porphyrin".[154]

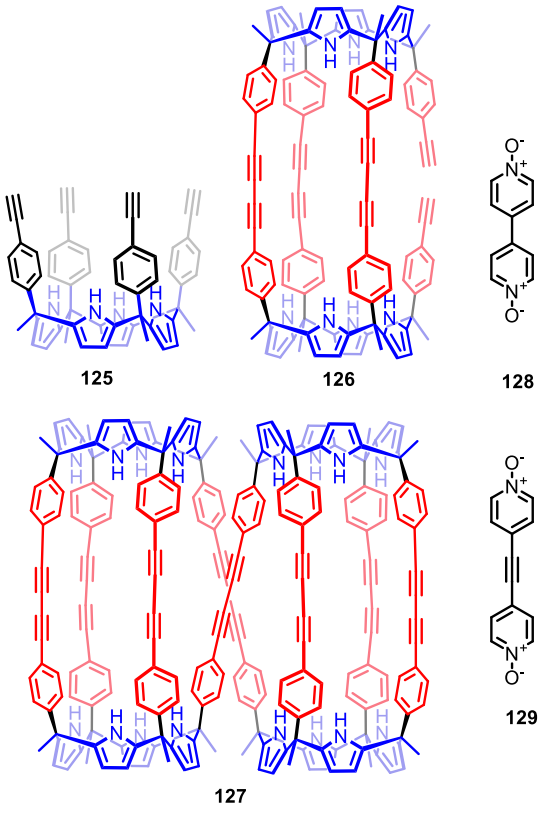

Fig. 101 Molecular structures of **125**–**129**.

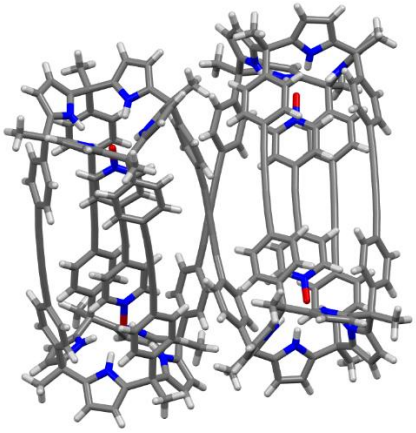

Fig. 102 X-ray single crystal structure of **129**$_2$⊂**127**. The figure was generated using data downloaded from the Cambridge Crystallographic Data Centre (CSD Nos. 1476422). Lattice solvents are removed for clarity.

The same group subsequently reported the successful synthesis of two calix[4]pyrrole homodimers (**130** and **131**). These systems, accessed via template-directed self-assembly, feature a large polar cavity.[155] As illustrated in Scheme 8, the condensation of 2 equiv. of the formyl-functionalized tetraaryl-extended calix[4]pyrrole **132** with 4 equiv. of diamines, in the presence of 1 equiv. of bipyridyl-N-oxide **129** as a template, afforded the target products **130** and **131**. As inferred from a ^{1}H NMR spectroscopic analysis, a sandwich-like complex, **129**⊂**132**$_2$, was formed in near quantitative yield in $CDCl_3$. On the basis of a molecular simulation study it was concluded that the binding of **129** as a guest serves to arrange the adjacent formyl units on the upper rim of **132** in a position suitable for pairwise reaction with the selected diamines (Fig. 103). In fact, the bis-calix[4]pyrrole capsules **130**/**131** were obtained in the form of inclusion complexes **129**⊂**130**/**131** (Fig. 104). These products were characterized by an almost perfect fit between the receptor and substrate.

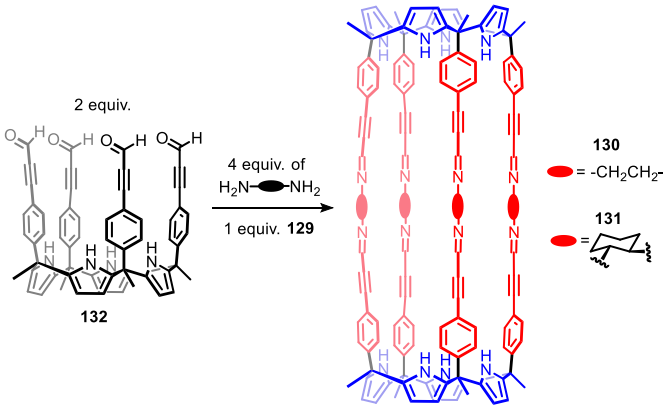

Scheme 8 Synthetic route and molecular structure of octaimine capsules **130** and **131.**

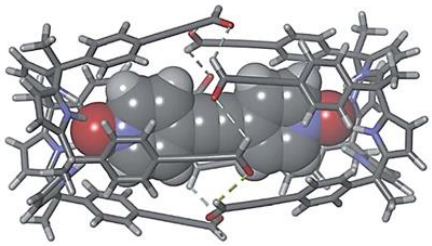

Fig. 103 Structure of the **129**⊂**132**$_2$ capsule with minimized energy in the molecular simulation studies. Reproduced from ref. 155 with permission. Copyright The Royal Society of Chemistry, 2017.

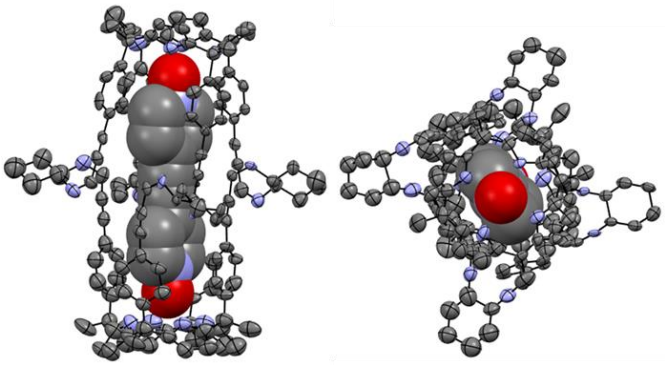

Fig. 104 Side and top view of the single-crystal X-ray structure of the host-guest inclusion complex **129**⊂**131**. Solvents and hydrogen atoms are omitted for clarity. These images were generated using data downloaded from the Cambridge Crystallographic Data Centre (CSD Nos. 1566200)

Using receptor **133**, a triethylenediamine-linked calix[4]pyrrole bisporphyrinate **135** could be generated in the presence of anionic substrate that interacts with the pyrrolic NH protons present in **133** (Fig. 105).[156, 157] Direct complexation of **133** with triethylenediamine generated a 1:2 stoichiometry host:guest complex, wherein the two amine guests interact separately with the two porphyrin fragments, as inferred from ^{1}H NMR spectroscopic studies carried out in CD_2Cl_2. In sharp contrast, the triethylenediamine-linked calix[4]pyrrole bisporphyrinate **135** was exclusively formed when the anion complexes **133**·F^-/Cl^- were used as the hosts. Binding of F^- or Cl^- to **133** stabilizes the cone conformation; presumably, this serves to shorten the distance between the two porphyrin fragments allowing for the two metalloporphyrin centres to approach one another to the point they can be bridged by an appropriately chosen diamine.

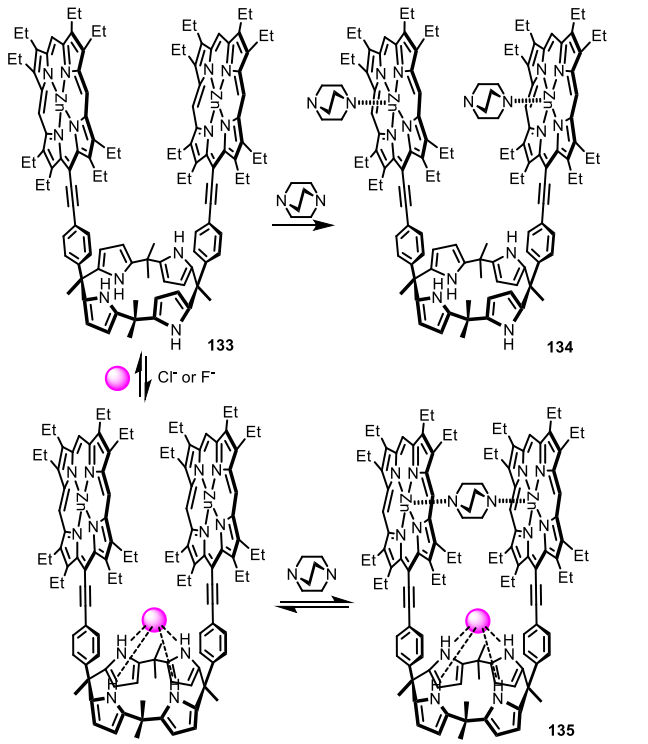

Fig. 105 Triethylenediamine-linked calix[4]pyrrole bisporphyrinate **135** created by pre-forming an anion complex.

Capsule-type calix[4]pyrrole dimers prepared via the coordination of a Cu^{II} cation to the carboxylate functionalized calix[4]pyrrole **136** and **137** were reported by Ballester (Fig. 106).[158] The nature of the solvent was found to play an important role in the formation of the capsular dimer. For instance, when dimethylformamide was used as the solvent, both **136** and **137** were found to form discrete capsules upon treatment with Cu^{II}. However, in diethylformamide only **137**, a system with a longer spacer, was able to support formation of the capsule-lime dimer.

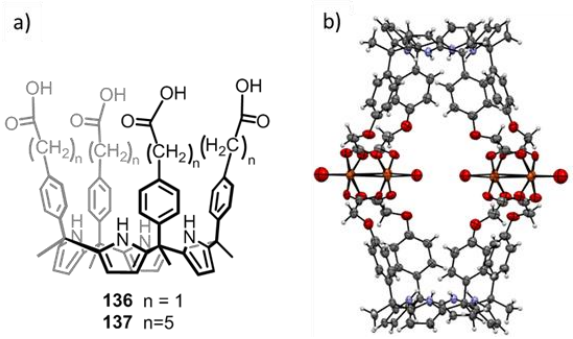

Fig. 106 (a) Structure of **136** and **137** and (b) the single crystal structure of a Cu^{II} complexation-driven capsule-type dimer formed from **136**. This figure was generated using data downloaded from the Cambridge Crystallographic Data Centre (CSD Nos. 1519366). Solvents are omitted for clarity.

In a report published in 2019, Ballester and co-workers disclosed a metal-capped calix[4]pyrrole wherein the upper rim of a *meso*-tetraaryl calix[4]pyrrole **138** (Fig. 107) is "sealed off" by means of Pd(II)-pyridyl coordination.[159] In this case, ^{1}H DOSY NMR experiments carried out in $CDCl_3$/CD_3CN (2:1 v/v) revealed

a cylindrical structure containing the [**138**·Pd]$^{2+}$ dication. When **138** was replaced by **139** the formation of analogous cage structure was not observed. Upon addition of 1 equiv. of **140** to **138** in a 2:1 $CDCl_3/CD_3CN$ solution, a 1:1 host:guest complex was formed. In this case, **140** resides within the deep aromatic cavity and is stabilized by presumed hydrogen bonding interaction with the pyrrolic NH protons. After adding 1 equiv. of Pd(II) to the above solution, an extra solvent molecule was required to stabilize the metallocage, as demonstrated by a single crystal X-ray diffraction analysis (Fig. 108a). The bis-N-oxide guest **128** was found to bind within capsule **138** (Fig. 108b).

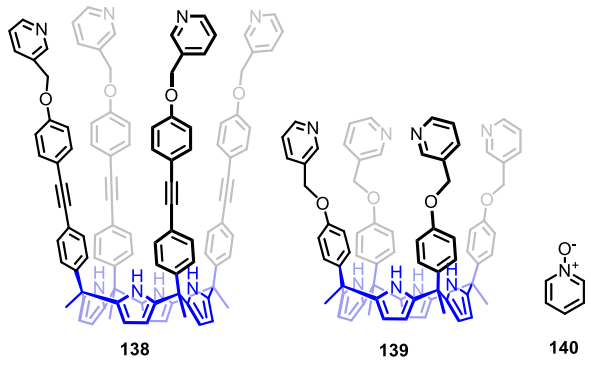

Fig. 107 Molecular structures of **138**–**140**.

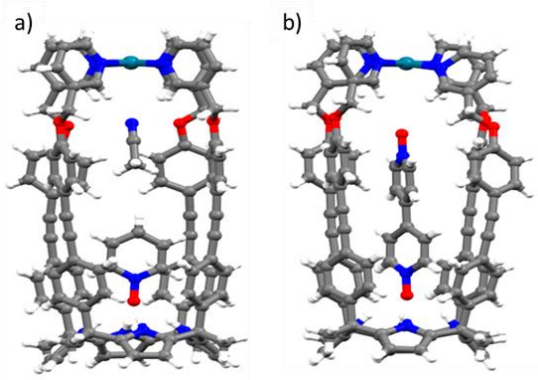

Fig. 108 X-ray crystal structures of (a) [**140**·CH_3CN]⊂[**138**·Pd]$^{2+}$ and (b) **128**⊂[**138**·Pd]$^{2+}$. These figures were generated using data downloaded from the Cambridge Crystallographic Data Centre (CSD Nos. 1876528 and 1876529). Counterions and lattice solvents are removed for clarity.

Doubly strapped calix[4]pyrroles featuring additional binding units and flexible strapped structures are attractive for the creation of new ion pair receptors.[62] In 2012, Lee, Gryko, and co-workers reported a new class of calix[4]pyrroles bearing proximal double straps on either side of the parent calix[4]pyrrole macrocycle (Fig. 109a and 109b).[160] The synthetic route is summarized in Scheme 9. Briefly, condensation of pyrrole with the bis-ketone **143** produces **141** or **142** along with a by-product (**145**) involving loss of a pyrrole. These two bis-ketones displayed distinctively different configurations in the solid state. As revealed by single-crystal X-ray diffraction analyses (Fig. 109c and 109d), **141** adopts a bowl shape with the calix[4]pyrrole unit in the 1,3-alternate form. In contrast, **142** is characterized by a scoop-like geometry with the calix[4]pyrrole macrocycle existing in a partial cone conformation. ITC studies of receptor **141** with Cl^- in acetonitrile revealed an exothermic binding pattern. The binding constant (K_a) corresponding to the formation of **141**·Cl^- was 2.65 × 10^5 M^{-1}. In contrast, the binding constant corresponding to the formation of the corresponding complex, **142**·Cl^- was one order of magnitude lower (K_a = 2.31 × 10^4 M^{-1}). The higher K_a value for the formation **142**·Cl^- was rationalized in terms of better pre-organization and improved cooperative binding relative to **141**.

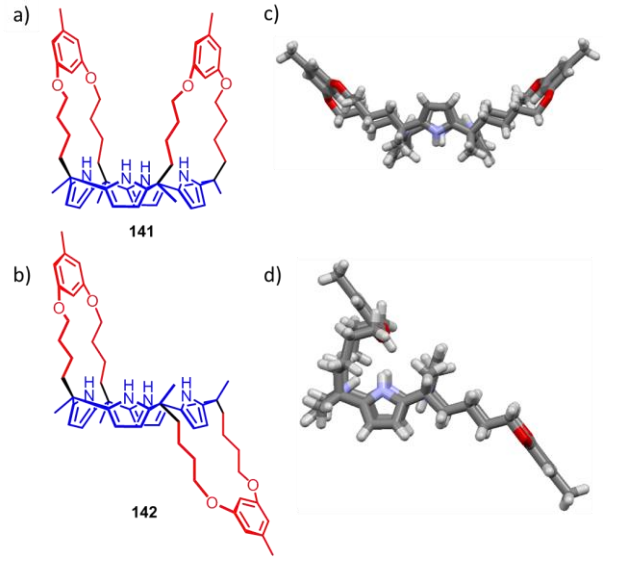

Fig. 109 Molecular structures of *meso-meso* strapped calix[4]pyrroles a) **141** and b) **142**, and X-ray single crystal structures of c) **141** and d) **142**. The X-ray images were generated using data downloaded from the Cambridge Crystallographic Data Centre (CSD Nos. 872113 and 872114). Solvent molecules have been omitted for clarity

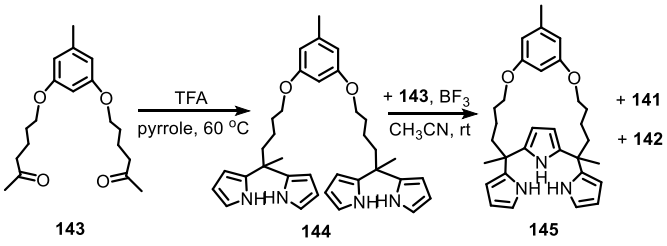

Scheme 9 Synthesis of **141** and **142**.

Ballester, Dalcanale, and co-workers reported three aryl-extended calix[4]pyrrole diastereomeric bis-phosphonate cavitands (structures **147ii**, **147io**, and **147oo** in Fig. 110).[161] The synthesis is shown in Fig. 110. Here, the tetrol **146** was chosen as the key calix[4]pyrrole starting material. The diastereoisomers obtained through reaction were found to differ in the relative spatial orientation of the P=O groups (ii = in, in; io = in, out; oo = out, out) present on the upper rims. Receptors **147** were found to bind ion pairs and to form a 1:1 complex with tetramethylphosphonium chloride (TMPCl) in dichloromethane solution. ^{1}H NMR and ^{31}P NMR spectroscopic analyses in dichloromethane-d_2 provided support for the notion that the chloride ion resides in the deep cavity of the host where it is stabilized via hydrogen bonding interactions with the four

pyrrolic NH protons. In contrast, a close contact binding mode was seen in the case of **147ii**·TMPCl. Ion-separated binding interactions were seen in the case of **147io/147oo**·TMPCl (Fig. 111). A single crystal X-ray structural analyses of this series of complexes revealed the presence of a columnar motif in the solid state (Fig. 112).

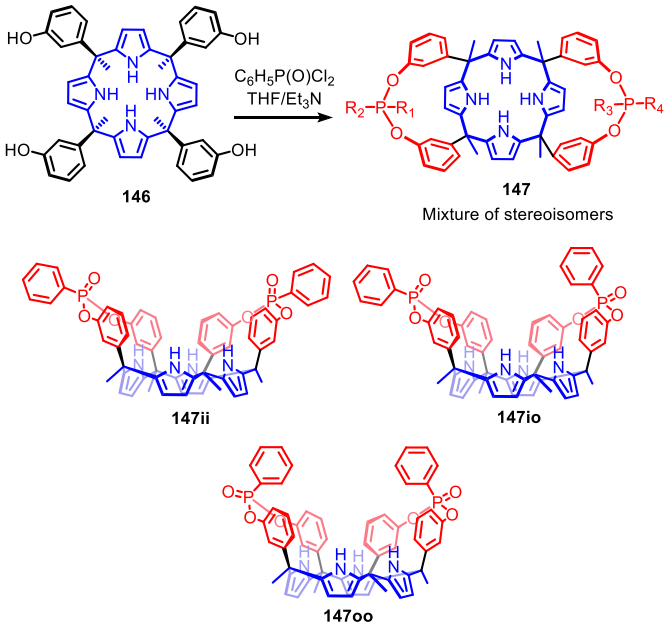

Fig. 110 Synthesis of a mixture of stereoisomers **147** and chemical structures of **147ii**, **147io**, and **147oo**.

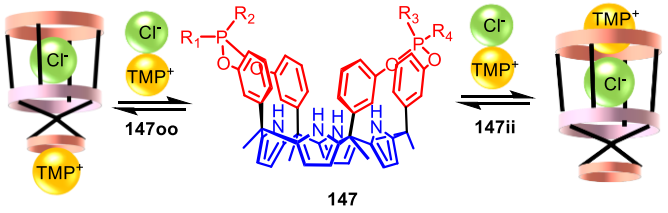

Fig. 111 Binding modes corresponding to the formation of the 1:1 complex **147**·TMPCl as inferred from the ^{1}H and ^{31}P NMR spectral data obtained from studies carried out in CD_2Cl_2 solutions.

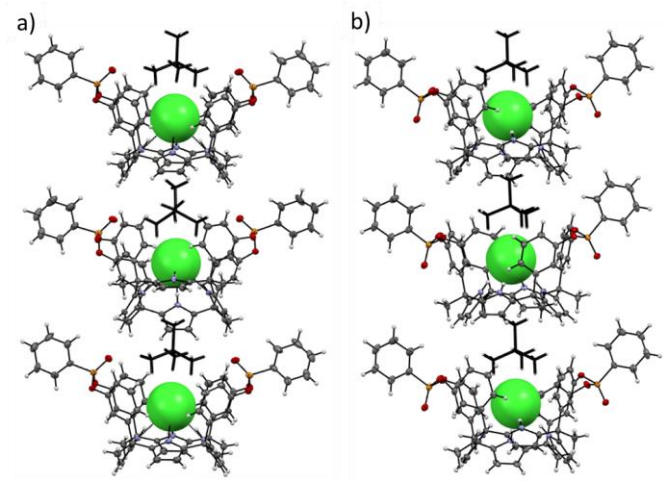

Fig. 112 Columnar motif seen for crystals of (a) **147ii**·TMPCl and (b) **147oo**·TMPCl as inferred from single crystal X-ray diffraction studies. Solvents are omitted for clarity. These figures were generated using data downloaded from the Cambridge Crystallographic Data Centre (CSD Nos. 913464 and 913474).

The binding affinities for receptors **147** interacting with TMPCl were found to be *K*(**147oo**·TMPCl) > *K*(**147io**·TMPCl) > *K*(**147ii**·TMPCl). A two-step binding process, involving anion recognition followed by cation complexation, analogous to what was put forward for simple calixpyrroles (e.g., **1**), was proposed by the authors (Fig. 113).[162, 163] Interestingly, when the cation was changed from a quaternary ammonium to a primary ammonium (octylammonium, OAM^+), the binding affinity sequence was reversed (i.e., *K*(**147ii**·OAMCl) > *K*(**147io**·OAMCl) > *K*(**147oo**·OAMCl). Both molecular modeling and ^{1}H NMR spectroscopic analyses provided support for the inclusion of OAM^+ in the upper rim, as well as formation of ion pair contact complex in the case of **147ii**·OAMCl.[164, 165]

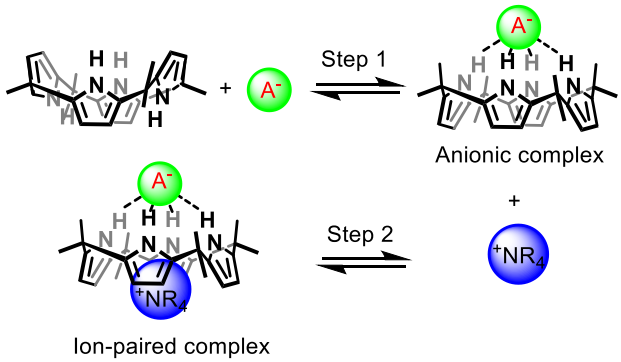

Fig. 113 The step-wise ion pair binding mechanism proposed previously for the interaction of ion pairs with the parent calix[4]pyrrole **1**.[162, 163]

Following this work, the same research group reported diastereomeric cavitands with four phosphonate groups on the upper rim of the scaffold (Fig. 114).[166] The isolated tetra-phosphonate receptors in this study were found to have either three (**148iooo**) or four (**148oooo**) of their P=O groups oriented away from the deep and functionalized aromatic cavity. Upon the titration of **148** with TMPCl in CD_2Cl_2, a 1:1 host:ion pair complex was formed, wherein the TMP^+ cation is exclusively bound to the electron-rich shallow cavity of the calix[4]pyrrole opposite to the chloride ion in a host-separated ion pair binding mode (Fig. 115), as inferred from ^{1}H and ^{31}P NMR spectroscopic analyses. It was found that the binding affinity corresponding to the formation of **148oooo**·TMPCl was about three times larger than that leading to **148iooo**·TMPCl in dichloromethane. This result was ascribed to the repulsive interaction between the bound chloride ion and the oxygen atom of the inwardly pointed P=O group present in **148iooo**. In a direct competitive binding experiment carried out in dichloromethane, the tetra-phosphonate calix[4]pyrrole **148oooo** exhibited an enhanced affinity toward the TMPCl salt (K_a[**148oooo**·TMPCl] = 16.0 × 10^7 M^{-1}) as compared to the bis-phosphonate calix[4]pyrroles discussed above (K_a[**147oo**·TMPCl] = 8.1 × 10^7 M^{-1}; K_a[**147io**·TMPCl] = 4 × 10^5 M^{-1}; K_a[**147ii**·TMPCl] = 2 × 10^5 M^{-1}). The higher binding constants seen for **148** were attributed to

two factors: (i) Conformational flexibility, and (ii) increased electrostatic interactions. When the organic cation was changed from a quaternary ammonium to a primary ammonium, host-separated binding was seen for **148oooo**·OAMCl, while a close-contact ion pair binding mode was found for **148iooo**·OAMCl (Fig. 116). Recently, ion pair recognition by **148oooo** was also investigated by means of DFT calculations with the recognition properties of **148iiii** also being predicted.[167]

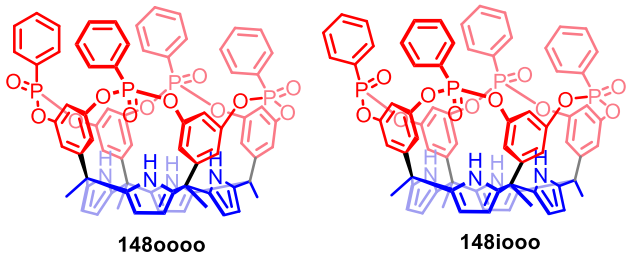

Fig. 114 Structures of **148oooo** and **148iooo**.

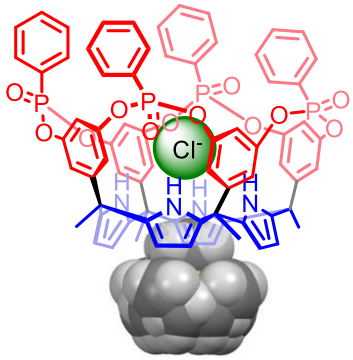

Fig. 115 Ion pair separated binding mode seen in **148oooo**·TMPCl as inferred from ^{1}H and ^{31}P NMR spectroscopic analyses. Complex **148iooo**·TMPCl was suggested to have a similar binding arrangement.

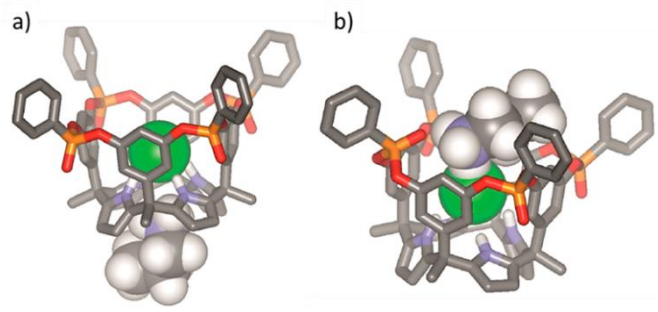

Fig. 116 Optimized structures of ion pair complexes with theoretically minimized energies (at BP86/dev2–SVP level). (a) **148oooo·OAMCl**; (b) **148iooo·OAMCl**. Reproduced from ref. 166 with permission. Copyright American Chemical Society, 2015.

A bis-loop calix[4]pyrrole **149** with a monophosphonate bridge was designed and synthesized for the specific recognition and sensing of creatinine (Fig. 117).[168] Creatinine is a metabolite present in urine, the concentration levels of which are often taken as indicative of kidney performance. A similar cavitand **151**, bridged by two methylene straps without the phosphonate group, was also synthesized as a reference. Receptor **149** was found capable of extracting neutral creatinine, which has limited solubility in dichloromethane, from the solid into the organic phase. ^{1}H and ^{31}P NMR spectra together with, 2D NOESY and ROESY experimental analyses in dichloromethane-d_2 led to the suggestion that a 1:1 host:guest complex is formed between receptor **149** and creatinine **150**. Support for the existence of such a complex came from a single crystal X-ray diffraction analysis (Fig. 118). In this case, the creatinine resided in the polar cavity of **149**, with the oxygen atom of the creatinine molecule bound to **149** via the four pyrrolic NH protons. One additional hydrogen bond is seen between the NH group in **150** and the oxygen of the P=O subunit (Fig. 118).[169] In the case of reference **151**, a system bearing two bridged methylene straps instead of a phosphate group and a methylene bridge, no appreciable extraction of creatinine was seen.

To function as an ionophore in an ion selective electrode (ISE), receptor **149** must be able to complex protonated creatinine (**150**·H$^+$). Therefore, the complexation behaviour of **149** with creatininium **150**·H$^+$ was investigated further using tetrakis(3,5–bis(trifluoromethyl)phenyl)borate (BARF$^-$, Fig. 117) as a non-competitive counter anion. The complex formed upon protonation (**150**·H$^+$) was characterized by a reduced affinity. The authors proposed that protonation of the creatinine at the nitrogen atom weakens the hydrogen-bonding-accepting ability of the adjacent carbonyl oxygen. A different complex **149**·(**150**·H$^+$)$_2$ (corresponding to the 1:2 host:guest complex) was observed upon increasing the concentration of **150**·H$^+$. Both **149** and **151** were incorporated into ISEs and used for the determination of **150**·H$^+$ concentrations in biological samples (urine and plasma). The sensor containing **149** showed obvious advantages in terms of both sensitivity and selectivity towards creatinine over the sensor based on **151** (Fig. 119). In fact, in 2019, the Ballester group reported the use of receptor **149** as the ionophore and a lipophilic pH indicator as an optical transducer in the creation of a creatinine optical sensing membrane that displayed a satisfactory response time. The system was also characterized by good optical selectivity coefficients.[170]

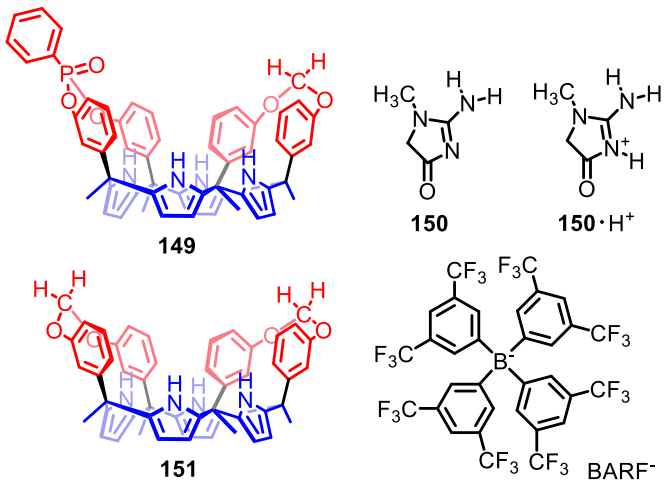

Fig. 117 Molecular structures of receptors **149** and **151**, and the creatinine and creatininium guests, **150** and **150**·H+, respectively.

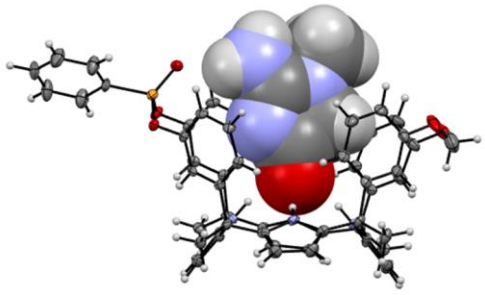

Fig. 118 Single crystal structure of the inclusion complex **149**·**150**. Solvent molecules are omitted for clarity. The figure was generated using data downloaded from the Cambridge Crystallographic Data Centre (CSD Nos. 1431012).

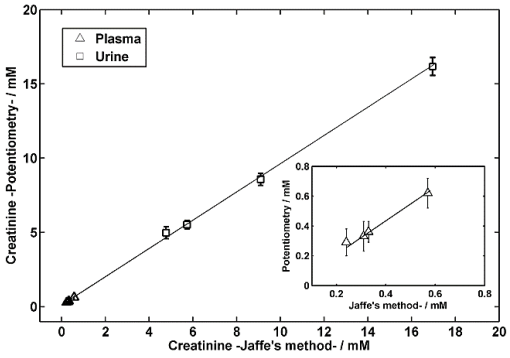

Fig. 119 Linear relationship between the creatinine concentration determined by an ISE based on **149** and the Jaffe's industry standard method. Reproduced from ref. 168 with permission. Copyright 2016 Wiley-VCH Verlag GmbH & Co. KGaA.

8 Conclusions and perspectives

Since the time of their first syntheses in 2002, strapped calix[4]pyrroles featuring at least one "closed" strap connected to the calix[4]pyrrole core have emerged as useful receptors for anions and ion pairs. The design is relatively straightforward. Moreover, in most cases the "strap effect" serves to enhance the corresponding binding affinities and selectivities. However, as the receptors increase in sophistication, the corresponding syntheses are becoming ever more challenging. Generally, there exist two synthetic strategies to access strapped calix[4]pyrroles: 1) Post-modification of a pre-formed calix[4]pyrrole system to introduce "closed straps"; 2) concurrent formation of multiple macrocycles, including the calix[4]pyrrole framework and the strapping moieties in one step.

Currently, increasing attention is being devoted to the functionalization of the straps. To achieve specific ion recognition goals (*e.g.*, selective extraction of CsCl or LiCl), some relatively complicated functional motifs have been introduced into the straps. Among representative systems prepared in this way are crown-ether-strapped calix[4]pyrroles, calixarene-strapped calix[4]pyrroles, hemispherand-strapped calix[4]pyrroles, and calix[4]pyrrole-strapped calix[4]pyrroles.

The practical uses of these and other strapped calix[4]pyrroles are currently being actively explored. Promising opportunities abound in the recognition of highly hydrated ion pairs (*e.g.*, LiCl, NaCl and CsOH). Further use in ion sensing, supramolecular extraction, mass transportation, and cancer cell targeting, are appealing; initial progress towards achieving these goals has been summarized in this review. On the fundamental research side, understanding further solvent effects and associated phenomena, such as ion pairing in the absence and presence of a given receptor, remain as challenges to be addressed.

Although progress has been made in the field of strapped calix[4]pyrroles, we believe that the best is yet to come. Since the calix[4]pyrrole core has at least eight meso positions and eight *β*-pyrrolic positions for modification, there are a myriad of possible ways to generate new functional strapped calix[4]pyrroles. We list 20 representative structures **a**-**t** in Fig. 120. To our knowledge, only few of them (*i.e.*, **a**, **b**, **c**, **d**, **p**) have been prepared to date. More specifically, most of the known strapped calix[4]pyrrole systems are of the **b**-type (cf. Fig. 120) due to their ease of synthesis and symmetry. Although the synthesis of the other structures may prove challenging, we feel they could afford the opportunity to target substrates that so far have remained beyond the horizon of calixpyrrole chemists. We hope that this review will provide a timely and useful reference for all those interested in ion recognition and supramolecular chemistry and will inspire researchers to prepare and study new functional macrocycles including novel strapped calix[4]pyrroles.

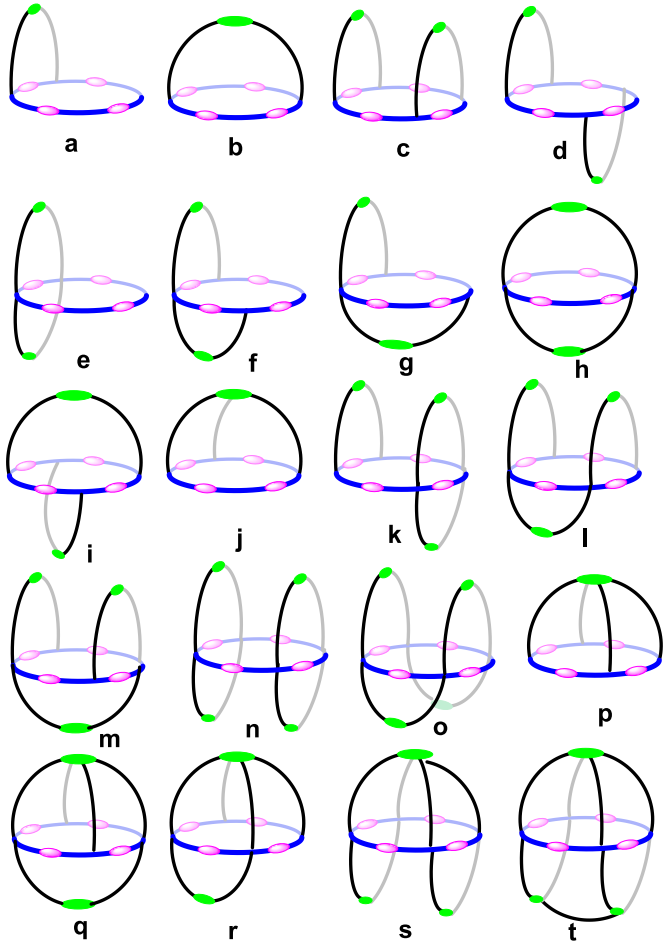

Fig. 120 Schematic representation showing various possible types of strapped calix[4]pyrrole (**a**–**t**). Most of these proposed systems are not yet synthetically accessible.

Conflicts of interest

The authors declare no competing financial interest.

Acknowledgements

This research was supported by the National Natural Science Foundation of China (21901069 to Q. H.), the Special Fund for Hunan's Plan on Innovative Province Construction (2019RS1018 to Q. H.), and the Fundamental Research Funds for the Central Universities (Startup Funds to Q. H. and S.P.). This work was supported by the National Research Foundation of Korea (NRF) grant funded by the Korea government (MSIT) (NRF-2019R1F1A1061780 to S.K.K.). Support is acknowledged from the Basic Science Research Program (NRF-2018R1A2A1A05077540 for C H. Lee) funded by the National Research Foundation under the Ministry of Science, ICT & Future Planning of Korea. Further support for this work was provided by the U.S. Department of Energy, Office of Science, Office of Basic Energy Sciences, Separation Science program under Award Number (DE-FG02-01ER15186 to J.L.S.), the National Institutes of Health (GM RO1 103790 to J.L.S.), and the Robert A. Welch Foundation (F-0018 to J.L.S.).

Notes and References

1. J. L. Atwood, *Comprehensive Supramolecular Chemistry II*, Elsevier, Oxford, 2 edn., 2017.
2. J. W. Steed and J. L. Atwood, *Supramolecular Chemistry* Wiley, Chichester, 2 edn., 2009.
3. I. V. Kolesnichenko and E. V. Anslyn, *Chem. Soc. Rev.*, 2017, 46, 2385-2390.
4. G. V. Oshovsky, D. N. Reinhoudt and W. Verboom, *Angew. Chem. Int. Ed.*, 2007, 46, 2366-2393.
5. W. D. Woggon and R. M. Wenger, *Chimia*, 2000, 54, 9-12.
6. J.-M. Lehn, *supramolecular chemistry: concepts and perspectives*, Wiley, Weinheim, 1996.
7. P. Neri, J. L. Sessler and M.-X. Wang, *Calixarenes and Beyond*, Springer, Berlin, 2016.
8. K. Bowman-James, A. Bianchi and E. García-España, *Anion Coordination Chemistry*, Wiley, New York, 2011.
9. Q. He, G. I. Vargas-Zuniga, S. H. Kim, S. K. Kim and J. L. Sessler, *Chem. Rev.*, 2019, 119, 9753-9835.
10. G. W. Gokel, W. M. Leevy and M. E. Weber, *Chem. Rev.*, 2004, 104, 2723-2750.
11. F. A. Christy and P. S. Shrivastav, *Crit. Rev. Anal. Chem.*, 2011, 41, 236-269.
12. J. S. Kim and D. T. Quang, *Chem. Rev.*, 2007, 107, 3780-3799.
13. L. Baldini, A. Casnati, F. Sansone and R. Ungaro, *Chem. Soc. Rev.*, 2007, 36, 254-266.
14. D. M. Homden and C. Redshaw, *Chem. Rev.*, 2008, 108, 5086-5130.
15. C. Redshaw, *Coord. Chem. Rev.*, 2003, 244, 45-70.
16. L. Mutihac, J. H. Lee, J. S. Kim and J. Vicens, *Chem. Soc. Rev.*, 2011, 40, 2777-2796.
17. G. Crini, *Chem. Rev.*, 2014, 114, 10940-10975.
18. E. M. M. Del Valle, *Process Biochem.*, 2004, 39, 1033-1046.
19. E. Engeldinger, D. Armspach and D. Matt, *Chem. Rev.*, 2003, 103, 4147-4173.
20. R. Gramage-Doria, D. Armspach and D. Matt, *Coord. Chem. Rev.*, 2013, 257, 776-816.
21. M. Xue, Y. Yang, X. D. Chi, Z. B. Zhang and F. H. Huang, *Acc. Chem. Res.*, 2012, 45, 1294-1308.
22. L. X. Chen, Y. M. Cai, W. Feng and L. H. Yuan, *Chem. Commun.*, 2019, 55, 7883-7898.
23. C. J. Li, *Chem. Commun.*, 2014, 50, 12420-12433.
24. H. Li, Y. Yang, F. F. Xu, T. X. Liang, H. R. Wen and W. Tian, *Chem. Commun.*, 2019, 55, 271-285.
25. T. Ogoshi and T. Yamagishi, *Eur. J. Org. Chem.*, 2013, 2961-2975.
26. K. I. Assaf and W. M. Nau, *Chem. Soc. Rev.*, 2015, 44, 394-418.
27. A. E. Kaifer, *Acc. Chem. Res.*, 2014, 47, 2160-2167.
28. N. J. Wheate, D. P. Buck, A. I. Day and J. G. Collins, *Dalton Trans.*, 2006, DOI: 10.1039/b513197a, 451-458.
29. H. D. Nguyen, D. T. Dang, J. L. van Dongen and L. Brunsveld, *Angew. Chem. Int. Ed.*, 2010, 49, 895-898.
30. C. Kim, S. S. Agasti, Z. Zhu, L. Isaacs and V. M. Rotello, *Nat. Chem.*, 2010, 2, 962-966.
31. D. H. Macartney, *Future Med. Chem.*, 2013, 5, 2075-2089.
32. G. Hettiarachchi, D. Nguyen, J. Wu, D. Lucas, D. Ma, L. Isaacs and V. Briken, *PloS one*, 2010, 5, e10514.
33. F. Biedermann, E. Elmalem, I. Ghosh, W. M. Nau and O. A. Scherman, *Angew. Chem. Int. Ed.*, 2012, 51, 7739-7743.
34. P. Montes-Navajas and H. Garcia, *Journal of Photochemistry and Photobiology A: Chemistry*, 2009, 204, 97-101.
35. N. Barooah, J. Mohanty, H. Pal and A. C. Bhasikuttan, *Org. Biomol. Chem.*, 2012, 10, 5055-5062.
36. G. Ghale and W. M. Nau, *Acc. Chem. Res.*, 2014, 47, 2150-2159.
37. E. Masson, X. Ling, R. Joseph, L. Kyeremeh-Mensah and X. Lu, *RSC Adv.*, 2012, 2, 1213-1247.

38. B. C. Pemberton, R. Raghunathan, S. Volla and J. Sivaguru, *Chem. Eur. J.*, 2012, 18, 12178-12190.
39. T. C. Lee, E. Kalenius, A. I. Lazar, K. I. Assaf, N. Kuhnert, C. H. Grun, J. Janis, O. A. Scherman and W. M. Nau, *Nat. Chem.*, 2013, 5, 376-382.
40. S. K. Kim and J. L. Sessler, *Acc. Chem. Res.*, 2014, 47, 2525-2536.
41. A. Baeyer, *Ber. Dtsch. Chem. Ges.*, 1886, 19, 2184–2185.
42. P. A. Gale, J. L. Sessler, V. Král and V. Lynch, *J. Am. Chem. Soc.*, 1996, 118, 5140-5141.
43. B. Turner, M. Botoshansky and Y. Eichen, *Angew. Chem. Int. Ed.*, 1998, 37, 2475-2478.
44. P. A. Gale, P. Anzenbacher and J. L. Sessler, *Coord. Chem. Rev.*, 2001, 222, 57-102.
45. W. Sliwa, *Heterocycles*, 2002, 57, 169-185.
46. C. H. Lee, H. Miyaji, D. W. Yoon and J. L. Sessler, *Chem. Commun.*, 2008, 24-34.
47. P. Ballester, *Isr. J. Chem.*, 2011, 51, 710-724.
48. D. S. Kim and J. L. Sessler, *Chem. Soc. Rev.*, 2015, 44, 532-546.
49. G. M. Mamardashvili, N. Z. Mamardashvili and O. I. Koifman, *Russ. Chem. Rev.*, 2015, 84, 275-287.
50. I. Saha, J. T. Lee and C.-H. Lee, *Eur. J. Org. Chem.*, 2015, 2015, 3859-3885.
51. D. W. Yoon, D. E. Gross, V. M. Lynch, J. L. Sessler, B. P. Hay and C. H. Lee, *Angew. Chem. Int. Ed.*, 2008, 47, 5038-5042.
52. P. K. Panda and C. H. Lee, *Org. Lett.*, 2004, 6, 671-674.
53. J. L. Sessler, S. K. Kim, D. E. Gross, C. H. Lee, J. S. Kim and V. M. Lynch, *J. Am. Chem. Soc.*, 2008, 130, 13162-13166.
54. M. G. Fisher, P. A. Gale, J. R. Hiscock, M. B. Hursthouse, M. E. Light, F. P. Schmidtchen and C. C. Tong, *Chem. Commun.*, 2009, DOI: 10.1039/b904089g, 3017-3019.
55. S. H. Kim, S. J. Hong, J. Yoo, S. K. Kim, J. L. Sessler and C. H. Lee, *Org. Lett.*, 2009, 11, 3626-3629.
56. M. Yano, C. C. Tong, M. E. Light, F. P. Schmidtchen and P. A. Gale, *Org. Biomol. Chem.*, 2010, 8, 4356-4363.
57. D. W. Yoon, H. Hwang and C. H. Lee, *Angew. Chem. Int. Ed.*, 2002, 41, 1757-1759.
58. S. P. Yu, L. M. T. Canzoniero and D. W. Choi, *Curr. Opin. Cell Biol.*, 2001, 13, 405-411.
59. C.-H. Lee, *B. Korean Chem. Soc.*, 2011, 32, 768-778.
60. C. H. Lee, H. K. Na, D. W. Yoon, D. H. Won, W. S. Cho, V. M. Lynch, S. V. Shevchuk and J. L. Sessler, *J. Am. Chem. Soc.*, 2003, 125, 7301-7306.
61. A. F. D. de Namor and M. Shehab, *J Phys Chem B*, 2003, 107, 6462-6468.
62. C. H. Lee, J. S. Lee, H. K. Na, D. W. Yoon, H. Miyaji, W. S. Cho and J. L. Sessler, *J. Org. Chem.*, 2005, 70, 2067-2074.
63. J. Xie, W. Feng, P. Lu and Y. Meng, *Comput. Theor. Chem.*, 2013, 1007, 1-8.
64. D. W. Yoon, D. E. Gross, V. M. Lynch, C. H. Lee, P. C. Bennett and J. L. Sessler, *Chem. Commun.*, 2009, DOI: 10.1039/b818077f, 1109-1111.
65. D. E. Gross, D. W. Yoon, V. M. Lynch, C. H. Lee and J. L. Sessler, *J. Incl. Phenom. Macrocycl. Chem.*, 2010, 66, 81-85.
66. S. K. Kim and J. L. Sessler, *Chem. Soc. Rev.*, 2010, 39, 3784-3809.
67. A. J. McConnell and P. D. Beer, *Angew. Chem. Int. Ed.*, 2012, 51, 5052-5061.
68. J. H. Yang, V. M. Lynch, J. L. Sessler and S. K. Kim, *Supramol. Chem.*, 2018, 31, 203-210.
69. S. J. Hong, J. Yoo, D. W. Yoon, J. Yoon, J. S. Kim and C. H. Lee, *Chem. Asian. J.*, 2010, 5, 768-772.
70. R. Samanta, S. P. Mahanta, S. Chaudhuri, P. K. Panda and A. Narahari, *Inorg. Chim. Acta*, 2011, 372, 281-285.
71. R. Samanta, S. P. Mahanta, S. Ghanta and P. K. Panda, *RSC Adv.*, 2012, 2, 7974-7977.
72. R. Samanta, B. S. Kumar and P. K. Panda, *Org. Lett.*, 2015, 17, 4140-4143.
73. Y. Marcus, *J. Chem. Soc., Faraday Trans.*, 1991, 87, 2995-2999.
74. S. K. Kim, J. Lee, N. J. Williams, V. M. Lynch, B. P. Hay, B. A. Moyer and J. L. Sessler, *J. Am. Chem. Soc.*, 2014, 136, 15079-15085.
75. R. P. Smith and D. E. Wilcox, *Crit. Rev. Toxicol.*, 1994, 24, 355-377.
76. C. R. Wade and F. P. Gabbai, *Z. Naturforsch. B: Chem Sci*, 2014, 69, 1199-1205.
77. Y. Kim, T. W. Hudnall, G. Bouhadir, D. Bourissou and F. P. Gabbai, *Chem. Commun.*, 2009, 25, 3729-3731.
78. E. D. Stevens and H. Hope, *Acta Crystallogr. A*, 1977, 33, 723-729.
79. S. H. Kim, J. Lee, G. I. Vargas-Zuniga, V. M. Lynch, B. P. Hay, J. L. Sessler and S. K. Kim, *J. Org. Chem.*, 2018, 83, 2686-2693.
80. H. Miyaji, P. Anzenbacher, J. L. Sessler, E. R. Bleasdale and P. A. Gale, *Chem. Commun.*, 1999, DOI: Doi 10.1039/A905054j, 1723-1724.
81. P. Anzenbacher, K. Jursikova and J. L. Sessler, *J. Am. Chem. Soc.*, 2000, 122, 9350-9351.
82. H. Miyaji, W. Sato and J. L. Sessler, *Angew. Chem. Int. Ed.*, 2000, 39, 1777-1780.
83. H. Miyaji, W. Sato, J. L. Sessler and V. M. Lynch, *Tetrahedron Lett.*, 2000, 41, 1369-1373.
84. H. Miyaji, W. Sato, D. Q. An and J. L. Sessler, *Collect. Czech. Chem. C.*, 2004, 69, 1027-1049.
85. H. Miyaji, H. K. Kim, E. K. Sim, C. K. Lee, W. S. Cho, J. L. Sessler and C. H. Lee, *J. Am. Chem. Soc.*, 2005, 127, 12510-12512.
86. S.-D. Jeong, J. Yoo, H.-K. Na, D. Y. Chi and C.-H. Lee, *Supramol. Chem.*, 2007, 19, 271-275.
87. J. Yoo, M. S. Kim, S. J. Hong, J. L. Sessler and C. H. Lee, *J. Org. Chem.*, 2009, 74, 1065-1069.
88. G. Park, K. Park and C.-H. Lee, *B. Korean Chem. Soc.*, 2013, 34, 283-286.
89. S. K. Kim, H. G. Lee, G. I. Vargas-Zúñiga, J. H. Oh, V. M. Lynch, M. H. Lee and J. L. Sessler, *Supramol. Chem.*, 2017, 29, 651-657.
90. A. P. Davis, D. N. Sheppard and B. D. Smith, *Chem. Soc. Rev.*, 2007, 36, 348-357.
91. H. J. Clarke, E. N. Howe, X. Wu, F. Sommer, M. Yano, M. E. Light, S. Kubik and P. A. Gale, *J. Am. Chem. Soc.*, 2016, 138, 16515-16522.
92. X. Wu, E. N. W. Howe and P. A. Gale, *Acc. Chem. Res.*, 2018, 51, 1870-1879.
93. S. J. Moore, M. G. Fisher, M. Yano, C. C. Tong and P. A. Gale, *Chem. Commun.*, 2011, 47, 689-691.
94. S. J. Moore, M. G. Fisher, M. Yano, C. C. Tong and P. A. Gale, *Dalton Trans.*, 2011, 40, 12017-12020.
95. C. Ji, R. B. Stockbridge and C. Miller, *J. Gen. Physiol.*, 2014, 144, 257-261.
96. R. B. Stockbridge, L. Kolmakova-Partensky, T. Shane, A. Koide, S. Koide, C. Miller and S. Newstead, *Nature*, 2015, 525, 548-551.
97. S. K. Ko, S. K. Kim, A. Share, V. M. Lynch, J. Park, W. Namkung, W. Van Rossom, N. Busschaert, P. A. Gale, J. L. Sessler and I. Shin, *Nat. Chem.*, 2014, 6, 885-892.
98. Y. Okada, T. Shimizu, E. Maeno, S. Tanabe, X. Wang and N. Takahashi, *J. Membr. Biol.*, 2006, 209, 21-29.
99. E. White, *Nat. Rev. Cancer*, 2012, 12, 401-410.
100. F. H. Igney and P. H. Krammer, *Nat. Rev. Cancer*, 2002, 2, 277-288.
101. K. H. Baek, J. Park and I. Shin, *Chem. Soc. Rev.*, 2012, 41, 3245-3263.
102. S. K. Ko, J. Kim, D. C. Na, S. Park, S. H. Park, J. Y. Hyun, K. H. Baek, N. D. Kim, N. K. Kim, Y. N. Park, K. Song and I. Shin, *Chem. Biol.*, 2015, 22, 391-403.
103. N. Busschaert, S. H. Park, K. H. Baek, Y. P. Choi, J. Park, E. N. W.

Howe, J. R. Hiscock, L. E. Karagiannidis, I. Marques, V. Felix, W. Namkung, J. L. Sessler, P. A. Gale and I. Shin, *Nat. Chem.*, 2017, 9, 667-675.
104. S. H. Park, S. H. Park, E. N. W. Howe, J. Y. Hyun, L. J. Chen, I. Hwang, G. Vargas-Zuniga, N. Busschaert, P. A. Gale, J. L. Sessler and I. Shin, *Chem*, 2019, 5, 2079-2098.
105. H. Miyaji, S. J. Hong, S. D. Jeong, D. W. Yoon, H. K. Na, J. Hong, S. Ham, J. L. Sessler and C. H. Lee, *Angew. Chem. Int. Ed.*, 2007, 46, 2508-2511.
106. I. W. Park, J. Yoo, B. Kim, S. Adhikari, S. K. Kim, Y. Yeon, C. J. Haynes, J. L. Sutton, C. C. Tong, V. M. Lynch, J. L. Sessler, P. A. Gale and C. H. Lee, *Chem. Eur. J.*, 2012, 18, 2514-2523.
107. I. W. Park, J. Yoo, S. Adhikari, J. S. Park, J. L. Sessler and C. H. Lee, *Chem. Eur. J.*, 2012, 18, 15073-15078.
108. S. K. Kim, H. G. Lee, G. I. Vargas-Zuniga, V. M. Lynch, C. Kim and J. L. Sessler, *Chem. Eur. J.*, 2014, 20, 11750-11759.
109. X. Chi, G. M. Peters, C. Brockman, V. M. Lynch and J. L. Sessler, *J. Am. Chem. Soc.*, 2018, 140, 13219-13222.
110. R. Kumar, A. Sharma, H. Singh, P. Suating, H. S. Kim, K. Sunwoo, I. Shim, B. C. Gibb and J. S. Kim, *Chem. Rev.*, 2019, 119, 9657-9721.
111. P. A. Gale, J. L. Sessler, V. Lynch and P. I. Sansom, *Tetrahedron Lett.*, 1996, 37, 7881-7884.
112. P. A. Gale, J. W. Genge, V. Král, M. A. McKervey, J. L. Sessler and A. Walker, *Tetrahedron Lett.*, 1997, 38, 8443-8444.
113. S. K. Kim, J. K. Lee, S. H. Lee, M. S. Lim, S. W. Lee, W. Sim and J. S. Kim, *J. Org. Chem.*, 2004, 69, 2877-2880.
114. J. K. Lee, S. K. Kim, R. A. Bartsch, J. Vicens, S. Miyano and J. S. Kim, *J. Org. Chem.*, 2003, 68, 6720-6725.
115. S. K. Kim, W. Sim, J. Vicens and J. S. Kim, *Tetrahedron Lett.*, 2003, 44, 805-809.
116. S. K. Kim, J. Vicens, K.-M. Park, S. S. Lee and J. S. Kim, *Tetrahedron Lett.*, 2003, 44, 993-997.
117. S. K. Kim, J. L. Sessler, D. E. Gross, C. H. Lee, J. S. Kim, V. M. Lynch, L. H. Delmau and B. P. Hay, *J. Am. Chem. Soc.*, 2010, 132, 5827-5836.
118. S. K. Kim, G. I. Vargas-Zuniga, B. P. Hay, N. J. Young, L. H. Delmau, C. Masselin, C. H. Lee, J. S. Kim, V. M. Lynch, B. A. Moyer and J. L. Sessler, *J. Am. Chem. Soc.*, 2012, 134, 1782-1792.
119. S. K. Kim, V. M. Lynch, N. J. Young, B. P. Hay, C. H. Lee, J. S. Kim, B. A. Moyer and J. L. Sessler, *J. Am. Chem. Soc.*, 2012, 134, 20837-20843.
120. B. Sadhu, M. Sundararajan, G. Velmurugan and P. Venuvanalingam, *Dalton Trans.*, 2015, 44, 15450-15462.
121. S. K. Kim, B. P. Hay, J. S. Kim, B. A. Moyer and J. L. Sessler, *Chem. Commun.*, 2013, 49, 2112-2114.
122. I. W. Park, S. K. Kim, M. J. Lee, V. M. Lynch, J. L. Sessler and C. H. Lee, *Chem. Asian. J.*, 2011, 6, 2911-2915.
123. S. K. Kim, V. M. Lynch, B. P. Hay, J. S. Kim and J. L. Sessler, *Chem. Sci.*, 2015, 6, 1404-1413.
124. S. K. Kim, V. M. Lynch and J. L. Sessler, *Org. Lett.*, 2014, 16, 6128-6131.
125. P. Thiampanya, N. Muangsin and B. Pulpoka, *Org. Lett.*, 2012, 14, 4050-4053.
126. Y. Yeon, S. Leem, C. Wagen, V. M. Lynch, S. K. Kim and J. L. Sessler, *Org. Lett.*, 2016, 18, 4396-4399.
127. A. Sonoc, J. Jeswiet and V. K. Soo, *Proc. Cirp.*, 2015, 29, 752-757.
128. M. K. Song, S. Park, F. M. Alamgir, J. Cho and M. L. Liu, *Mat. Sci. Eng. R.*, 2011, 72, 203-252.
129. R. Oruch, M. A. Elderbi, H. A. Khattab, I. F. Pryme and A. Lund, *Eur. J. Pharmacol.*, 2014, 740, 464-473.
130. Q. He, Z. Zhang, J. T. Brewster, V. M. Lynch, S. K. Kim and J. L. Sessler, *J. Am. Chem. Soc.*, 2016, 138, 9779-9782.
131. Q. He, G. M. Peters, V. M. Lynch and J. L. Sessler, *Angew. Chem. Int. Ed.*, 2017, 56, 13396-13400.
132. M. Y., *J. Chem. Soc., Faraday Trans.*, 1991, 87, 2995-2999.
133. S. E. Kesler, P. W. Gruber, P. A. Medina, G. A. Keoleian, M. P. Everson and T. J. Wallington, *Ore. Geol. Rev.*, 2012, 48, 55-69.
134. Q. He, N. J. Williams, J. H. Oh, V. M. Lynch, S. K. Kim, B. A. Moyer and J. L. Sessler, *Angew. Chem. Int. Ed.*, 2018, 57, 11924-11928.
135. D. R. Lide, *CRC Handbook of Chemistry and Physics, 75th ed., CRC, Boca Raton*, 1994, pp. 12-13.
136. V. Valderrey, E. C. Escudero-Adan and P. Ballester, *J. Am. Chem. Soc.*, 2012, 134, 10733-10736.
137. V. Valderrey, E. C. Escudero-Adan and P. Ballester, *Angew. Chem. Int. Ed.*, 2013, 52, 6898-6902.
138. J. R. Romero, G. Aragay and P. Ballester, *Chem. Sci.*, 2017, 8, 491-498.
139. R. Molina-Muriel, G. Aragay, E. C. Escudero-Adan and P. Ballester, *J. Org. Chem.*, 2018, 83, 13507-13514.
140. I. Saha, J. H. Lee, H. Hwang, T. S. Kim and C. H. Lee, *Chem. Commun.*, 2015, 51, 5679-5682.
141. Q. He, M. Kelliher, S. Bahring, V. M. Lynch and J. L. Sessler, *J. Am. Chem. Soc.*, 2017, 139, 7140-7143.
142. P. K. Panda and C. H. Lee, *J. Org. Chem.*, 2005, 70, 3148-3156.
143. D.-W. Yoon, S.-D. Jeong, M.-Y. Song and C.-H. Lee, *Supramol. Chem.*, 2007, 19, 265-270.
144. M. Chas, G. n. Gil-Ramírez and P. Ballester, *Org. Lett.*, 2011, 13, 3402-3405.
145. M. Chas and P. Ballester, *Chem. Sci.*, 2012, 3, 186-191.
146. A. Galan, G. Gil-Ramirez and P. Ballester, *Org. Lett.*, 2013, 15, 4976-4979.
147. M. Espelt, G. Aragay and P. Ballester, *Chimia*, 2015, 69, 652-658.
148. S. K. Korner, F. C. Tucci, D. M. Rudkevich, T. Heinz and J. Rebek, *Chem. Eur. J.*, 2000, 6, 187-195.
149. T. Heinz, D. M. Rudkevich and J. Rebek, *Nature*, 1998, 394, 764-766.
150. X. Liu and R. Warmuth, *J. Am. Chem. Soc.*, 2006, 128, 14120-14127.
151. S. Rieth, K. Hermann, B. Y. Wang and J. D. Badjic, *Chem. Soc. Rev.*, 2011, 40, 1609-1622.
152. A. Galan, E. C. Escudero-Adan, A. Frontera and P. Ballester, *J. Org. Chem.*, 2014, 79, 5545-5557.
153. A. Galan, G. Aragay and P. Ballester, *Chem. Sci.*, 2016, 7, 5976-5982.
154. L. K. Frensch, K. Propper, M. John, S. Demeshko, C. Bruckner and F. Meyer, *Angew. Chem. Int. Ed.*, 2011, 50, 1420-1424.
155. A. Galan, E. C. Escudero-Adan and P. Ballester, *Chem. Sci.*, 2017, 8, 7746-7750.
156. O. I. Koifman and N. Z. Mamardashvili, *Russ. Chem. Bull., Int. Ed.*, 2013, 62, 123-132.
157. N. Z. Mamardashvili, M. O. Koifman and O. I. Koifman, *Russ. J. Org. Chem.*, 2014, 50, 559-566.
158. J. Aguilera-Sigalat, C. Sáenz de Pipaón, D. Hernández-Alonso, E. C. Escudero-Adán, J. R. Galan-Mascarós and P. Ballester, *Cryst. Growth Des.*, 2017, 17, 1328-1338.
159. L. Escobar, D. Villaron, E. C. Escudero-Adan and P. Ballester, *Chem. Commun.*, 2019, 55, 604-607.
160. J. Y. Park, K. Skonieczny, N. Aratani, A. Osuka, D. T. Gryko and C. H. Lee, *Chem. Commun.*, 2012, 48, 8060-8062.
161. M. Ciardi, F. Tancini, G. Gil-Ramírez, E. C. Escudero Adán, C. Massera, E. Dalcanale and P. Ballester, *J. Am. Chem. Soc.*, 2012, 134, 13121-13132.
162. J. L. Sessler, D. E. Gross, W. S. Cho, V. M. Lynch, F. P. Schmidtchen, G. W. Bates, M. E. Light and P. A. Gale, *J. Am. Chem. Soc.*, 2006, 128, 12281-12288.

163. D. E. Gross, F. P. Schmidtchen, W. Antonius, P. A. Gale, V. M. Lynch and J. L. Sessler, *Chem. Eur. J.*, 2008, 14, 7822-7827.
164. T. Wang, J. Liu, H. Sun, L. Chen, J. Dong, L. Sun and Y. Bi, *RSC Adv.*, 2014, 4, 1864-1873.
165. T. Wang, J. Liu, D. Zhang and H. Sun, *RSC Adv.*, 2014, 4, 44948-44958.
166. M. Ciardi, A. Galán and P. Ballester, *J. Am. Chem. Soc.*, 2015, 137, 2047-2055.
167. T. Wang and J. Liu, *Adv. Theory Simul.*, 2018, 1, 1700010.
168. T. Guinovart, D. Hernandez-Alonso, L. Adriaenssens, P. Blondeau, M. Martinez-Belmonte, F. X. Rius, F. J. Andrade and P. Ballester, *Angew. Chem. Int. Ed.*, 2016, 55, 2435-2440.
169. D. N. Lande, S. A. Bhadane and S. P. Gejji, *J. Mol. Liq.*, 2017, 247, 456-466.
170. M. M. Erenas, I. Ortiz-Gomez, I. de Orbe-Paya, D. Hernandez-Alonso, P. Ballester, P. Blondeau, F. J. Andrade, A. Salinas-Castillo and L. F. Capitan-Vallvey, *ACS sensors*, 2019, 4, 421-426.

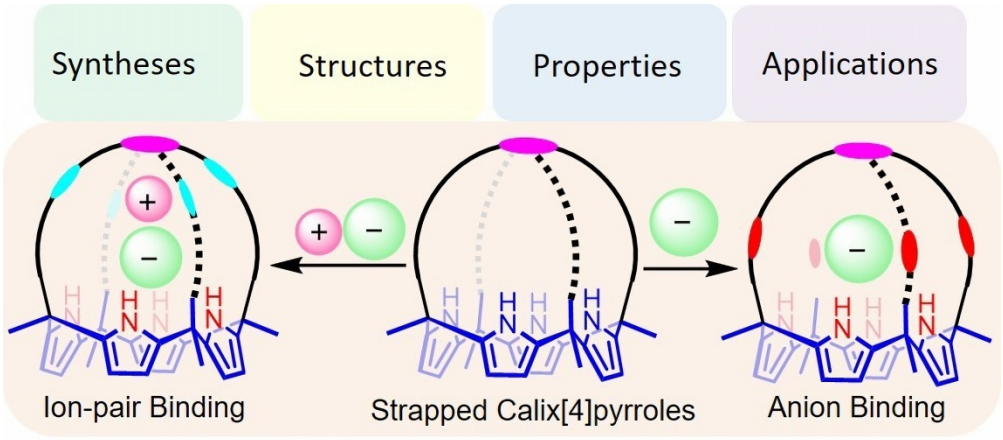

1319x582mm (72 x 72 DPI)